ABSTRACT

Title of Document: INVESTIGATIONS OF THE EFFECTS OF OYSTER ALLOMETRY AND REEF MORPHOLOGY ON FILTRATION RATE AND PARTICLE CAPTURE USING NUMERICAL MODELS

Melinda K. Forsyth, Master of Science 2014

Directed By: Assistant Professor Dr. Lora A. Harris
Marine-Estuarine-Environmental Sciences

Crassostrea virginica, the eastern oyster, is a filter-feeding bivalve currently found at low numbers in Chesapeake Bay. Accurately modeling the particles removed from the water column by feeding is important for determining the impact oysters have on water quality and can be a tool for planning restoration. Upon thorough assessment of three oyster models, each incorporating a filtration rate formulation, I established a new filtration rate model that is dependent on individual size and the environmental limitations of salinity, temperature, and suspended solids. This equation was then coupled with two particle models, each designed to account for the gradient of particles across a reef with varying degrees of complexity. The model including both advection and diffusion resulted in a better depiction of reef particle gradients. I used steady-state solutions over a range of conditions to determine that oyster reefs in lower velocity environments with high oyster densities are more susceptible to food limitation.

INVESTIGATIONS OF THE EFFECTS OF OYSTER ALLOMETRY AND REEF MORPHOLOGY ON FILTRATION RATE AND PARTICLE CAPTURE USING NUMERICAL MODELS

By

Melinda K. Forsyth

Thesis submitted to the Faculty of the Graduate School of the
University of Maryland, College Park, in partial fulfillment
of the requirements for the degree of
Master of Science
2014

Advisory Committee:
Assistant Professor Dr. Lora Harris, Chair
Professor Dr. Larry Sanford
Research Professor Dr. Mario Tamburri

Acknowledgements

I would like to thank my advisor Dr. Lora Harris for her guidance and support in completion of my thesis. I appreciate her patience when I struggled with writing and the help with understanding and creating mathematical models. I would also like to thank my committee members including Dr. Larry Sanford, for his patience in explaining hydrodynamics over and over, and Dr. Mario Tamburri, for his insight and support.

I want to acknowledge members of my lab group, both past and present members, and the base of friends that I gained in Southern Maryland. Special thanks to Melissa Day, Casey Hodgkins, and Nicole Bransome Mehaffie.

I would also like to thank those I have crossed paths with in my graduate career that expanded my knowledge of oysters and gave me support. I would like to especially thank Dr. Elizabeth North for her help in the beginning stages of my thesis development.

My research would not have been possible without funding from DC Water and their internship program. Also, thanks to Dr. Ed Houde for providing me with another position at CBL while I completed my thesis.

I would especially like to thank my fiancé and soon to be husband Daniel Ehrich. Thanks for moving to Southern Maryland with me, and being there when times were tough. Also, thanks to Layla for putting a smile on my face every day.

Table of Contents

List of Tables

List of Figures

Chapter 1: A Review and Improvement of Existing Eastern Oyster Filtration Rate Models

ABSTRACT

Crassostrea virginica, the eastern oyster, is a filter-feeding, particle clearing bivalve currently at low numbers in Chesapeake Bay. Accurately describing the filtration rate of these bivalves is essential to estuarine management and associated efforts to understand the impact of oyster populations on water quality. Here, the filtration rate equations for three existing models (Cerco and Noel (2005), Fulford et al. (2007), and Powell et al. (1992)) are assessed. I examine how each of the models define the maximum filtration rate and explore the various limitation factors that modify these maximum rates via environmental conditions that include salinity, temperature, total suspended solids, and dissolved oxygen. Based on the individual model strengths found in the model comparison and a literature review, I determine a maximum filtration rate of 0.17 m^3 g^{-1} DW day^{-1} for a 1 g DW oyster to be a better filtration rate, which is then modified by a combination of limitation factors taken from a variety of sources. These include those described by Fulford et al. (2007) for total suspended solids and salinity, and a newly developed function to describe temperature dependence. Differences in size are incorporated by using a basic allometric formulation where a weight exponent alters filtration rate based on individual oyster size.

1. INTRODUCTION AND OBJECTIVES

The eastern oyster, *Crassostrea virginica*, is a sessile filter feeding bivalve mollusk that can be classified as an ecosystem engineer (Gutierrez et al. 2003). According to Newell (1988), oysters filter water at a typical rate of 0.12 m^3 g^{-1} dry weight (DW) day^{-1}, removing suspended organic and inorganic particles from the water column to affect water column clarity and nutrient cycling. As autogenic engineers (Wilberg et al. 2013), oysters, which are gregarious, form reefs by accumulating shell, providing substrate for oyster larvae settlement as well as habitat for other organisms (Newell 1988; Chesapeake Bay Program 2009, NOAA 2007).

Chesapeake Bay was home to a productive oyster fishery in the 1880s before a substantial decline, attributed to overfishing depleting the stock and dismantling the hard substrate that oysters need. In the 1950s, the outbreak of MSX (*Haplosporidium nelsoni)* and Dermo (*Perkinsus marinus*), parasitic diseases, further decreased the oyster population (Newell 1988; Kemp et al. 2005). Recent modeling efforts to consider both fishery pressure and disease presence for *C. virginica* revealed the abundance of oysters in Chesapeake Bay has declined by 99.7% (Wilberg et al. 2011), greatly affecting the ecological services that oysters provide.

Figure 1 graphs the decline in oyster abundance and filtration capacity as reported by Kemp et al. (2005). Using similar estimates of abundance, Newell (1988) calculated that the 19th century oyster population could filter a volume of water equivalent to the upper and middle of the Bay in about 3.6 days. Because of declines in the population, this estimate must be revised to hundreds of days (Newell 1988).

Wilberg et al.'s (2013) population model of Chesapeake Bay oysters integrates fishery related habitat changes that affect the carrying capacity of this estuarine ecosystem. This moves us towards a better understanding of the oyster habitat dependence and stock assessment of oysters. However, there is still a need for model formulations that include the secondary role of these species as ecosystem engineers that filter the water column.

Oyster filtration is regulated by the movement of cilia on the gills, decreasing or increasing pumping and particle uptake (Newell and Langdon 1996; Ward 1994). The particles collected follow varying pathways within the oyster anatomical system. Particles first reach the gills, an organ also necessary for respiration. The gills capture particles, with varying degrees of efficiency, with greater efficiency for particles larger than 4 μm in diameter (Tamburri and Zimmer-Faust 1996). These particles can either be rejected or transferred to the labial palps, a site of further particle sorting. Different stimuli allow for selection of preferred particles, including organic rather than inorganic particles. The labial palps surround the mouth, and deliver the desired particles to the digestive track (Newell and Langdon 1996; Tamburri and Zimmer-Faust 1996; Ward et al. 1994).

Particle movement within the system occurs as the particles form mucous slurries and strings and these are moved with cilia. Particles that are rejected, either due to being undesirable or in excess of the digestive capacity of the oyster, are excreted as pseudofeces (Newell and Langdon 1996; Tamburri and Zimmer-Faust 1996; Ward et al. 1994). Particles ingested follow the alimentary system and are

excreted as feces (Ward et al. 1994). Filtered water exits the oyster with the exhalent current.

Numerous eastern oyster (*Crassostrea virginica*) models incorporating the feeding mechanism of oysters have been established, spanning a diversity of approaches that include the efforts of Powell et al. (1992), Cerco and Noel (2005), and Fulford et al. (2007). Cerco and Noel (2005) numerically model oyster growth in terms of changes in total carbon, Powell et al. (1992) calculate population dynamics in terms of increases and decreases in size classes of oysters, and Fulford et al. (2007) predict filtration rates to determine clearance of phytoplankton.

For oyster models describing bioenergetics (e.g. Powell et al.1992; Cerco and Noel 2005), the filtration rate is the major determinant of growth that in turn affects changes in oyster biomass. In addition to being a component of growth rate formulations, the filtration rate is also indicative of the impact oysters may have on the ecosystem via such processes as phytoplankton clearance. Estimating the magnitude of this impact on phytoplankton biomass is a focus of the oyster model developed by Fulford et al. (2007). The volume of water and associated particles that oysters can remove via filter feeding is of interest to managers in ecosystems where nutrient pollution may lead to phytoplankton blooms and deteriorated water quality. Feedbacks between a decline in water quality and the eastern oyster are of interest to current efforts to restore the oyster population and meet Total Maximum Daily Load regulatory requirements in Chesapeake Bay (Clean Water Act section 303(d)).

All too frequently, we lack the time to thoroughly examine the dynamics of models, even though sensitivity analyses and exploration of model dynamics are

important to understand model strengths and weaknesses (Fulton et al. 2003). For example, Brush et al. (2002) finds that phytoplankton biomass, a state variable commonly used as currency in Nutrient-Phytoplankton-Zooplankton-Depth (NPZD) models, is often predicted correctly even though different models have different formulations for the rate process of primary production. In calculating primary production with these varied formulations, drastically different numbers are predicted and this diversity of output indicates great quantitative uncertainty in the mechanisms that drive primary production. In the case of oysters, it is especially crucial that we provide reliable filtration rates as these formulations are critical in linking these organisms to the ecosystem services they provide in improving water clarity.

The objective of this chapter is to compare three oyster models (Cerco and Noel (2005), Fulford et al. (2007), and Powell et al. (1992)) with a focus on filtration rates. Here, I consider the oyster to be a perfect sieve of the water column, assuming no particles are released with the outflow of water. Therefore, clearance rates and filtration rates are considered synonymous. The filtration rates depend on both the critical selection of a maximum filtration rate and data-driven formulations that describe environmental limitation factors and mechanisms. Comparisons of these approaches, with further literature review, naturally leads to the development of a new filtration rate and determination of weaknesses or data gaps that can be pursued in future empirical efforts.

1.1 Existing Oyster Models

1.1.1. Cerco and Noel (2005) Oyster Model

The Cerco and Noel (2005) bioenergetics oyster model describes changes in oyster biomass (*O*, g oyster C m^{-2}) with time (*t*, day) as:

$$\frac{dO}{dt} = [\text{POC Consumption}] - [\text{Respiration}] - [\text{Mortality}] \quad (1)$$

The particulate organic carbon (POC) consumption term is the amount of organic carbon oysters consume and incorporates a filtration rate that describes the rate oysters uptake water. This rate is a function of the maximum filtration rate, Fr_{max}, and limitations from temperature (T), salinity (S), total suspended solids (TSS), and dissolved oxygen (DO), which can be expressed as.

$$Fr = Fr_{max} * f(T) * f(S) * f(TSS) * f(DO) \quad (2)$$

The maximum filtration, Fr_{max}, is the maximum rate oysters can filter water (m^3 g^{-1} oyster C day^{-1}). Equations for each environmental limitation, *f(S), f(T), f(TSS), f(DO),* scaled between 0 and 1, are multiplied by the Fr_{max}. These environmental effects on filtration are listed in Table 1 (Cerco and Noel 2005).

Cerco and Noel (2005) estimate the change of oyster biomass in relation to environmental variables that affect the bioenergetics of the oyster population. This model approach is both similar to, and different from the following models, with the main difference a focus on carbon exchange and oyster growth in terms of total oyster carbon biomass in a square meter, rather than per individual organism.

1.1.2. Fulford et al. (2007) Oyster Clearance Model

The Fulford et al. (2007) model objective is specifically targeted at understanding the effect of oysters on phytoplankton removal, rather than changes in

biomass of oysters per unit area. Particle uptake is oyster size and particle size dependent. The main model equations describe filtration rate, or clearance rate, with a formulation expressed similarly to Cerco and Noel (2005) (refer to Equation 2), but with size dependent filtration rates. This equation is

$$CR_{(i)} = CR_{\max(i)} * f(T) * f(S) * f(TSS) * f(DO) \quad (3)$$

where $CR_{(i)}$ is the oyster clearance rate ($m^3\ g^{-1}$ oyster C day^{-1}) dependent on the size *(i)* of the oyster, $CR_{max(i)}$ is the maximum clearance rate ($m^3\ g^{-1}$ oyster C day^{-1}) for the oysters of size *(i)*, and the functions of environmental variables or *f(T, S, TSS, DO)* are limitation factors to the maximum clearance rate, scaled between 0 and 1 (Fulford et al. 2007). These environmental limitation functions are listed in Table 1.

Equation 3 calculates the filtration rate for one size class of oyster. The mean filtration for a population is expressed as

$$CR_{pop} = \sum CR_{(i)} * P_{(i)} \quad (4)$$

Where CR_{pop} is the mean clearance rate ($m^3\ g^{-1}$ oyster C day^{-1}) of the population, $CR_{(i)}$ is clearance rate ($m^3\ g^{-1}$ oyster C day^{-1}) of an oyster of size *(i)* (g DW) and $P_{(i)}$ is the proportion of the population that are size *(i)*. Phytoplankton removal can then be calculated from the total filtration and the phytoplankton concentration. The filtration efficiency is also altered depending on the particle sizes with size classes of <2 μm, 2 to 4 μm, and >4 μm (Fulford et al. 2007).

This model examines the ecosystem function of a population of oysters rather determining growth and changes in biomass. Unlike the Cerco and Noel (2005) model, Fulford et al. (2007) incorporates a different filtration rate depending on the sizes of oysters in the population.

1.1.3. Powell et al. (1992) Population Dynamics Model

The Powell et al. (1992) model is a size-based oyster population model. Categories of oysters, such as juvenile and market sized, and the associated biomasses (g DW) make up ten different size classes.

In the Powell et al. (1992) model, the change in standing stock of oysters, based on caloric units, is equal to the net production within the size class, additions to the size class from the larger or smaller size class, and losses to the larger and smaller size class. The governing equation for the change in the standing stock, *O*, (calories m^{-2}) of each size class *(j)* is:

$$\frac{dO_{(j)}}{dt} = Pg_{(j)} + Pr_{(j)} + (\text{gain and loss from/to j} - 1) + (\text{gain and loss from/to j} + 1) \quad (5)$$

Where *Pg* is growth energy (calories m^{-2} day^{-1}), and *Pr* is reproductive energy (calories m^{-2} day^{-1}).

Filtration rate (mL $individual^{-1}$ min^{-1}), *Fr*, used to determine *Pg*, is formulated as

$$Fr = Fr_{max} * f(S) * f(TSS) \quad (6)$$

where Fr_{max} is the maximum filtration rate (mL $individual^{-1}$ min^{-1}). Fr_{max} is dependent on the size of the oysters in each size class and temperature. Unlike the above models, there is no *f(T)*, as it is incorporated into the maximum filtration rate. This maximum filtration is then multiplied by limitation factors of *f(S)* and *f(TSS)*. These environmental limitations are listed in Table 1. Dissolved oxygen is not a factor in the model (Powell et al. 1992).

The Powell et al. (1992) model is different from the other models in that it is a population model, where the changes in size classes are the desired output. Secondly, filtration rate is modeled on an individual basis rather than in units of carbon.

2. METHODS

2.1 Model Comparison

Filtration rate formulations were compared amongst the three models previously described. This comparative effort included identifying an empirical data source for parameterization of each model's filtration rate, contrasting the various limitation factors, and performing a sensitivity analysis to evaluate how simulated filtration rates responded to variations in T, S, and TSS.

Each of the three models' filtration rate equations were programmed in Simile (http://www.simulistics.com/), a modeling software. I calculated daily filtration rates ($m^3\ g^{-1}$ oyster C day^{-1}) for 1 g DW oysters with monitoring data from the lower Potomac River, a tributary of the Chesapeake Bay where historical oyster reefs are located (Maryland Department of Natural Resources 1997).

I obtained the Maryland Department of Natural Resources (MDNR)'s 2009 monthly monitoring water data for station LE 2.2 in the lower Potomac River, pictured in Figure 2. Data used as forcing functions included S, T, and TSS; with DO assumed optimal and set to a value of "1". I interpolated the data between sampling time frames to avoid missing data. Moving averages and standard deviations were computed at two-week increments to determine an estimated minimum and maximum for each forcing function that fluctuated over the annual cycle. These values were then used to constrain the random selection of a daily value for each day of the year

when field measurements were not available. Figure 3 shows the interpolated daily water quality for TSS, T, and S.

To evaluate the effectiveness of this method, the interpolated data for T and S were compared to nearby continuous monitoring stations that included Breton Bay, located further north of station LE 2.2, and St. Mary's College, located in the St Mary's River (Figure 2). At these stations, TSS is not measured continuously and was therefore not included in this comparison. Only slight differences were revealed between the continuous monitoring data and the interpolated values. While using the near-continuous monitoring data from these shallow sites would be preferable, TSS is critical to simulating filtration rates, necessitating the use of the interpolated dataset. The interpolated values were used to force T, S, and TSS for each model simulation to facilitate the evaluation and comparison of filtration rates under the same environmental conditions.

The next step was to examine the sensitivity of the models to changes in the environmental variables. Model sensitivity analysis was broken into two general approaches that included first determining how the magnitude of forcing functions affect filtration rate, and then testing how sensitive model output was to each of the limitation factors individually.

To determine the effect of forcing function magnitude, I iteratively manipulated single environmental parameters to be high and low values. Within the available long term dataset, the year 2009 was an intermediate year for T and S, and a low year for TSS. To have filtration rates for intermediate values of all three environmental parameters, the TSS for 2009 was multiplied by 1.6. This new

interpolated dataset was used to find filtration rates for conditions that represented intermediate conditions for all three variables. One environmental factor at a time was then manipulated to represent high or low values. For example, one model run for this sensitivity analysis would include using the high T values while keeping S and TSS forcing functions at the intermediate level. To simulate the high and low conditions, environmental forcings were multiplied by factors shown in Table 2. These multiplicative factors were determined by examining means for each variable for 1990 to 2010 for the LE 2.2 station and finding factors to adjust the intermediate interpolated dataset to be high or low values represented by the annual means.

I then compared filtration rates affected by one limitation factor at a time, assuming the other environmental factors were optimal. For instance, the *f(T)* would be dependent on the day of the year in the intermediate interpolated dataset, but the other functions of *f(TSS)* and *f(S)* were set at values of "1" and held constant over the time frame of the simulation.

2.2. Filtration Rate Model

After comparing the models, I defined an individual maximum filtration rate affected by T, S, and TSS limitations by searching the literature for empirically measured and modeled oyster filtration rates. Because filtration per unit weight varies with size, literature values required normalization for proper comparison and a 1 g DW oyster filtration rate was calculated in each case (See Appendix A for conversions). I then determined the maximum filtration rate for a 1 g DW oyster by taking a mean of the published maximums, including those of the three compared models.

Because individual size can alter the filtration rate (Newell and Langdon 1996), I included allometric constraints. Oyster size or dry weight, *W*, is assumed to affect the maximum filtration, *FR*, represented by the power formula:

$$FR=a_f W^b \quad (7)$$

where a_f is a constant (Peters 1983) related to filtration and *b* is the weight exponent (Newell and Langdon 1996). In this case, a_f is the maximum filtration rate for a 1 g DW oyster. I used a literature review to evaluate values of *b*, and used the morphological indicator of gape area as a proxy for filtration rate.

The general trend for bivalves is that as gape increases, filtration rate increases. This has been documented for mussels that possess filtering siphons (Jorgensen, 1990), with some caveats described for the more complicated case of oysters that remove particles through their mantles using gills (Collier et al. 1953). Collier et al. (1953) recorded pumping rates and shell movements, finding that the highest filtration rate occurs when the oyster is completely opened, but with some variation from this maximum rate when the oyster remained fully gaping. I chose to examine the maximum of the gape areas and assume a proportional relationship to the maximum filtration as G∝FR, where G is the gape area. I then solved for $G=a_g W^b$, where W is the dry weight, in which the value of *b* could be applied to $FR=a_f W^b$. Newell and Langdon (1996) found that gill size proportionally decreased as oyster size increased, providing added confirmation that this allometric relationship is appropriate.

Laboratory methods to determine the constants of a_g and *b* included measuring gape areas and dry weights for different sized oysters. Oysters ages 1 to 3 years old

were purchased from Marinetics, Inc. in Cambridge, MD, and larger oysters, of unknown ages, were donated by the oyster hatchery at Morgan State University's location at Jefferson Patterson Park in St. Leonard, MD. Five pictures of each oyster with a ruler were taken in the same dimensional plane and analyzed with Image-J (http://rsb.info.nih.gov/ij/) for gape width over a period of an hour after a minimum of 7 days of acclimation. The maximum gape width and the length around the oyster (excluding the hinge) measured with a string and ruler were multiplied to calculate the maximum gaping area, as shown in Figure 4. This was likely a slight overestimate since the width decreases closer to the hinge. After measurement, I shucked each oyster and placed the wet tissue in a pre-weighed tin, dried it for at least 72 hours at 65°C, and weighed it to calculate a dry weight. The *b* exponent in the gape area to weight relationship of $G=a_g W^b$ became the exponent *b* in $FR=a_f W^b$.

After defining the individual maximum filtration rate in this final stage of the modeling analysis, I determined which limitation formulations and parameterizations from T, S, and TSS should affect the filtration. Results from model analyses were used to select the best *f(TSS)* and *f(S)* to affect the new filtration rate maximum. The *f(T)* was formulated and re-parameterized based on model analysis and other temperature vs. filtration rate empirical studies.

3. RESULTS AND DISCUSSION

3.1. Model Comparison

3.1.1. Maximum Filtration Rates

The maximum filtration rate of an oyster is essential to parameterize as accurately as possible in any model that uses this value to simulate filtration in

relation to environmental limitation factors. Cerco and Noel (2005) set the maximum filtration rate at 0.55 m^3 g^{-1} oyster C day^{-1} based upon values reported by Jordan (1987) as weight specific biodepositon rates (mg g^{-1} DW hr^{-1}), and the clearance rates (L g^{-1} DW hr^{-1}) measured by Newell and Koch (2004). Both of these studies examine eastern oysters from the Choptank River, MD. Cerco and Noel (2005) calculate filtration rates from Jordan (1987) by dividing the measured biodeposition rates at varying water temperatures by the measured TSS concentrations (Cerco and Noel 2005). The functional relationship between these filtration rates and temperature reveal 0.55 m^3 g^{-1} oyster C day^{-1} at 27°C as the optimum value.

Similarly, Fulford et al. (2007) set the maximum at 0.55 m^3 g^{-1} oyster C day^{-1}, citing both Cerco and Noel (2005) and Newell and Langdon (1996), each with filtration rates originating from the Jordan (1987) empirical data. Unlike Cerco and Noel (2005), Fulford et al. (2007) alters this maximum rate by the size structure of a population. The individual *(i)* maximum filtration rate, $CR_{max(i)}$ (m^3 g^{-1} oyster C day^{-1}), for an individual of weight, $W_{(i)}$ (g DW), adapted from Newell and Langdon (1996), is:

$$CR_{\max(i)} = 0.55 * (W_{(i)})^{-0.28} \quad (8)$$

In other words, as weight increases, the maximum filtration per unit weight decreases (Newell and Langdon 1996). This is a common allometric function. Metabolic rates frequently scale with body size as a power function that exhibits quarter power scaling (Savage 2004).

Unlike the Cerco and Noel (2005) and Fulford et al. (2007) models, the Powell et al. (1992) model maximum filtration rate is dependent on both oyster

length, L (cm), and daily T (°C). The individual (j) maximum filtration, $FR_{max(j)}$ (mL individual^{-1} min^{-1}) is calculated as:

$$FR_{max(j)} = \frac{L_{(j)}{}^{0.96} T^{0.95}}{2.95} \quad (9)$$

(Powell et al. 1992). These filtration rates originated from a study by Doering and Oviatt (1986), which used mesocosm experiments with different sized *Mercenaria mercenaria*, hard shell clams, and calculated filtration based flow and ^{14}C concentration changes.

Figure 5a graphs Powell et al. (1992) individual maximum filtration rates (mL individual^{-1} min^{-1}) against temperature for three different lengths of oysters, representing 1, 2, and 3 year old oysters, showing increased filtration with increasing oyster size. For comparison to Cerco and Noel (2005) and Fulford et al. (2007) models, these filtration rates were converted to be biomass specific (m^3 g^{-1} oyster C day^{-1}) (See Appendix A for conversion), which are graphed against temperature in Figure 5b. With this normalization, the pattern of size with filtration rate is reversed. A 1 g DW, 7.62 cm, oyster at 27°C has a filtration rate of 0.16 m^3 g^{-1} oyster C day^{-1}, which is 3-4 fold lower than the 0.55 m^3 g^{-1} oyster C day^{-1} filtration of the other two models. Figure 5b also reveals that smaller oysters have a larger filtration rate per unit size than 0.16 m^3 g^{-1} oyster C day^{-1}. This non-linear change in filtration with size is a result of the power function in the filtration rate formulation (Equation 8).

The maximum filtration rate used for both Cerco and Noel (2005) and Fulford et al. (2007) both originate from oyster studies. Using the *M. mercenaria* maximum filtration rate, Powell et al. (1992) suggests that modeled filtration rates are often too high and unrealistic and are not continuously maintained. Yet, hard clams, which use

siphons (Doering and Oviatt 1986), and eastern oysters have different filtration rates. For example, Riisgard (1988) reports oyster filtration and clam filtration rates (L hr^{-1}) as $FR=6.79W^{0.73}$ and $FR=1.24W^{0.8}$ respectively, where W is g DW (Riisgard 1988).

Figure 6 graphs the filtration rate in the units of $m^3 g^{-1}$ organism C day^{-1} for clams and oysters using Riisgard (1988) and measured filtration rates from Newell and Koch (2004) at 25°C, corrected for 1 g DW of bivalve (See Appendix A for conversions). Oysters have much higher filtration rates than clams on a dry weight basis. This result informs my assessment that Powell et al. (1992) underestimate filtration rates simulated for oysters, a finding that conflicts with their conclusions.

3.1.2. Environmental Limitation Factors

The maximum filtration rates are affected by environmental limitation factors, each listed in Table 1. These limitation factors include temperature, salinity, TSS, and dissolved oxygen, which are normalized to give fractions between 0 and 1 and multiplied by the maximum filtration rate.

3.1.2.1. Temperature Limitation Factors

Oysters prefer higher temperatures for filtration. In a temperate climate, oysters are exposed to a broad range of water temperatures, which can have a great impact on filtration. Cerco and Noel (2005) and Fulford et al. (2007) employ the same function of temperature, or *f(T)*, as listed in Table 1 and graphed in Figure 7. Cerco and Noel (2005) formulate the *f(T)* by comparing filtration rates with temperature from the Newell and Koch (2004) and Jordan (1987) studies, and Fulford et al. (2007) acquire their *f(T)* from Cerco and Noel (2005).

The Powell et al. (1992) model has temperature as a component of the maximum filtration equation, as described previously and adopted from the study by Doering and Oviatt (1986), thus there is no standalone *f(T)*. The weight standardized filtration rates (m^3 g^{-1} oyster C day^{-1}) (See Appendix A for conversion) for 1 g DW or 7.62 cm oysters are graphed against temperature in Figure 7. Unlike the other models, the Powell et al. (1992) model does not have a decrease in filtration at higher temperatures. Rather, rates increase near linearly. Predicted filtration rates vary from 0 to above 0.2 m^3 g^{-1} oyster C day^{-1}, over a range of realistic water temperatures (Figure 7).

3.1.2.2. Salinity Limitation Factors

The *f(S)* selected for each of the models illustrates the general mechanistic response of oysters where higher salinities favor higher filtration rates. These salinity limitation functions are listed in Table 1, and vary from a single equation to stepwise functions. A comparison of the functional form of these limitation formulations is graphed in Figure 8.

The salinity limitation functions for each model are derived from different sources. Cerco and Noel (2005) adopt a formulation of *f(S)* found in other parts of the Chesapeake Bay Environmental Model Package for which the oyster model is a component, parameterized using the functional response with salinity reported by Loosanoff (1953). Powell et al. (1992) also cite Loosanoff (1953), where filtration begins decreasing below a salinity of 7.5 and ceases below a salinity of 3.5. Powell et al. (1992) then formulate a *f(S)*=0 for S less than 3.5, a *f(S)*=1 for S greater than 7.5,

and a linear increase from *f(S)*=0 to *f(S)*=1 between the salinities of 3.5 and 7.5. Fulford et al. (2007) cite R.I.E. Newell's unpublished data.

The models differ most in the mid-range salinities (4-12) where the increase from a *f(S)*=0 to a *f(S)*=1 occurs, shown in Figure 8. The model differences of these mid-range salinities are notable at a salinity of 7, where Cerco and Noel (2005) predict a *f(S)*=0.27, Fulford et al. (2007) a *f(S)*=0.51, and Powell et al. (1992) a *f(S)*=0.86. This near three-fold difference in predicted limitation effects deserves additional study.

3.1.2.3. Total Suspended Solids Limitation Factors

Very high and very low levels of particulate load or TSS decrease filtration. TSS consists of both inorganic and organic particles, and oysters feed on the phytoplankton that make up a portion of these organic particles. Low TSS indicates there is low availability of phytoplankton, so oysters decrease their feeding activity (Cerco and Noel 2005). At higher TSS levels, there may be physiological issues that decrease filtration (Loosanoff 1962) such as clogging of the gills (Newell and Langdon 1996).

The models' various *f(TSS)* equations are listed in Table 1 and graphed in Figure 9. Cerco and Noel (2005) use the Jordan (1987) biodeposition rates measured under varying TSS to formulate a general stepwise function. Fulford et al. (2007) formulate *f(TSS)* using results from Loosanoff (1962), which examined the effect of different concentrations and types of seston on the filtration of Long Island Sound oysters. Fulford et al. (2007) also cite Newell and Langdon (1996), who describe clearance rates that increase until TSS reaches about 25 mg L^{-1}, a conclusion that can

also be drawn from analyzing Jordan (1987) data. Powell et al. (1992) formulate the *f(TSS)* using Loosanoff and Tommers (1948), which is a brief article on silt effects on feeding, expanded upon in Loosanoff (1962), which the Fulford et al. (2007) model cites. In general, these studies all appear to depend on a few experiments that indicate minimum and saturating bounds to rates of filtration in response to suspended particle concentrations.

As seen in Figure 9, Fulford et al. (2007) and Cerco and Noel (2005) have similar responses of filtration to TSS up to a concentration of 25 mg L^{-1}, at which point the two functions diverge. Cerco and Noel (2005) eventually predicts a value of 0, while the function of Fulford et al. (2007) levels out around a value of 0.4.

Powell et al. (1992) do not have a low TSS negatively affecting filtration like the other models (Figure 9; Table 1). Rather, they use a logarithmically decreasing function, eventually mimicking that of Fulford et al. (2007) at higher TSS levels. The differences among all three models for *f(TSS)* is highlighted in Table 3, where different levels of TSS can have very different outcomes of *f(TSS)* depending on the model used.

3.1.2.4. Dissolved Oxygen Limitations

Oysters prefer higher levels of dissolved oxygen for feeding (Fulford et al. 2007; Cerco and Noel 2005). The Fulford et al. (2007) and Cerco and Noel (2005) models include dissolved oxygen limitations. The *f(DO)* equations for the two models are similar in formulation but differ in parameterization as listed in Table 1 and graphed Figure 10. Cerco and Noel (2005) took an equation from their benthos model to formulate *f(DO),* while Fulford et al. (2007) parameterized their *f(DO)* using

the study by Bayne (1971 a and b), which examined the responses of bivalve mollusks to dissolved oxygen.

3.1.3. 2009 Filtration Rate

The daily filtration rates for the three models were graphed for comparison in Figure 11, all showing a pattern of increased filtration during warmer months. The yearly pattern for Cerco and Noel (2005) and Fulford et al. (2007) are quite similar, with variability in the daily simulated output ranging between 0 and maximum values. In contrast, Powell et al. (1992) is substantially different than the other models, having 3-4 folds consistently lower filtration in the summer months and substantially less variability. The extremes in predicted filtration rates in the late spring and summer months for all the models are likely due to variability in the salinity forcing function.

I summed the daily filtration rates to obtain the total 2009 filtration ($m^3 g^{-1}$ oyster C), listed in Table 4. The total filtration for the Powell et al. (1992) model is about half that of the Cerco and Noel (2005) total. As shown in Figure 11, the Powell et al. (1992) model has higher filtration in the cooler months than the other models, so even though the maximum rate is 3-4 fold less than the other two models, the yearly filtration for Powell et al. (1992) is only about 2-folds lower. In terms of uptake capabilities, this may not result in more uptake due to low food particle concentrations associated with these cooler months.

3.1.4. Model Sensitivity Analysis

Two types of sensitivity were run with the three models, the first altering one environmental variable to be “high”, “intermediate”, and “low” levels, while keeping

other variables constant, and the second multiplying one environmental variable at a time by the maximum filtration, assuming other conditions were optimal. Sensitivity to these changes varied for the models depending on the environmental parameters tested. The main findings from the sensitivity analysis are listed in Table 6 for temperature, salinity, and TSS, and further explained here.

3.1.4.1. Temperature

Higher temperatures increased the filtration for all models, as expected from the *f(T)* definitions (Table 1). However, when temperature is too high, the Cerco and Noel (2005) and Fulford et al. (2007) models exhibit a dip in filtration, as depicted in Figure 12, which graphs the results of manipulating the field-based environmental forcing conditions to reflect low, intermediate, and high conditions for the Fulford et al. (2007) model.

3.1.4.2. Salinity

For Powell et al. (1992), there are only slight differences with changes in salinity. However, low salinity decreases filtration for both the Fulford et al. (2007) model and Cerco and Noel (2005) models as shown in Figure 13 that graphs the outcome of altering the forcing conditions.

To further isolate the effect of salinity on maximum filtration, Figure 14 examines the effect of this limitation factor on filtration rates while keeping the other factors at an optimal value of "1". It is clear that low salinity affected filtration between days 100 and 200 for the Fulford et al. (2007) and Cerco and Noel (2005) models. The limiting effect of salinity is greater for Cerco and Noel (2005) due to the steeper slope from $f(S)=1$ to $f(S)=0$ in the salinity limitation equation. This contrasts

with a second period of lower *f(S)* between days 300-365 for Fulford et al. (2007) that lowers filtration, which does not appear in the predictions of Cerco and Noel (2005). The *f(S)* slope for Fulford et al. (2007) affects a wider range of salinities, and during the days of 300-365, Cerco and Noel (2005) considers the S optimal and Fulford et al. (2007) does not.

3.1.4.3 Total Suspended Solids

When TSS was altered to be low, medium, and high, Powell et al. (1992) demonstrates a clear decrease in filtration with the increase in TSS (Figure 15), where the filtration rate for a 7.6 cm oyster is plotted over the time period of the simulation. Cerco and Noel (2005) and Fulford et al. (2007) show minimal changes in filtration rate in response to the TSS levels forced in this simulation exercise. When *f(TSS)* is only multiplied by the maximum filtration, some variability between Cerco and Noel (2005) and Fulford et al. (2007) are seen as shown in the sensitivity results in Figure 16. Generally, the TSS is in the optimal range for both the Cerco and Noel (2005) and Fulford et al. (2007) models, but there are some days with suboptimal TSS levels. These suboptimal days are more frequent when using the *f(TSS)* provided by Cerco and Noel (2005). In this instance, the suboptimal TSS levels are created from TSS concentrations that are at the lower threshold of the *f(TSS)* functions, and the difference between the number of days between the models was due to Cerco and Noel (2005) encompassing concentrations less than 5 mg L^{-1} in the low range while Fulford et al. (2007) has low concentrations as less than 4 mg L^{-1} (Table 1).

3.2 Filtration Rate Model

3.2.1. Individual-based Maximum Filtration Rate

The three models I assessed are examples of filtration rates in the literature, but other filtration rate empirical studies and models were also explored to more fully determine what might be the best way of simulating this process in oysters. A compilation of this literature review is presented in Table 5, listing those studies and models examining oyster filtration, including a range of filtration rates ($m^3 g^{-1}$ oyster C day^{-1}), maximum filtration rates ($m^3 g^{-1}$ oyster C day^{-1}) corrected for 1 g DW oysters (See Appendix A for conversions), the variable examined in the study, and the method of measurement.

The three models and the studies listed in Table 5 report a range of 0.08 to 0.54 for 1 g DW oyster maximum filtration rates ($m^3 g^{-1}$ oyster C day^{-1}). This is an extraordinarily wide range of values. Some of this variation may be attributed to the way the filtration rate is measured. Ideally, the methods should be similar as different methods can result in different calculated filtration rates, making comparisons of filtration rates problematic (Riisgard 2001). The most common approach to measure filtration is to examine changes in concentrations of particles. Also, changes in light attenuation, measured with irradiance sensors, have been used as an indicator of feeding activity (Newell and Koch 2004). The older studies in Table 5 (Loosanoff and Nomejko 1946 and Loosanoff 1958) used a kymograph, which is a recording mechanism that marks each time a certain volume of water is pumped by an oyster (Loosanoff and Engle 1947).

Another issue is that most filtration rates are measured in the lab, but *in situ* measurements may be different. Grizzle et al. (2008) found that filtration rates in the field were comparable to the Powell et al. (1992) and Riisgard (1988) models, but more variability was found in the field, so the rate *in situ* may be lower on average.

To find a maximum filtration rate for the purposes of this modeling effort, I calculated the mean maximum rate from the sources in Table 5 and the three models used in the comparison, excluding Comeau et al. (2008) that experimented with low temperatures and Gerritsen (1994), which looked at bivalves in general. This mean rate is calculated to be 0.34 m^3 g^{-1} oyster C day^{-1} for a market sized, 1 g DW oyster, comparable to the maximum rate in Riisgard (1988) (Table 5). For simplicity in modeling oyster filtration, this rate is translated from per g oyster C to per g DW (See Appendix A for conversions), converting the filtration rate to 0.17 m^3 g^{-1} DW day^{-1}.

Gape is assumed to be related to filtration, and I determine the weight exponent, *b*, in the equation $FR=aW^b$ from the relationship of dry weight and gape area, as graphed in Figure 17. Using a nonlinear least squares model in R (http://www.r-project.org/), the fitted model is $G = 501.76 * W^{.64862}$, also graphed in Figure 17. The calculated weight exponent, *b*, is thus 0.65, which is comparable to other allometric exponents found in the literature. Newell and Langdon (1996) report a value of 0.67 for oysters, originating from the gill proportion of the oyster, which decreases with oyster size. Rissgard (1998) report the exponent to be 0.73±0.22. Fulford et al. (2007) also adjust filtration rate on a weight basis (Equation 7). The exponent is negative in this case in order to have the filtration rate on a per weight basis of m^3 g^{-1} oyster C day^{-1} rather than m^3 day^{-1}. This formulation is also common

in the metabolic theory of ecology in which the exponent b has been found to fall between $^2/_3$ and 1, with $^3/_4$ being the standard and theoretically derived value (Sibly et al. 2013; Brown et al. 2004; Savage et al. 2004).

From these findings, the maximum filtration formulation of $FR=aW^b$ is parameterized using a value of 0.65 for the weight exponent, *b*, and the constant *a* is defined as the maximum filtration rate, 0.17 $m^3 g^{-1}$ DW day^{-1}. This can be used to determine the filtration rate of an individual of weight, *W* (g DW).

3.2.2. Limitation Factors

I assessed the limitation factors for which functions should be included in the new model. For this model, DO is assumed optimal and is not incorporated. The model comparison resulted in my conclusion that the temperature function needs to be modified from the Cerco and Noel (2005) and Fulford et al. (2007) models. These models have very low filtration in the winter months and high filtration in the summer, while Powell et al. (1992) has more filtration during the winter months than the other models. According to Comeau et al. (2008) (Table 5), at low temperatures, there should be some filtration. This is better represented by the Powell et al. (1992) predictions. Upon examining the filtration rates calculated by Cerco and Noel (2005) from the Jordan (1987) study, which Cerco and Noel (2005) used for their formulation and parameterization of equations, oysters exhibit a slightly higher filtration rate than Cerco and Noel (2005)'s *f(T)* approximated at lower temperatures. The *f(T)* is set to go to essentially 0 in the winter months by the models, but there is some filtration that continues to occur. On the other hand, this filtration change may

not lead to drastic uptake changes because food is limited in the winter months as well.

Given these considerations, I parameterized a new *f(T)*, using the Cerco and Noel (2005) and Fulford et al (2007) formulation for *f(T)*, for simplicity here referred to as Fulford et al. (2007). Figure 18 graphs the *f(T)* for Gerristen (1994) (Table 5), which reports general bioenergetics bivalve equations, and Fulford et al. (2007). Figure 18 also shows Loosanoff (1958) (Table 5) filtration rates, dependent on temperature, translated into fractions of the maximum rate. Upon examining these studies, each with varying temperature functions, the *f(T)* formulation was re-parameterized to give a new *f(T)* for the new model, also plotted in Figure 18:

$$f(T) = e^{(-0.006*(T-27)^2)} \quad (10)$$

Fulford et al. (2007) limitations for S and TSS (Table 1) will be incorporated in the new model. Roger Newell, an experienced oyster scientist, per personal communication with Fulford et al. (2007), set the salinity limitation. This *f(S)* captures more variability in filtration from salinity changes, and there are less drastic decreases in filtration, which occur using the Cerco and Noel (2005) model for salinities of 7 to 10.

The Fulford et al. (2007) TSS limitation combines the better components of the limitations of Cerco and Noel (2005) and Powell et al. (1992). There is no filtration at very low concentrations, in agreement with Cerco and Noel (2005), but it also incorporates a logistic decrease at higher concentrations, similar to Powell et al. (1992). High TSS can significantly decrease the filtration rate (Table 1; Figure 9), but this was not seen in the sensitivity analysis as the TSS did not reach these levels.

The Fulford et al. (2007) model's use of a logarithmic function after 25 mg L^{-1}, reaching a *f(TSS)* of about 0.4 for the higher TSS levels, would give less drastic effects on filtration than the Cerco and Noel (2005) model (Table 1; Figure 9).

3.2.3. Model Equations

Combining all the elements of the above analysis together, and assuming there is no limit on oxygen, results in an amended filtration rate model $FR_{(i)}$ (m^3 $oyster^{-1}$ day^{-1}) that includes limitation factors for T, S, and TSS for individual *(i)* of weight, *W* (g DW):

$$FR_{(i)} = 0.17 * W^{0.65} * f(T) * f(S) * f(TSS) \quad (11)$$

The environmental limitation equations include:

$$f(T) = e^{(-0.006*(T-27)^2)} \quad (12)$$

$f(S)$=0 when S<5; $0.0926 * S - 0.139$ when 5≤S≤12; 1 when S>12 (13)

(Fulford et al. 2007)

$f(TSS)$=0.1 when TSS<4 mg L^{-1}; 1 when 4≤TSS≤25 mg L^{-1}; (14)

$10.364 * \log(TSS)^{-2.0477}$ when TSS>25 mg L^{-1}

(Fulford et al. 2007)

4. CONCLUSION

The Cerco and Noel (2005), Fulford et al. (2007), and Powell et al. (1992) models are similar and different in their definitions of filtration rates, each with their own strengths and weaknesses. With this variety of filtration rate models comes the opportunity to entertain a "Goldilocks" assessment, selecting the best aspect of each formulation to promote evolution of our ability to better model oyster filtration rates.

Cerco and Noel (2004) and Fulford et al. (2007) had high maximum filtration rates in comparison to other literature values, while Powell et al. (1992) had a relatively low maximum filtration rate, which was based on clams, not the eastern oyster. Fulford et al. (2007) had the least drastic effects from S and TSS changes, in comparison to Cerco and Noel (2005). Fulford et al. (2007) and Cerco and Noel (2005) did not capture winter filtration with their *f(T),* while Powell et al. (1992) showed higher filtration in the cooler months.

Accurate filtration rates are imperative to understanding the impacts oysters can have on water quality, thus analysis of these models allowed us to delve into which components are best. From analysis of these models and a thorough literature search, I conclude this study by proposing a maximum filtration of 0.17 m^3 g^{-1} DW day^{-1} for a 1 g DW oyster.

This filtration rate should then be limited by a new *f(T)* (Equation 10), to account for more winter filtration, and the Fulford et al. (2007) limitation factors of *f(TSS)* and *f(S),* listed in Table 4. Along with a weight component, these components make up a new filtration rate model (Equations 11-14). In the next chapter, this filtration model will be combined with a particle model to calculate the particle capture capabilities of oysters.

LITERATURE CITED

Barrera-Escorcia, G., Vanegas-Perez, C., & Wong-Chang, I. (2012). Filtration rate, assimilation and assimilation efficiency in *Crassostrea virginica* (Gmelin) fed with *Tetraselmis suecica* under cadmium exposure. *Journal of Environmental Science and Health Part A, 45*, 14-22.

Bayne, B.L. (1971a) Oxygen consumption by three species of lamellibranch mollusk in declining ambient oxygen tension. *Comparative Biochemistry and Physiology A, 40*, 955-970.

Bayne, B.L. (1971b). Ventilation, the heart heat and oxygen uptake by *Mytilus edulis* in declining oxygen tension. *Comparative Biochemistry and Physiology A, 40*, 1065-1085.

Brown, J.H., Gillooly, J.F., Allen, A.P., Savage, V.M., & West, G.B. (2004). Toward a metabolic theory of ecology. *Ecology, 85* (7), 1771-1789.

Brush, M.J., Brawley, J.W., Nixon, S.W., & Kremer, J.N. (2002). Modeling phytoplankton production: problems with the Eppley curve and an empirical alternative. *Marine Ecology Progress Series, 238*, 31-45.

Cerco, C.F. & Noel, M.R. (2005). Evaluating ecosystem effects of oyster restoration in Chesapeake Bay. *A Report to the Maryland Department of Natural Resources*.

Chesapeake Bay Program (2009, Nov. 2). *Eastern Oyster*. Retrieved November 11, 2010, from Bay Field Guide: http://www.chesapeakebay.net/american_oyster.htm

Collier, A., Ray, S.M., Magnitzky, A.W., & Bell, J.O. (1953). Effect of dissolved organic substances on oysters. *Fishery Bulletin 84*, 54.

Comeau, L.A., Fabrice, P., Tremblay, R, Bates, S.S., & LeBlanc A. (2008). Comparison of eastern oyster (*Crassostrea virginica*) and blue mussel (*Mytilus edulis*) filtration rates at low temperature. *Canadian Technical Report of Fisheries and Aquatic Sciences 2810.*

Dame, R.F. (1972). The ecological energies of growth, respiration and assimilation in the intertidal American Oyster *Crassostrea virginica. Marine Biology, 17*, 243-250.

Doering, P.H. & Oviatt, C.A. (1986). Application of filtration rate models to field populations of bivalves: an assessment using experimental mesocosms. *Marine Ecology Progress Series, 31*, 265-275.

Fulford, R.S., Breitburg, D.L., Newell, R.I.E., Kemp, W. M., & Luckenbach, M. (2007). Effects of oyster population restoration strategies on phytoplankton biomass in Chesapeake Bay: A flexible modeling approach. *Marine Ecology Progress Series, 336*, 43-61.

Fulton, E.A., Smith, A.D.M., & Johnson, C.R. (2003). Effect of complexity on marine ecosystem models. *Marine Ecology Progress Series, 253*, 1-16.

Gerritsen, J., Holland, A.F., & Irvine, D.E. (1994). Suspension-feeding bivalves and the fate of primary production: An estuarine model applied to the Chesapeake Bay. *Estuaries, 17* (2), 403-416.

Grizzle, R.E., Greene, J.K., & Coen, L.D. (2008). Seston removal by natural and constructed intertidal eastern oyster (*Crassostrea virginica*) reefs: A comparison with previous laboratory studies, and the value of in situ methods. *Estuaries and Coasts, 31*, 1208-1220.

Gutierrez, J.L., Jones, C.G., Strayer, D.L, & Iribarne, O.O. (2003). Mollusks as ecosystem engineers: the role of shell production in aquatic habitats. *Oikos 101*, 79-90.

Jordan, S. (1987). Sedimentation and remineralization associated with biodeposition by the American oyster *Crassostrea virginica* (Gmelin). (Doctoral Dissertation). University of Maryland, College Park, Maryland.

Kemp, W. M., Boynton, W. R., Adolf, J. E., Boesch, D. F., Boicourt, W. C., Brush, G., et al. (2005). Eutrophication of Chesapeake Bay: Historical trends and ecological interactions. *Marine Ecology Progress Series, 303*, 1-29.

Langefoss, C. M. & Maurer D. (1975). Energy portioning in the American oyster, *Crassostrea virginica* (Gmelin). *Proceedings of the National Shellfisheries Association, 65*, 20-25.

Loosanoff, V.L. & Engle, J.B. (1947). Effect of different concentrations of micro-organisms on the feeding of oysters (*O. virginica*). *Fishery Bulletin 42, 51*, 31-57.

Loosanoff, V.L. & Nomejko C.A. (1946). Feeding of oysters in relation to tidal stages and to periods of light and darkness. *Biological Bulletin, 90*(3), 244-264.

Loosanoff, V.L. & Tommers, F.D. (1948). Effect of suspended silt and other substances on rate of feeding of oysters. *Science, 107*(2768), 69-70.

Loosanoff, V.L. (1953). Behavior of oysters in water of low salinities. *Proceedings of the National Shellfisheries Association, 43*, 135-151.

Loosanoff, V.L. (1958). Some aspects of behavior of oysters at different temperatures. *Biological Bulletin, 114*(1), 57-70.

Loosanoff, V.L. (1962). Effects of turbidity on some larval and adult bivalves. *Proceedings of the Fourteenth Annual Gulf and Caribbean Fisheries Institute, 14*, 80-94.

Maryland Department of Natural Resources. (1997). Report: Maryland's historic oyster bottom; A geographic representation of the traditional named oyster bars.

Newell R.I.E. & Langdon C.J. (1996) Mechanisms and physiology of larval and adult feeding. In: Kennedy V.S., Newell R.I.E, & Eble A. (eds) The eastern oyster *Crassostrea virginica*. Maryland Sea Grant College, College Park, MD, 185-230.

Newell, R.I.E & Koch, E.W. (2004). Modeling seagrass density and distribution in response to changes in turbidity stemming from bivalve filtration and seagrass sediment stabilization. *Estuaries, 27* (5), 793-806.

Newell, R.I.E. (1988). Ecological changes in Chesapeake Bay: Are they the result of overharvesting the American Oyster, *Crassostrea virginica*? *Understanding the Estuary: Advances in Chesapeake Bay Research. Chesapeake Research Consortium Publication 129*, 536-546.

Newell, R.I.E., Fisher, T.R., Holyoke, R.R., & Cornwell, J.C. (2005). Influence of eastern oysters on nitrogen and phosphorus regeneration in Chesapeake Bay, USA. In: Dame, R. & Olenin, S. (eds) The comparative roles of suspension feeders in ecosystems. NATO Science Series: IV-Earth and Environmental Sciences. Springer, Netherlands, 47, 93-120.

NOAA Fisheries Eastern Oyster Biological Review Team. (2007). Status review of the Eastern Oyster (Crassostrea virginica): Report to the National Marine Fisheries Service, Northeast Regional Office. *NOAA.*

Palmer, R.E. (1980). Behavioral and rhythmic aspects of filtration in the bay scallop, *Argopecten irradians concentricus* (Say), and the oyster, *Crassostrea virginica* (Gmelin). *Journal of Experimental Marine Biology and Ecology*, 45, 273-295.

Peters, R.H (1983). The ecological implications of body size. Cambridge University Press, New York, 1-23.

Powell, E.N, Hofmann, E.E., Klinck, J.M., & Ray, S.M. (1992). Modeling oyster populations I. A commentary on filtration rate. Is faster always better? *Journal of Shellfish Research, 11*(2), 387-398.

Powell, E.N, Hofmann, E.E., Klinck, J.M., & Ray, S.M. (1994). Modeling oyster populations IV: Rates of mortality, population crashes, and management. *Fishery Bulletin, 92*, 347-373.

Riisgard, H.U. (1988). Efficiency of particle retention and filtration rate in 6 species of Northeast American bivalves. *Marine Ecology Progress Series, 45* (3), 217-223.

Riisgard, H.U. (2001). On measurement of filtration rates in bivalves-the stony road to reliable data: review and interpretation. *Marine Ecology Progress Series, 211*, 275-291.

Ross, P.G., & Luckenbach, M.W. (2006). Relationships between shell height and dry tissue biomass for the eastern oyster (*Crassostrea virginica)*. 9th International Conference on Shellfish Restoration, Charleston, S.C. November 2006.

Savage, V.M., Gillooly, J.F., Brown, J.H., West, G.B., & Charnov, E.L. (2004). Effects of body size and temperature on population growth. *The American Naturalist, 163*(3), 429-441.

Sibly, R.M., Grimm, V., Martin, B.T., Johnston, A.S.A, Kulakowska, K, Topping, C.J., et al. (2013). Representing the acquisition and use of energy by inidviduals in agent-based models of animal populations. *Methods in Ecology and Evolution, 4*, 151-161.

Tamburri, M.N. & Zimmer-Faust, R.K. (1996). Suspension feeding: Basic mechanisms controlling recognition and ingestion of larvae. *Limnology and Oceanography, 41*(6), 1188-1197.

Ward, J.E., Newell, R.I.E., Thompson, R.J., & MacDonald, B.A. (1994). In vivo studies of suspension-feeding processes in the eastern oyster, *Crassostrea virginica* (Gmelin). *Biological Bulletin, 186*, 221-240.

Wilberg, M.J, Livings, M.E., Barkman, J.S., Morris, B.T., & Robinson, J.M. (2011). Overfishing, disease, habitat loss, and potential extirpation of oysters in upper Chesapeake Bay. *Marine Ecology Progress Series, 436*, 131-144.

Wilberg, M.J., Wiedenmann, J.R., & Robinson, J.M. (2013). Sustainable exploitation and management of autogenic ecosystem engineers: application to oysters in Chesapeake Bay. *Ecological Applications, 23*(4), 766-776.

TABLES

Function	Model: Cerco and Noel 2005	Model: Fulford et al. 2007	Model: Powell et al. 1992*
f(T)	$= e^{(-0.015*(T-27))}$	$= e^{(-0.015*(T-27))}$	Incorporated in maximum filtration with oyster length
f(TSS)	= 0.1 when TSS<5 g m^{-3} = 1.0 when 5≤TSS≤25 g m^{-3} = 0.2 when 25<TSS<100 g m^{-3} = 0.0 when TSS>100 g m^{-3}	= 0.1 when TSS<4 mg L^{-1} = 1 when 4≤TSS≤25 mg L^{-1} $= 10.364 * \ln(TSS)^{-2.0477}$ when TSS>25 mg L^{-1}	$= 1 - 0.01 * \frac{\log\left(\frac{TSS}{1000}\right) + 3.38}{0.0418}$
f(S)	$= 0.5 * (1 + \tanh(S - 7.5))$	= 0 when S<5 $= 0.0926 * S - 0.139$ when 5≤S≤12 = 1 when S>12	= 0 when S≤ 3.5 $= \frac{S-3.5}{4}$ when 3.5<S<7.5 = 1 when S≥ 7.5
f(DO)	$= \frac{1}{1 + e^{1.1*((1.0-DO)/(1.0-0.7))}}$	$= \frac{1}{1 + e^{1.1*((1.75-DO)/(1.75-1.5))}}$	N/A

Table 1. Environmental limitation factors for temperature (*f(T)*), salinity (*f(S)*), total suspended solids (*f(TSS)*), and dissolved oxygen (*f(DO)*) for the Cerco and Noel (2005), Fulford et al. (2007), and Powell et al. (1992) models. *f(S) came from Powell et al. (1994).

Environmental Variable	Low	High
T	0.93	1.07
TSS	0.625	1.6875
S	0.65	1.43

Table 2: Sensitivity analysis scaling factors. These factors were multiplied by the dataset used as forcing functions in the model to scale yearly environmental variables to be low and high.

Model	TSS		
	20 mg L^{-1}	30 mg L^{-1}	120 mg L^{-1}
Cerco and Noel 2005	1	0.2	0
Fulford et al. 2007	1	0.86	0.42
Powell et al. 1992	0.6	0.56	0.41

Table 3: Model comparison of calculated *f(TSS)*s for different TSS levels.

Model	2009 Total Filtration (m^3 g^{-1} oyster C)
Cerco and Noel (2005)	45.51
Fulford et al. (2007)	56.96
Powell et al. (1992)	22.59

Table 4. Model total yearly filtration rates (m^3 g^{-1} oyster C) for 2009 found from summation of daily filtration rates.

Source	Range of Filtration Rates ($m^3 g^{-1}$ oyster C day^{-1})	Oyster Size Given	Maximum Rate Standardized for 1 g DW ($m^3 g^{-1}$ oyster C day^{-1})	Measurement Method	Parameter Tested
Barrera-Escorcia et al. (2012)	0.02-0.07	1.38 g DW	0.08*	Change in algal cells using a Nebauer chamber	NA
Comeau et al. (2008)	0.01-0.12	77-84 mm (1.1 g DW)	0.12*	Change in particles using a Coulter Counter	T 0-9 °C
Gerritsen (1994)	0.24	1 g DW	0.24	Literature search	NA
Grizzle (2008)	0-0.48	36.1 mm (0.19 g DW)	0.30*	In situ cholropyll-a changes	None
Langefoss and Maurer (1975)	0.13-0.40	0.211-0.422 g DW	0.28*	Change in algal cells using a Coulter Counter	food content
Loosanoff (1958)	0-0.39	100-110 mm (1.99 g DW)	0.47*	Kymograph	T 2-38 °C
Loosanoof & Nomejko (1946)	0.32-0.46	4 inches (1.87 g DW)	0.54*	Dockside kymograph	tide and light
Newell et al. (2005)	0-0.46	1 g DW	0.46	Interpretation of Jordan (1987)	NA
Newell & Koch (2004)	0.04-0.46	corrected to 1 g DW	0.46	Change in light measurements	T 15-25 °C
Palmer (1980)	0-0.26	corrected to 1 g DW	0.26	Change in algal cells using a Coulter Counter	light and food type
Riisgard (1988)	0.33-0.69	0.063-0.994 g DW	0.33	Change in particles using a Coulter Counter	NA

() Calculated dry weight * Calculated 1 g DW filtration

Table 5. A review of oyster filtration rates**.** This table compiles filtration rates from a number of studies and includes the study's citation, filtration rate ($m^3 g^{-1}$ oyster C day^{-1}), oyster size, filtration rate standardized for a1 g DW oyster ($m^3 g^{-1}$ oyster C day^{-1}), method used to measure filtration rate, and the parameter tested in each study. Calculated dry weights and standardized filtration rates for 1 gram oysters are listed in parenthesis and indicated by a star respectively.

Parameter	Sensitivity Key Findings
T	• Increases in T cause increase in filtration for all models. • Cerco and Noel 2005 and Fulford et al. (2007) have a dip in filtration when T increased.
S	• Decreases in S decreased filtration for Cerco and Noel (2005) and Fulford et al. (2007). • Cerco and Noel (2005) had more dramatic decreases from low S. • Fulford et al. (2007) catches more variation in changing filtration when S was low.
TSS	• Powell et al. (1992) has decreased filtration with increased TSS. • TSS mostly stayed in the optimal range, even when altered, so only slight difference seen between Cerco and Noel (2005) and Fulford et al. (2007).

Table 6. Key findings from the sensitivity analysis of the Cerco and Noel (2005), Fulford et al. (2007), and Powell et al. (1992) models.

FIGURES

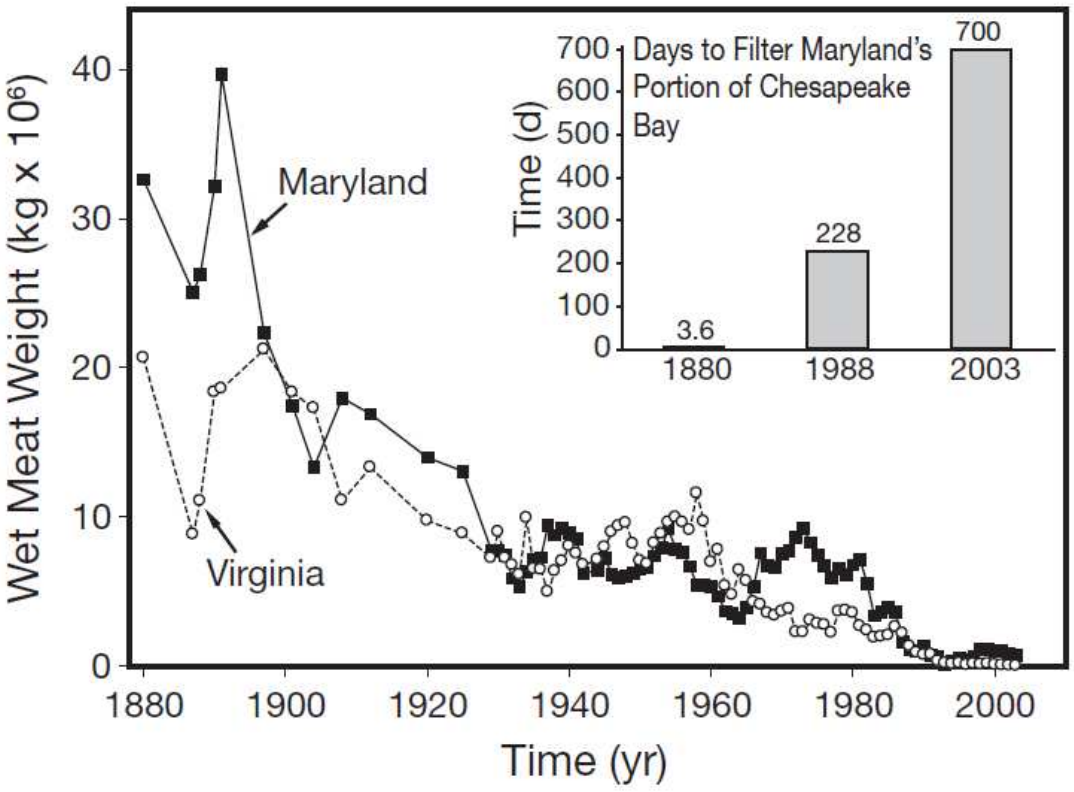

Figure 1. The harvest of the eastern oyster in Maryland and Virginia from 1880-2000 and the days it would take to filter a volume equivalent to that of Maryland's portion of the Bay (reproduced from Kemp et al. 2005; adapted from Newell 1988).

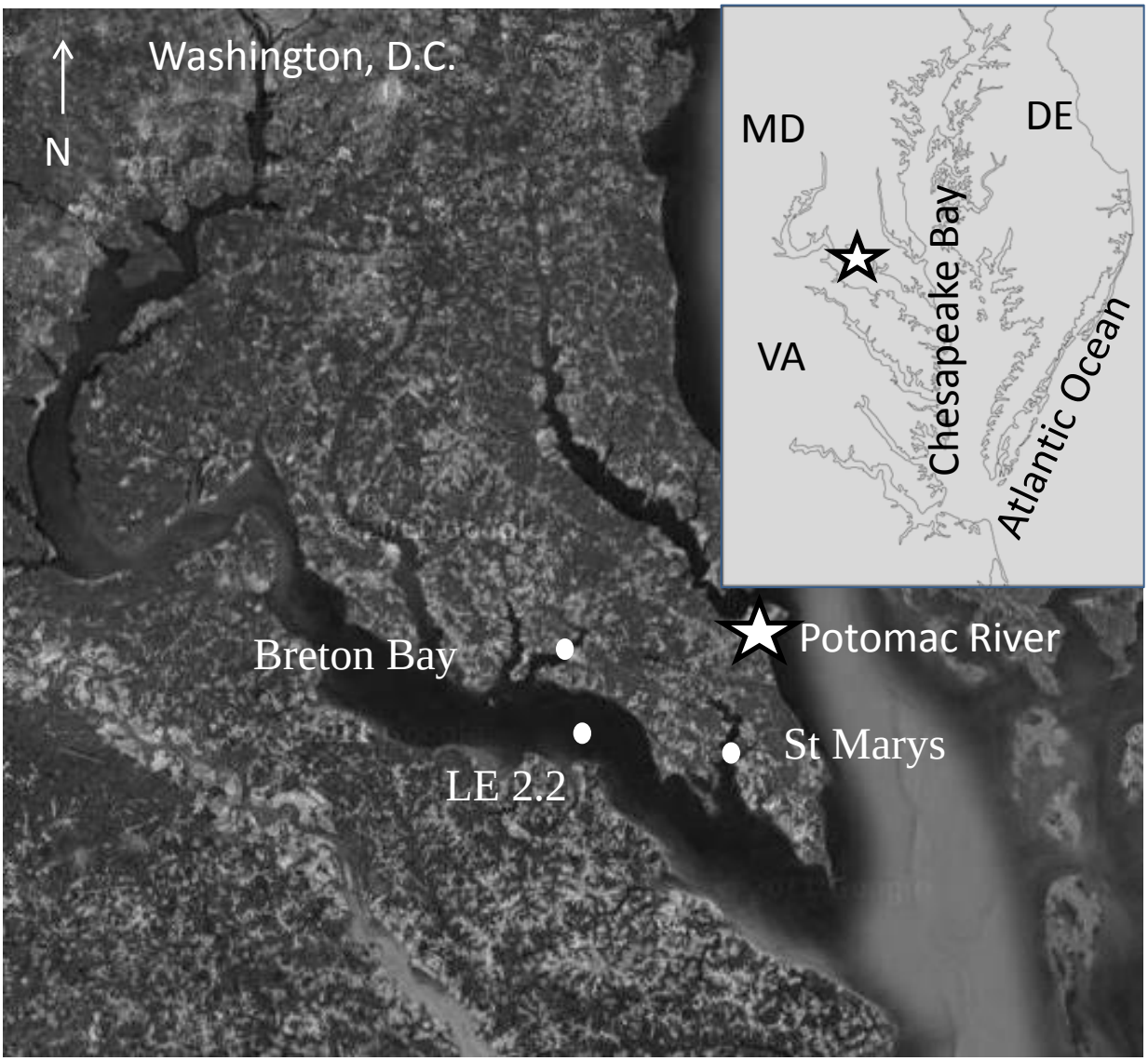

Figure 2. Locations of monitoring site LE2.2 and continuous monitoring sites St. Marys and Breton Bay.

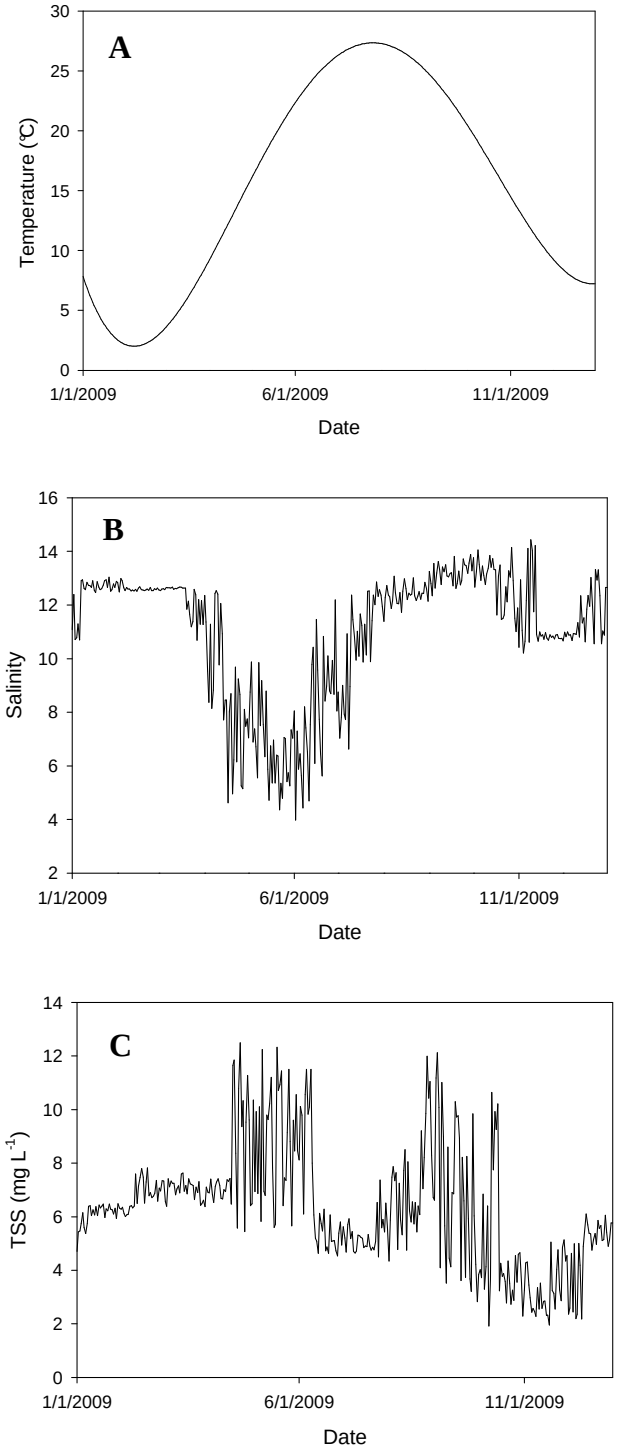

Figure 3. Extrapolated daily forcing functions for 2009 used for model simulations including (a) temperature (°C), (b) salinity, and (c) TSS (mg L^{-1}).

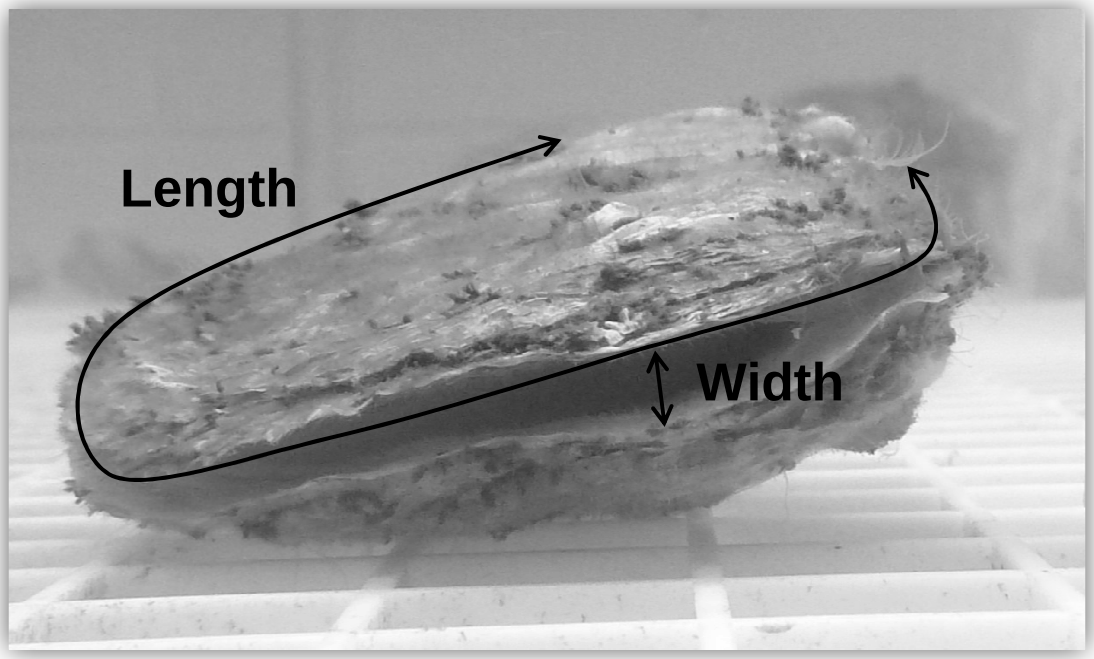

Figure 4. Laboratory length and maximum gape width measurements.

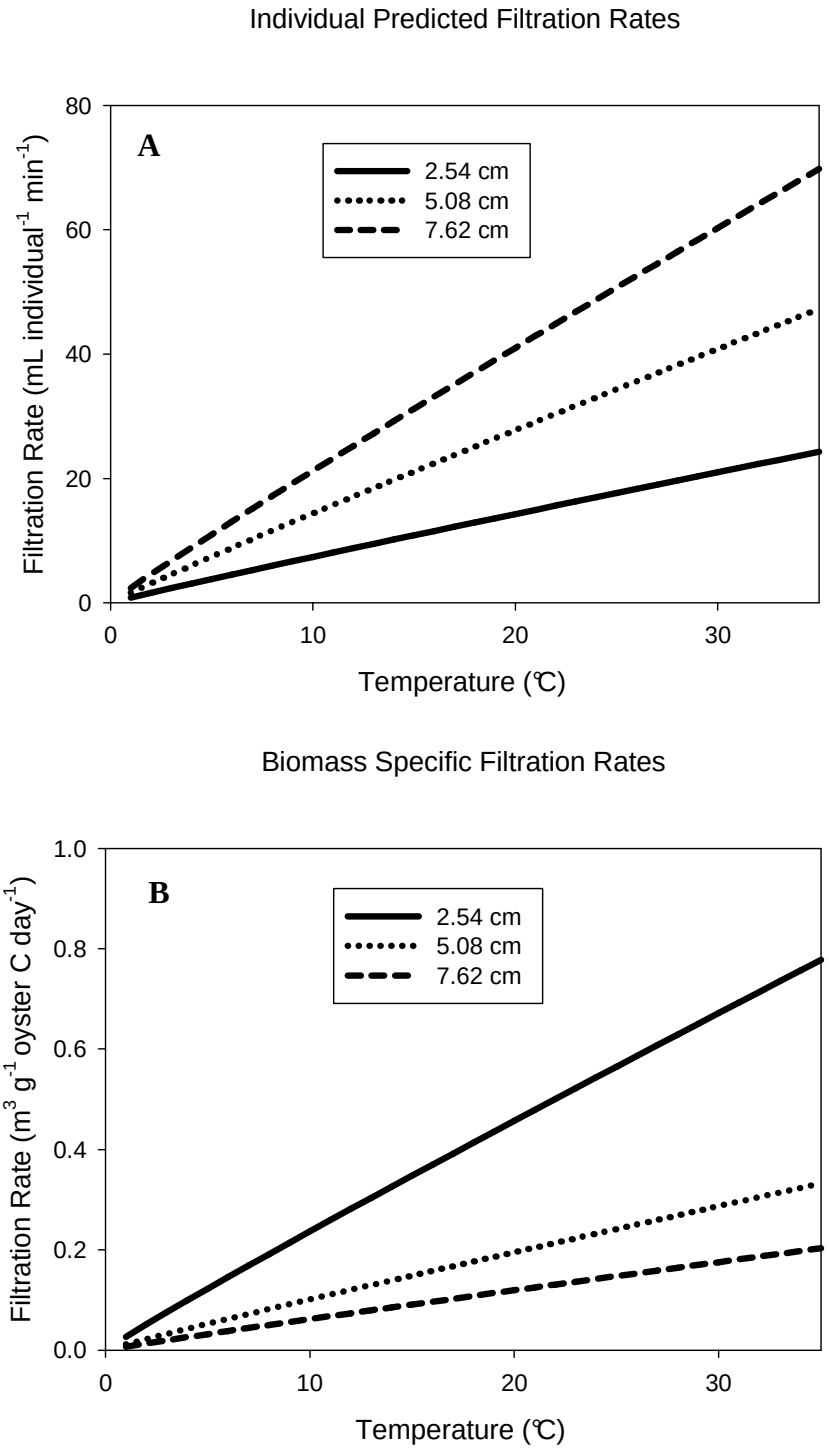

Figure 5. (a) Predicted individual maximum filtration rates (mL individual^{-1} min^{-1}) of the Powell et al. (1992) model for 1 inch (2.54 cm), 2 inch (5.08 cm), and 3 inch (7.62 cm) oysters and (b) filtration rates converted to biomass specific maximum filtration rates (m^3 g^{-1} oyster C day^{-1}) for the three oyster sizes.

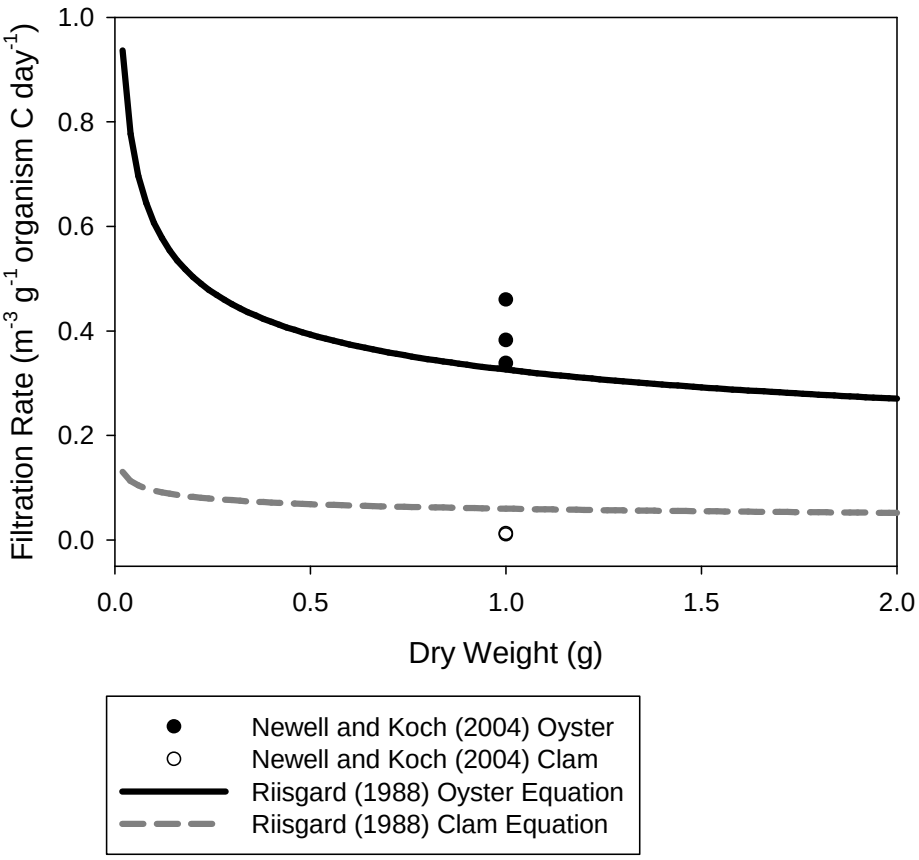

Figure 6. Comparison of predicted and measured filtration rates for oysters and clams. Regression lines of filtration rates for clams and oysters vs. the individual g DW by Riisgard (1988) and data points of filtration rates for 1 g DW oysters and clams at 25°C found by Newell and Koch (2004).

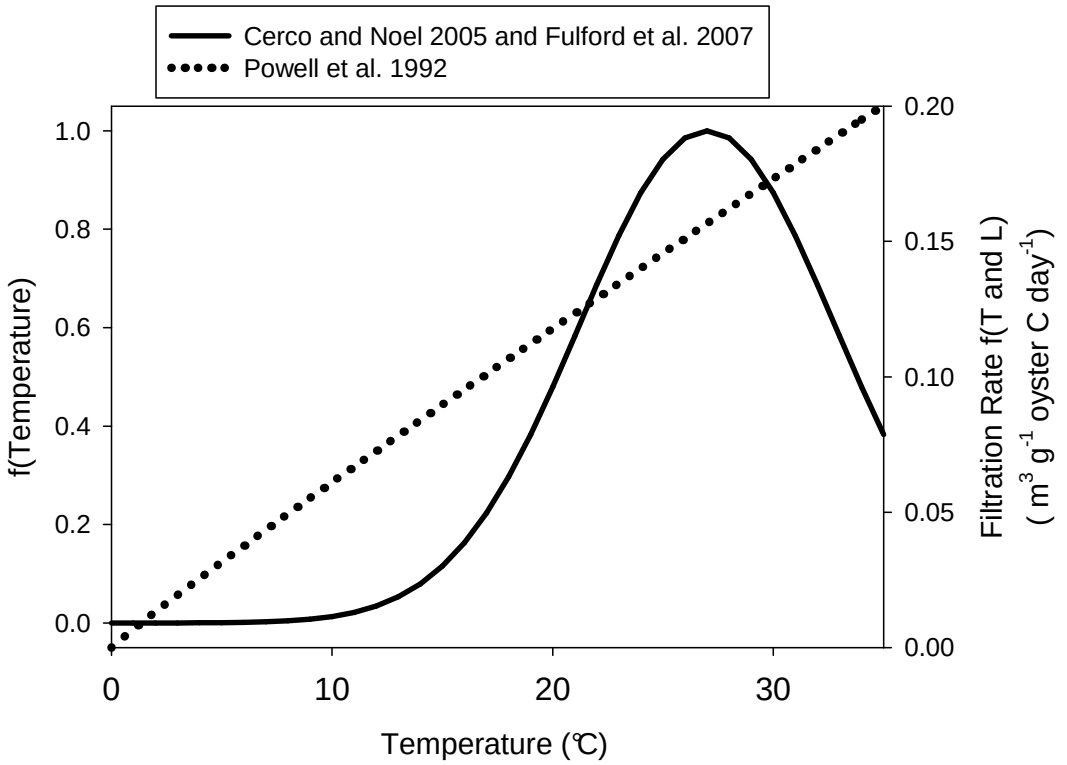

Figure 7. Model temperature limitation functions. The *f(T)* for the Cerco and Noel (2005) and Fulford et al. (2007) models, and the Powell et al. (1992) model's temperature dependent weight based filtration rate ($m^3\ g^{-1}$ oyster C day^{-1}) for a market sized oyster.

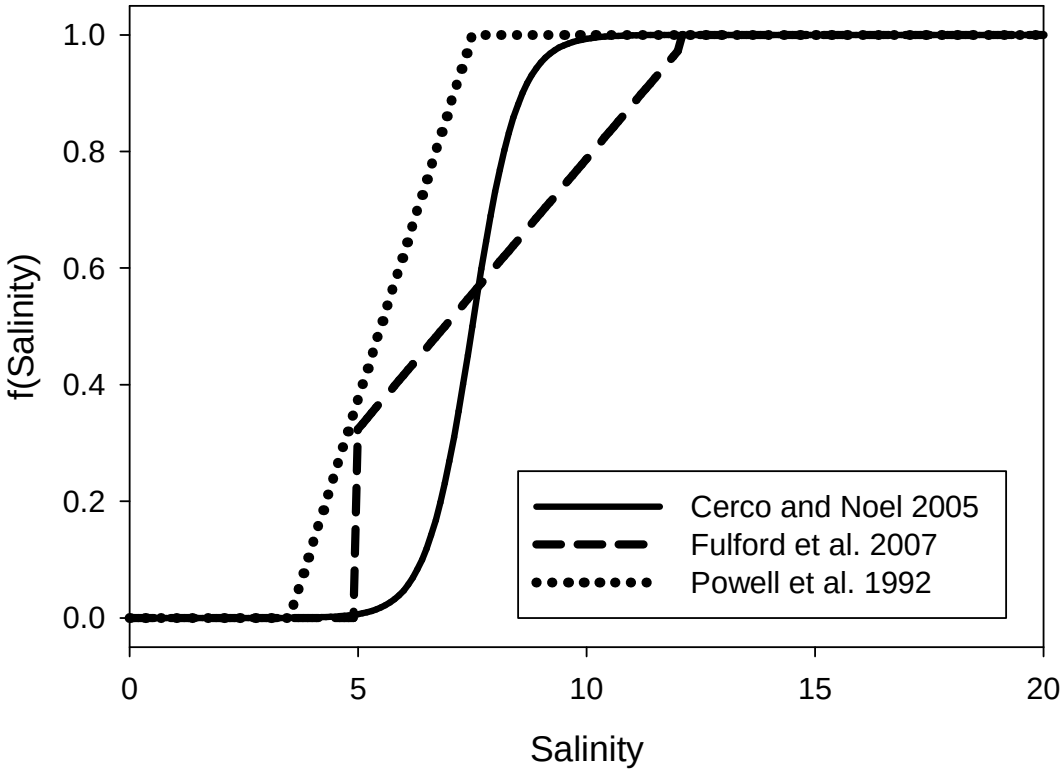

Figure 8. Model salinity limitation functions. The *f(S)* over different salinity ranges for the three different models.

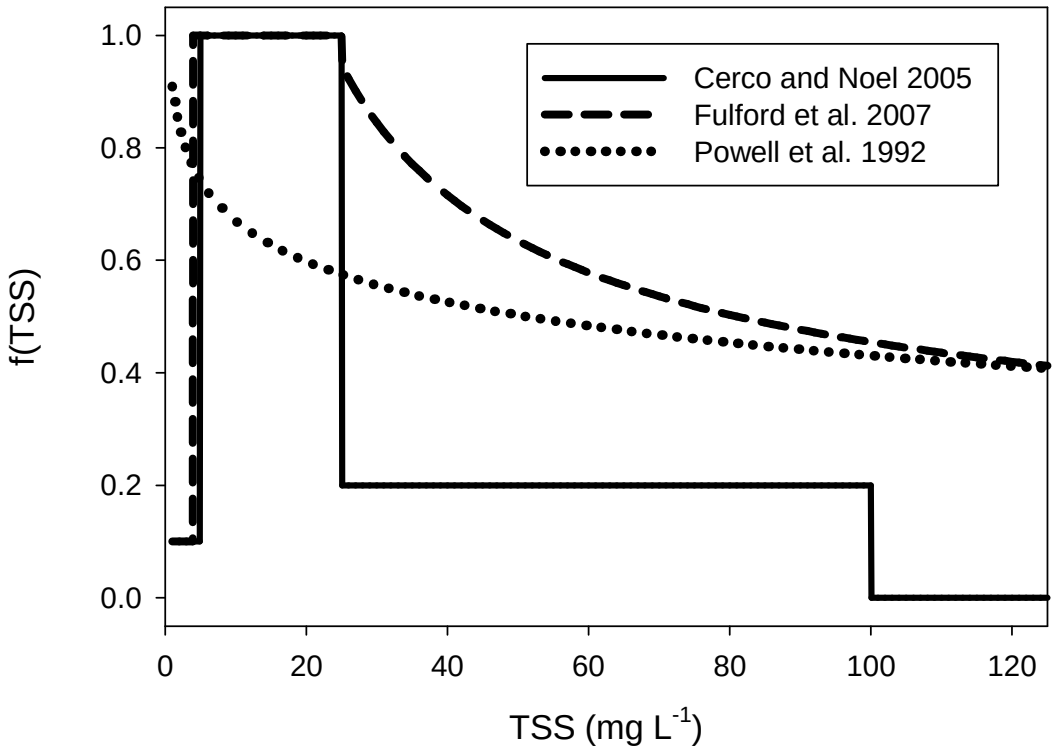

Figure 9. Model TSS limitation functions. The *f(TSS)* over different total suspended solid ranges for the three different models.

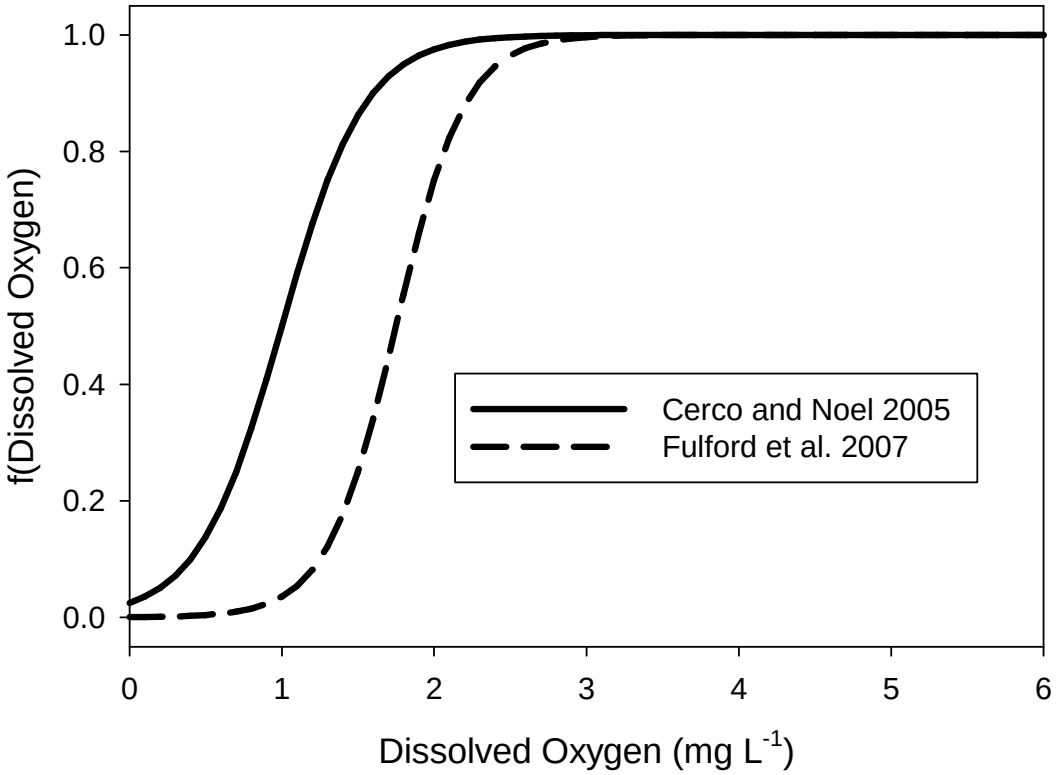

Figure 10. Model DO limitation functions. The *f(DO)*over a range of dissolved oxygens for the Cerco and Noel (2005) and Fulford et al. (2007) models.

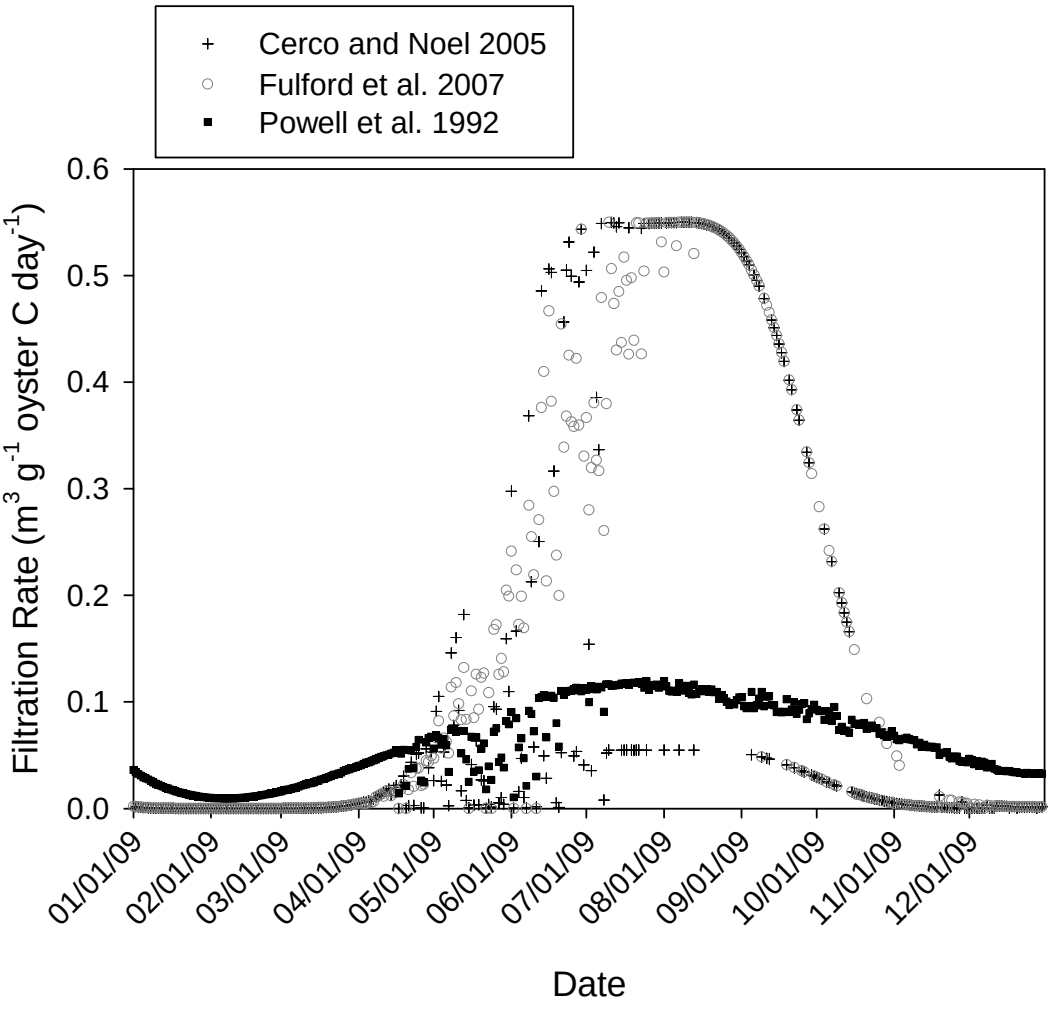

Figure 11. Simulated 2009 biomass specific daily filtration rates (m^3 g^{-1} oyster C day^{-1}) for each model.

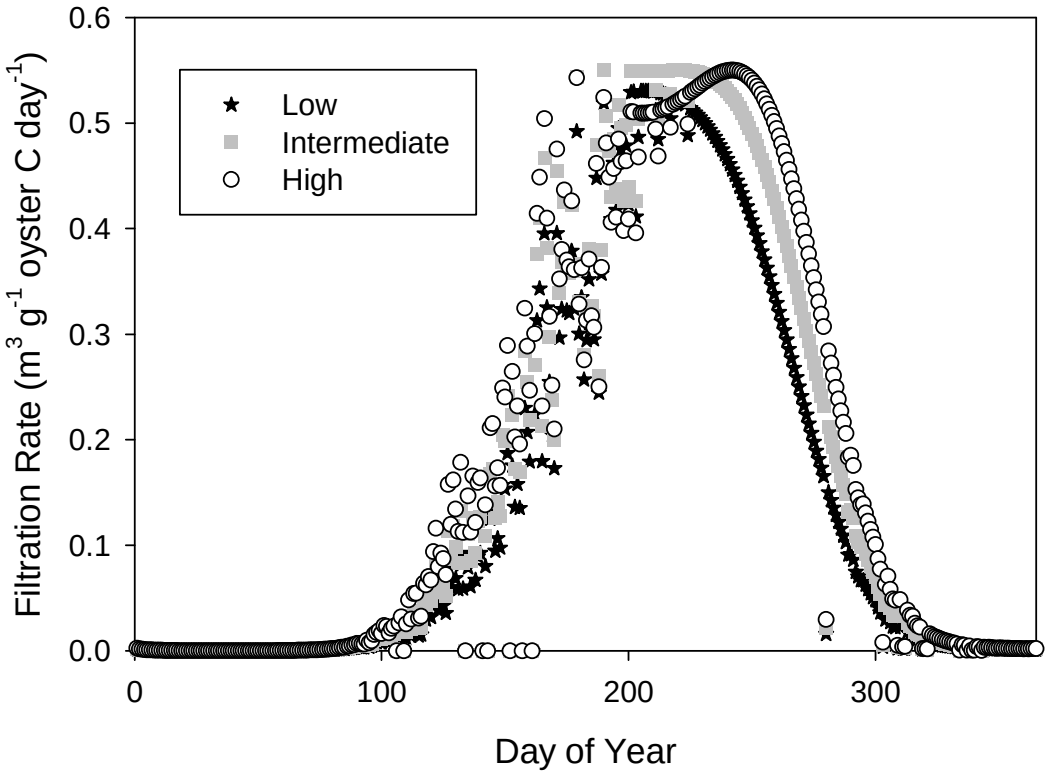

Figure 12. Sensitivity results of daily simulated filtration rates (m^3 g^{-1} oyster C day^{-1}) for the Fulford et al. (2007) model at three levels of T.

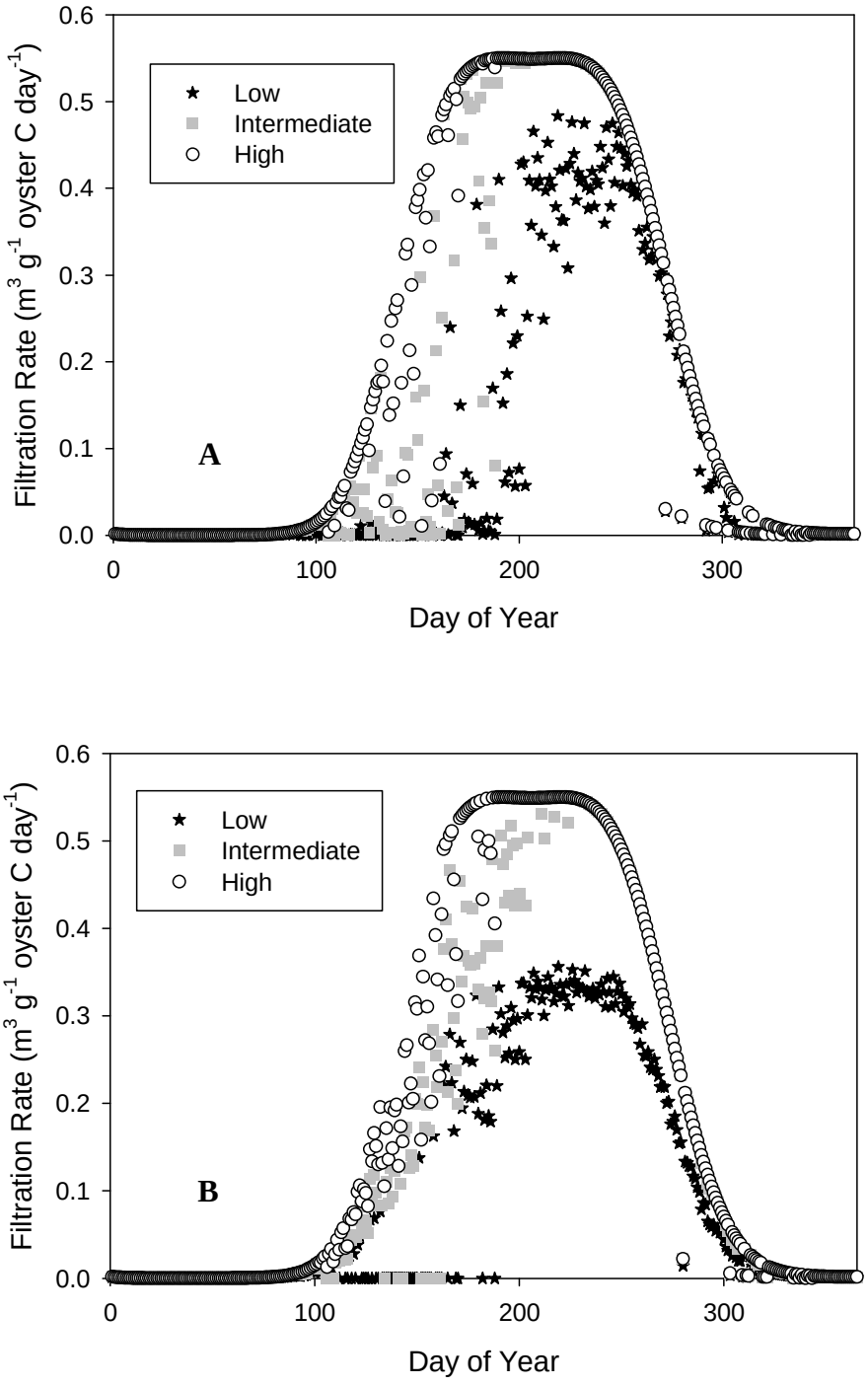

Figure 13. Sensitivity results of daily simulated filtration rates (m^3 g^{-1} oyster C day^{-1}) for the (a) Cerco and Noel (2005) and (b) Fulford et al. (2007) models at three levels of S.

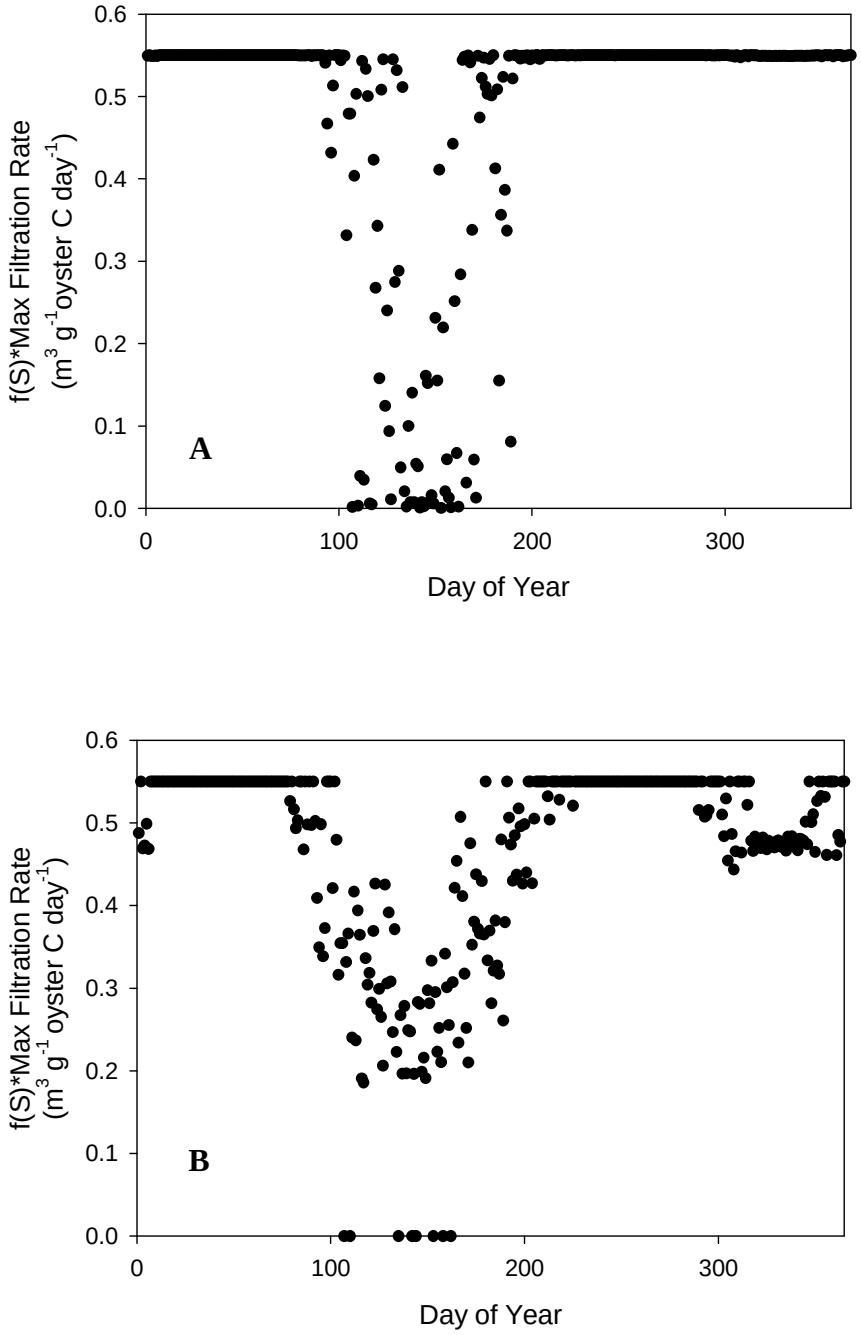

Figure 14. Sensitivity results of salinity influenced simulated filtration rates (m^3 g^{-1} oyster C day^{-1}) for the (a) Cerco and Noel (2005) and (b) Fulford et al. (2007) models.

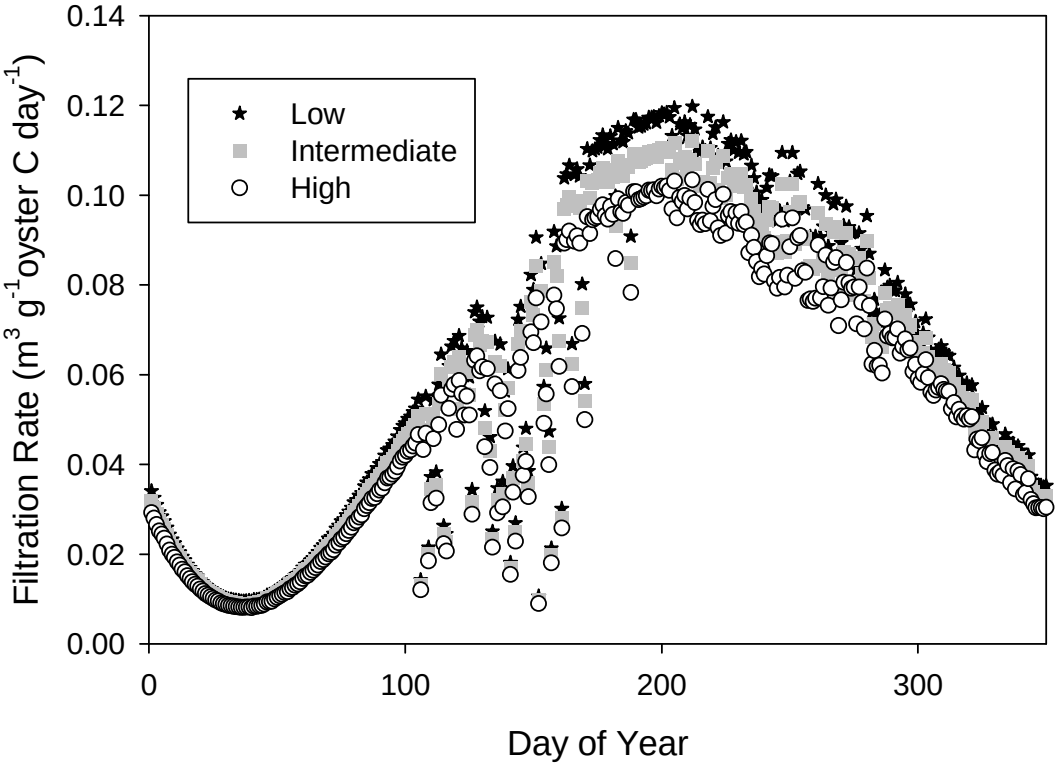

Figure 15. Sensitivity results of daily simulated filtration rates (m^3 g^{-1} oyster C day^{-1}) for the Powell et al. (1992) model at three levels of TSS.

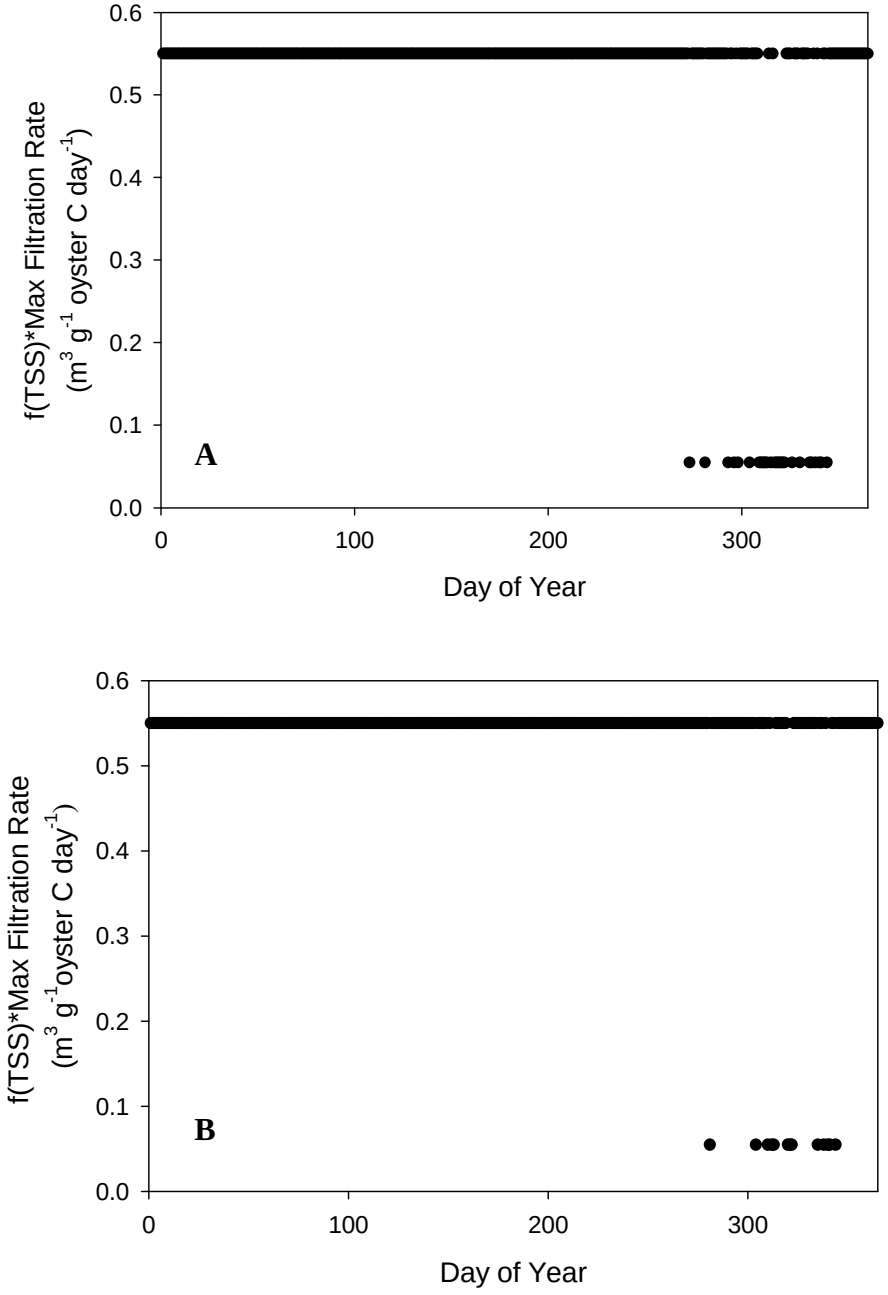

Figure 16. Sensitivity results of TSS influenced simulated filtration rates (m^3 g^{-1} oyster C day^{-1}) for the (a) Cerco and Noel (2005) and (b) Fulford et al. (2007) models.

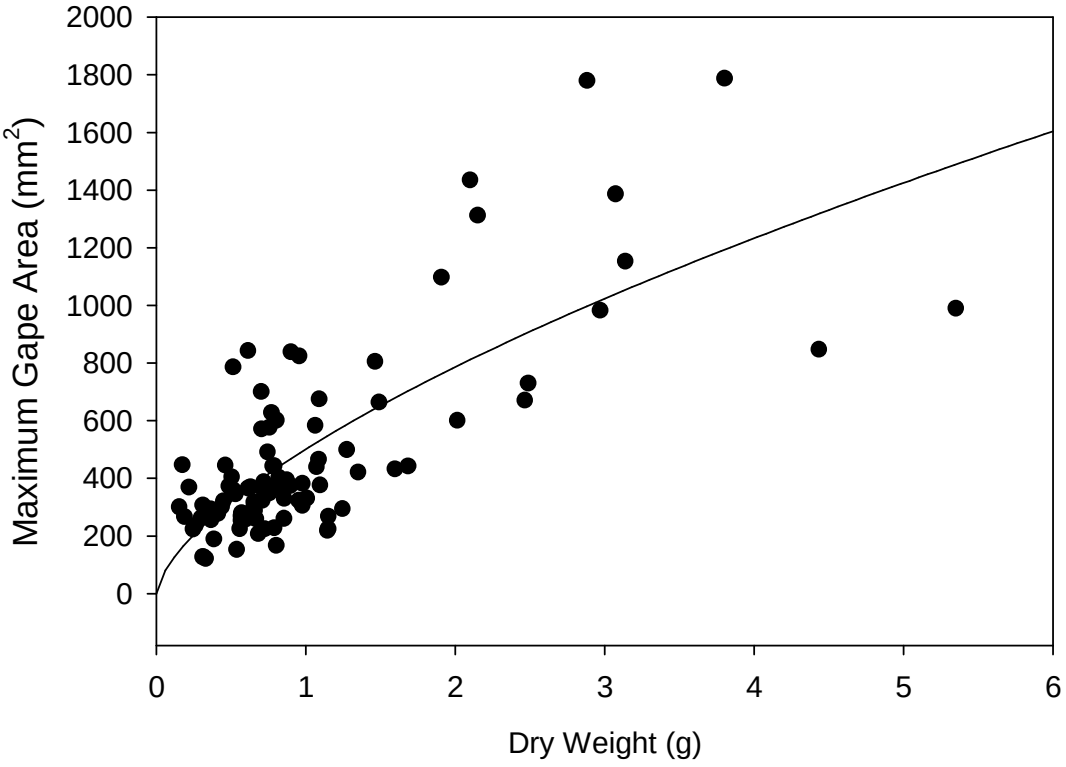

Figure 17. Laboratory dry weights and maximum gape areas and the power function model fitted to the data.

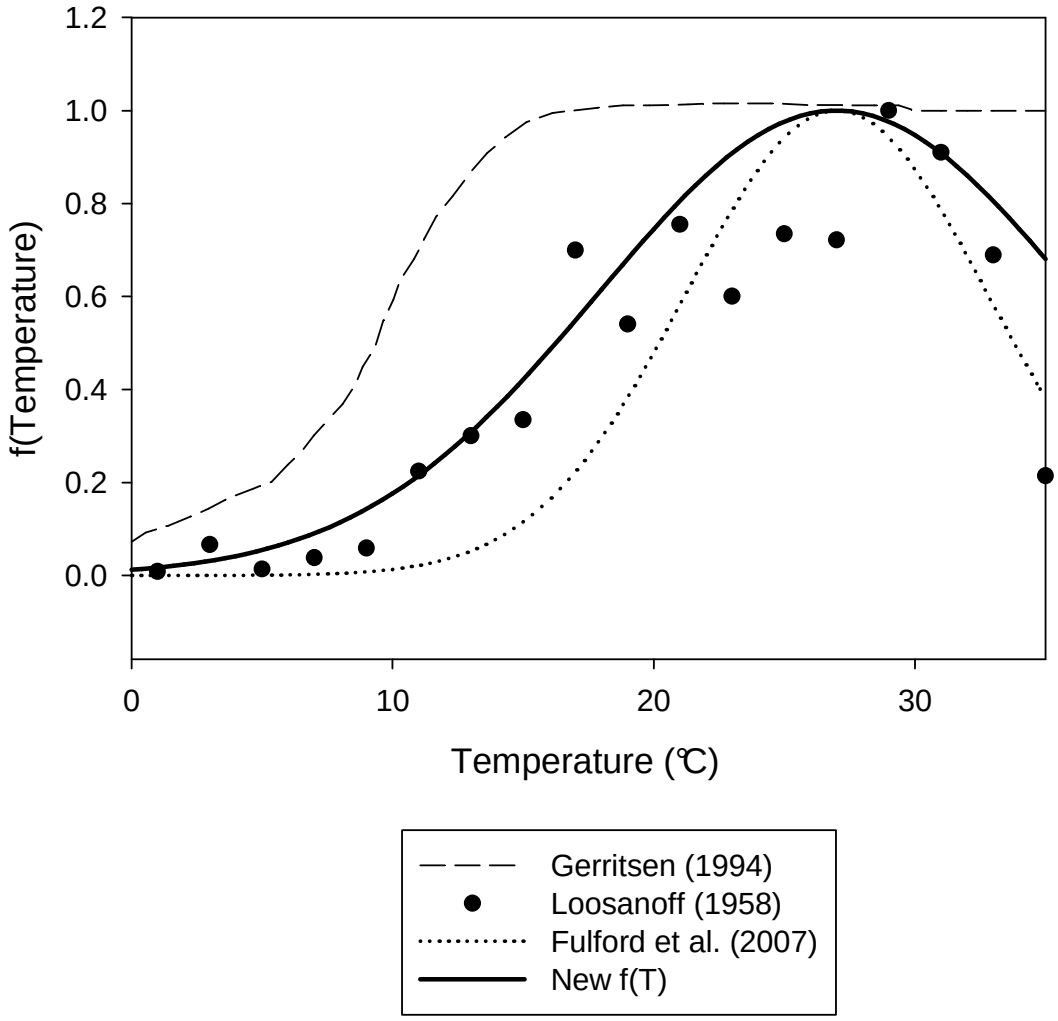

Figure 18. Comparison of temperature limitations, including the *f(T)* found in Gerristen (1994), Fulford et al. (2007), and Loosanoff (1958), and the new *f(T)*.

Chapter 2: Coupled Filtration Rate and Particle Models as Indicators of Supportive Oyster Reef Sizes

ABSTRACT

Restoration and aquaculture are amongst the management strategies used to increase populations of the filter-feeding eastern oyster, a depleted resource in Chesapeake Bay. The concentration of chlorophyll an oyster filters from the water column depends on both the individual filtration rate and the phytoplankton concentration of the overlying water. Particle availability to suspension feeders has been documented to decrease from the leading edge of the reef and create decreasing concentrations near the reef in comparison to the overlying water column. Here, two particle hydrodynamic models are used to account for these patterns, one describing advective flows, and the second and more complex model incorporating vertical diffusion and changes in velocity with water column height. A filtration rate model is then coupled with these two different particle models. Additional model complexity generates lower uptakes for the advection-diffusion model. Simulated results when using the advection-diffusion model indicate low velocities and high oyster densities lead to greater particle depletion. The use of the filtration rate model and the advection-diffusion particle model would be beneficial for both improving current models and determining sustainable reef sizes for restoration and aquaculture.

1. INTRODUCTION

Suspension feeders are important regulators of phytoplankton in aquatic ecosystems. Since these organisms are restricted in movement, feeding is dependent on both the individual filtration rate and delivery of phytoplankton particles to each organism. Environmental parameters such as salinity, temperature, and total suspended solids (TSS) affect the rate at which these organisms can filter the water column. Hydrodynamic conditions around a reef regulate particle transport, leading to changes in food availability or particle concentrations that may result in feedback effects on the filtration rate.

Phytoplankton concentrations above a bed of filter feeders depend on physical conditions of the water column and the effects of the organism itself in removing particulate organic matter. Particle gradients on reefs have been documented in many studies, especially those focusing on mussels, with widely reported findings of downstream reduction of particles (Wilson-Oromond et al. 1997; Butman et al. 1994) and depletion near the bed in comparison to the remaining water column (Butman et al. 1994; Jones et al. 2009; Petersen et al. 2013; Saurel et al. 2013; Wildish and Kristmanson 1984; Frechette et al. 1989). The removal of particles by upstream organisms combined with the magnitude of the water's velocity create these patterns, reducing the food availability to benthic feeders further from the leading edge of the reef.

The work of Butman et al. (1994) illustrates the patterns of hydrodynamic conditions and particle changes around mussels. In a flume experiment, Butman et al. (1994) measured fluorescence as a proxy for phytoplankton concentration, sampling

the water column at locations up- and down-stream of a bed of mussels under average flume velocity conditions of 5 cm s^{-1} and 15 cm s^{-1}. Velocity varied with water column height and decreased toward the mussel bed, creating a velocity structure following what is called the law of the wall, where velocity decreases logarithmically toward the substrate (Clauser 1956). The range of velocities along this vertical profile was greatest for the faster (15 cm s^{-1}) flume conditions due to this logarithmic change. For two experimental runs, ambient phytoplankton concentrations were used, while in a third experiment, cultured phytoplankton were added, thus increasing initial concentrations of particles. The experiment using cultured additions of phytoplankton produced results that were easier to interpret. Regardless of flume velocity conditions, fluorescence decreased downstream, with a significant difference in concentrations between the upper water column and the lower water column. For the higher velocity, measurements with a laser Doppler velocimeter (LDV) supported the observation that turbulent stress areas increased in height with distance downstream, here as a result of bottom roughness, indicating the growth of a boundary layer.

A boundary layer is an area where conditions near the substrate are different than the overlying water column. Turbulence, velocity changes, and biological effects can create these layers. Here, my reference to boundary layers should be understood as a concentration boundary layer. In this case, phytoplankton concentration is depleted in comparison to the above water column as a result of the velocity gradient and benthic feeding. From the leading edge of the reef, the thickness of this depleted layer increases in size (e.g. Wildish and Kristmanson 1984).

Understanding the relationships among suspended particle concentrations, hydrodynamic conditions, and feeding rates is important to informing our knowledge of the factors that affect feedbacks between shellfish and the aquatic ecosystem. Numerical modeling provides one tool for exploring these mechanisms. Most published models (Frechette et al. 1989; Petersen et al. 2013; Simpson 2007) describing particle gradients have been applied to mussels, but this approach has been limited for oyster reefs. In the Chesapeake Bay, the eastern oyster, *Crassostrea virginica*, is of interest in modeling efforts as part of restoration. The eastern oyster has declined from historic levels by 99.7% in the Chesapeake Bay (Wilberg et al. 2011), greatly affecting the ecological services provided, and also leading to a decline of the oyster fishery. Furthermore, the Chesapeake Bay has faced an influx of nutrients, concurrently degrading the water quality with decreasing oyster populations (Cerco and Noel 2007). Today, there is a large restoration effort underway, as well as an increase in aquaculture to restore both the seafood industry and improve water quality. Restoration efforts are being led by such organizations as the Chesapeake Bay Foundation (/www.cbf.org/oysters) and the Oyster Recovery Partnership (www.oysterrecovery.org/). To date, *C. virginica* models have focused on simulating oyster bioenergetics and growth (Cerco and Noel 2005; Cerco and Noel 2007), oyster standing stocks (Powell et al. 1992, Wilberg et al. 2011), larval transport (North et al. 2008), or the capacity of oyster populations to filter the water column and affect nutrient concentrations (Fulford et al. 2007).

Developing models that accurately describe particle concentrations across an oyster reef is fundamental to defining the food availability for existing, restored, or

farmed oysters, thus giving insight to the uptake capabilities of an oyster at a specific location. These models can also help to ensure a reef does not face large particle gradients.

As suspension feeders, oysters depend on the organic matter that makes up a portion of the suspended material that is transported over a reef for feeding and growth. Models calculating filtration and particle uptake often do not include hydrodynamic processes, including those developed by Cerco and Noel (2005), Fulford et al. (2007), and Powell et al. (1992). In these models, particle uptake is determined by multiplying an average, "ambient" particle concentration by the predicted filtration rate, without accounting for spatial changes of particle concentration across the reef. Therefore, these models may overestimate particle uptake, and often do not account for particle depletions away from reef edges.

The goal of this study is to establish a particle uptake model, accounting for phytoplankton gradients that are evidenced in other, empirical studies of clustering filter feeders (Butman et al. 1994; Jones et al. 2009; Petersen et al. 2013; Saurel et al. 2013; Wildish and Kristmanson 1984; Frechette et al. 1989). I couple an oyster filtration rate model with two different particle models of varying complexity, one incorporating horizontal, advective flows, and the second incorporating advective and diffusive vertical flows. The objectives of this modeling effort included assessing the impacts of increasing model complexity, formulating a model that predicts better oyster particle uptake in relation to hydrodynamic forcings, predicting where along a reef food limitation may occur, and presenting this model as a tool for planning restoration and aquaculture strategies.

2. METHODS

I established two particle models for use in conjunction with an individual-based filtration rate model. The first particle model adds advective flows, while the second, more complex model includes advection, vertical diffusion, and water column height-dependent velocity. Particle uptake was calculated using both models to assess the impact of added complexity, and additional simulations were run with the more complex, advection-diffusion model. Models were coded and simulations were run using Matlab R2012a, and these programs are included in Appendix B.

2.1. Modeling Overview

The general objective of this study was to create coupled physical-biological models describing the transport and uptake of particles across an oyster reef. I developed conceptual models to describe the two modeling approaches, pictured in Figures 1-3. The first diagram includes advective flows in the horizontal, *x*, direction (Figure 1), and the second has additional diffusive flows in the vertical, *z*, direction (Figure 2). Details describing fluxes for grid cells in the vertical direction in the advection-diffusion model are provided in Figure 3. Each of the models requires specification of grid cells to simulate flow and movement of particles in space. Flow was unidirectional for a 1 meter wide section of reef and divided into grid cells lengthwise, each with a length of *dx*, in the *x* direction, parallel to the flow. For the second model that incorporates diffusion, grid points were also included in the *z* direction, each with a height of *dz* (Figure 3). The depth of the water column was kept at 3 meters for both simulation frameworks.

Sizing of the grid cells was kept small enough to ensure stability of the steady state solution. Having the grid cells small enough inhibits mathematical oscillations and unrealistic results, which can occur when the grid cell size is too large. The stability criteria set for the advection model required that $dx < (0.5u_{bar}h)/FR$ where *FR* is the filtration rate, u_{bar} is current velocity, and *h* is water column depth. Mimicking the method of Hornberger and Wiberg (2005), the stability criteria for the advection-diffusion model was set to $dx < (dz^2u_z)/(5K_z)$, where u_z is the velocity at a given height, *z*, and K_z is the diffusivity at *z*. Keeping these limits in mind, the grid sizes for all simulations were smaller in size than the stability criteria defined for any of the selected conditions. The grid cell size was set at *dx*=0.1 m and the depth of the water column, *h*, for the advection model. The advection-diffusion model was parameterized with *dx*=0.1 m and *dz*=0.15 m.

2.2. Filtration Rate Model

Having an equation that accurately describes filtration rates of oysters is the first step in modeling oyster uptake, as this process represents a feedback on water column particle concentrations. Filtration rate is dependent on both oyster size and functions of temperature, salinity, and total suspended solids (TSS). The filtration rate (m^3 $oyster^{-1}$ day^{-1}) for an individual, described in more detail in Chapter 1, is

$$FR_{(i)} = 0.17 * W^{0.65} * f(T) * f(S) * f(TSS) \quad (1)$$

where W is oyster weight (g DW). The functions of the environmental variables, scaled between 0 and 1, are listed in Table 1.

Using Equation 1 to calculate individual filtration rate, $FR_{(i)}$ (m^3 $oyster^{-1}$ day^{-1}), the area-based filtration rate in units of cm^3 hr^{-1} cm^{-2} for a given grid cell location, x, becomes:

$$FR_x = [\sum FR_{(i)} * N_{(i)} \ ] * conversions \ (2)$$

where N is the density of individuals (oysters m^{-2}) in each size class *i*, with necessary conversions for FR_x from units of m^3 day^{-1} m^{-2} to cm^3 hr^{-1} cm^{-2}. The total filtration which occurs in a grid cell is then dependent on the area of the cell.

2.3. Particle Models

Both organic and inorganic particles are of importance to oyster feeding as phytoplankton provide nutrition, while inorganic particles can hinder filtration. In the models, I have chosen to use chlorophyll concentrations (*C*) as the main currency in simulating suspended particles, as my research questions in designing this modeling framework focuses predominantly on food availability. Because the filtration model requires estimates of TSS to determine whether filtration is being inhibited by especially high or low concentrations of material in the water column, the model also computes TSS, including inorganic and organic material, as a multiple of the chlorophyll concentration (*C*).

For each model, I programmed solutions to compute the time-independent steady states, using forward approximation to calculate outcomes of subsequent grid cells for chlorophyll concentration (*C*), TSS concentration, and filtration rate, *FR*. In these solutions, the concentration for one grid cell, $C_{x+1,}$ was dependent on the previous grid cell filtration rate, FR_x. For reference, the model variables are listed in Table 2.

2.3.1. Advection Model

The advection model adapts the approach of Wilson-Ormond et al. (1996), with food supply as a function of flow and filtration. As depicted in Figure 1, the entire height of the water column is available to oysters. The particle concentration advection model is governed by the differential equation (Wilson-Ormond et al. 1996):

$$\frac{dC}{dx} = -\frac{(FR_x * w * dx)}{u_{bar}V} C_x \quad (3)$$

Here, particle concentrations (C) are modeled with changing, horizontal distance (dx) across the reef as a function of filtration rate (FR_x), surface area of the grid cell ($w*dx$), velocity (u_{bar}), and grid cell volume (V). Discretization of this governing equation illustrates more clearly the way that this formulation simply models particle or chlorophyll movement:

$$C_x * A * u_{bar} = C_{x+1} * A * u_{bar} + C_x * FR_x * w * dx \quad (4)$$

Advected In Advected Out Filtered Out

A is the area of incoming and outgoing flow, which is depth (h) multiplied by cell width (w), while $w*dx$ is the flat surface area of the grid cell. The model is essentially a mass balance equation, computing inputs and outputs to and from a grid cell via advection and removal of particles from filtration. Rearranging and simplifying Equation 4 results in an equation for solving concentrations as particles move from one grid cell (C_x) to the adjacent, subsequent grid cell (C_{x+1}):

$$C_{x+1} = C_x \left(1 - \frac{FR_x * dx}{u_{bar} * h}\right) \quad (5)$$

This equation was used to implement the model, as detailed in the programming provided in Appendix B.

To link these transport processes to the filtration model, chlorophyll concentrations (*C*) must be converted to values of suspended solids, TSS (mg L^{-1}), to provide a feedback effect to the filtration rates down-reef. The concentration of the next grid cell, C_{x+1}, is multiplied by a set fraction to convert this concentration to TSS. This TSS_{x+1} value is then used to compute the filtration rate of the next grid, FR_{x+1} (Equation 1, Table 1 *f(TSS)*). I used a ratio of 1,309,916 TSS (mg L^{-1}) : 1 chlorophyll (mg cm^{-3}) in this conversion after examination of monitoring data in the lower Potomac River estuary.

2.3.2. Advection-Diffusion Model

The second model incorporates advection and diffusion, dividing a reef into grid cells in both the *x* and *z* direction as indicated in Figure 3. In this model, oyster feeding and changes in velocity with water column height, *z*, are included to create a particle gradient as illustrated in the conceptual diagram (Figure 2). No internal boundary layer (momentum boundary layer) is explicitly modeled, though the addition of this mechanism represents another potential component that could be included in the future. The oysters feed from the bottom grid cell only, or location *z*=1. TSS is calculated in these grid cells using the same conversion factor described for the advection model. Filtration rates respond to these concentrations as described by Table 1 (Equation 1, *f(TSS)*), with upper and lower thresholds to simulate the effect of TSS concentration.

The 2-D particle mass balance for any given grid cell can be described as:

$$\frac{\partial C}{\partial t} + \frac{\partial uC}{\partial x} + \frac{\partial wC}{\partial z} = \frac{\partial}{\partial z}\left(K_z \frac{\partial C}{\partial z}\right) + S \qquad (6)$$

S computed only in bottom cells

The governing equation includes terms for change in concentration with time $\left(\frac{\partial C}{\partial t}\right)$, advection $\left(\frac{\partial uC}{\partial x}\right)$, sinking$\left(\frac{\partial wC}{\partial z}\right)$, and vertical turbulent diffusion $\left(\frac{\partial}{\partial z}\left(K_z \frac{\partial C}{\partial z}\right)\right)$ (Frechette et al. 1989; Jones et al. 2008; Simpson 2007). In this case, *w* is the sinking velocity and *S* is the removal of particles from filtration. Concentrations are assumed to not vary with time, indicating no growth or changes to the phytoplankton supply over the reef, and sinking is assumed to be minimal, eliminating the $\frac{\partial C}{\partial t}$ and $\frac{\partial wc}{\partial z}$ terms (Frechette et al. 1989). These assumptions permit simplifying Equation 6 to Equation 7, which expands to Equation 8.

$$u_z \frac{\partial C}{\partial x} = \frac{\partial}{\partial z}\left(K_z \frac{\partial C}{\partial z}\right) + S \qquad (7)$$

S only in bottom cells

$$u_z \frac{\partial C}{\partial x} = \frac{\partial K_z}{\partial z}\frac{\partial C}{\partial z} + K_z \frac{\partial^2 C}{\partial z^2} + S \qquad (8)$$

S only in bottom cells

Following the example of Hornberger and Wiberg (2005) for expanding $\frac{\partial C}{\partial x}$ and $\frac{\partial^2 C}{\partial z^2}$, chlorophyll concentrations for given grid cells can be computed as indicated in Equation 9. This equation is then rearranged in Equation 10 to have *C* in the adjacent grid cell, or $C_{x+1,z}$, as the desired output.

$$u_z \frac{C_{x+1,z} - C_{x,z}}{\partial x} = \frac{\partial K_z}{\partial z}\frac{C_{x,z+1} - C_{x,z-1}}{2\partial z} + K_z \frac{C_{x,z+1} - 2C_{x,z} - C_{x,z-1}}{\partial z^2} + S \qquad (9)$$

S only in bottom cell

$$C_{x+1,z} = C_{x,z} + \frac{\partial x}{u_z}\begin{bmatrix} C_{x,z+1}\left(\frac{\partial K_z/\partial z}{2\partial z} + \frac{K_z}{\partial z^2}\right) + C_{x,z}\left(\frac{-2K_z}{\partial z^2}\right) \\ +C_{x,z-1}\left(\frac{-\partial K_z/\partial z}{2\partial z} + \frac{K_z}{\partial z^2}\right) - S \end{bmatrix} \quad (10)$$

S only in bottom cell

Velocity (u_z), vertical diffusivity (K_z), and thus the derivative $\left(\frac{\partial K_z}{\partial z}\right)$, vary with height ($z$) in the water column as depicted in Figure 3. Following the law of the wall with logarithmically increasing velocity; velocity at a given height (u_z) depends on the roughness parameter (z_0), and shear velocity (u_*), all defined in Equations 11 (Butman et al. 1994), 12 (L. Sanford, personal communication), and 13 (Butman et al. 1989; Frechette et al. 1989).

$$z_0 \approx \frac{oyster\ height}{30} \quad (11)$$

$$u_* = \frac{2u_{bar}(h - z_0)}{5\left(z_0 + h\left(\ln\left(\frac{h}{z_0}\right) - 1\right)\right)} \quad (12)$$

$$u_z = \frac{u_*}{0.4}\ln\left(\frac{z}{z_0}\right) \quad (13)$$

The vertical turbulent diffusivity (K_z) is calculated as a function of shear velocity as specified in Equation 14 (Jones et al. 2009; Simpson et al. 2007), and Equation 15 is the derivative of Equation 14, both necessary variables in Equation 10.

$$K_z = 0.4u_* z\left(1 - \frac{z}{h}\right) \quad (14)$$

$$\frac{\partial K_z}{\partial z} = 0.4u_*\left(1 - 2\frac{z}{h}\right) \quad (15)$$

Filtration only occurs in the bottom box, as indicated by *S*. At grid points where z=1, this term can be substituted by:

$$S = -C_{x,1}\left(\frac{FR_x}{\partial z}\right) \quad (16)$$

The removed chlorophyll is dependent on the concentration and the rate at which it is filtered. The *dz* accounts for the size of the given grid cell as FR_x is calculated in terms of per unit area ($cm^3\ hr^{-1}\ cm^{-2}$).

2.4. Boundary Conditions

The conditions in the first grid cell in the direction of flow (location x=1) are dependent on the outside particle concentrations. For both models, the initial filtration rate is dependent on the upstream, forced TSS concentration. This filtration rate is then used in the calculation of $C_{1,z}$ (or simply C_1 in the advection model) with the outside or initial concentration, C_0, as the upstream concentration. The upstream chlorophyll concentrations in the simulations are both comparable to and higher than those concentrations recorded, using a vertical profiler between August 14-18, 2013 around a depth of 2 meters, at Harris Creek, a site of ongoing oyster restoration (http://mddnr.chesapeakebay.net/eyesonthebay/profiler.cfm).

In the advection-diffusion model, boundary conditions are needed above and below the water column, since movement occurs in the vertical direction as well as the horizontal direction. A common approach of dealing with boundaries is to have no flux through the boundaries (Edelstein-Keshet 2005). Since no actual movement occurs at these boundaries and no particle concentrations exist at the top and bottom boundaries of the water column, a concentration was needed for the calculations that would prevent unrealistic fluxes at these locations. For the top grid calculation in Equation 10, the value of $C_{x,z}$ substitutes for $C_{x,z+1}$, and in the lower grid calculations, $C_{x,z}$ is substituted for $C_{x,\,z-1}$, thus creating zero flux.

2.5. Particle Uptake

Uptake (mg hr^{-1} grid $cell^{-1}$) is simply the summation of the particles (Equations 5 and 10) in each grid cell multiplied by the corresponding filtration rate (Equation 2), corrected for grid cell size, expressed as

$$Uptake_{x,1} = \sum [FR_{x,1} * w * dx]\, C_{x,1} \quad (17)$$

In the advection model, there is no *z* direction to consider. In the advection-diffusion model, this uptake is only calculated in the bottom grid cells (location *z*=1).

2.6. Simulations

These simulations are designed to numerically experiment with the models. Numerous questions could be applied to these models, and I focus on the following.

1. ***How do these models compare? Do the added factors of diffusivity and changing velocity affect the outcomes?***

To explore the extent to which complexity changes outputs, particle uptake was calculated for four simulations parameterized with the conditions listed in Table 3. These scenarios all took place over a 1 m wide by 10 m long simulated reef, changing the combinations of oyster density (50 and 700 oysters m^{-2}) and water velocity (34,000 and 3,400 cm hr^{-1}) values. A density of 50 oysters m^{-2} is comparable to restoration goals on natural oyster reefs according to the Oyster Metrics Workgroup (Allen et al. 2011). Aquaculture often uses floating bags to grow oysters, but these densities could be applied to the near bottom environment in a first cut to explore aquaculture conditions with these models. A density of 700 oysters m^{-2} was calculated from an aquaculture bag holding 200-250 market sized oysters, with the size of a bag described as a third of a square meter (Doiron 2008).

A velocity of 34,000 cm hr^{-1} was selected as it is likely in shallow regions of the Potomac River, where oysters are found. The second velocity is simply a magnitude lower. In the simulation, the beginning concentration of particles remained the same, with temperature, initial particle concentration (related to TSS as previously described), and salinity being optimal. The size of the oysters was also standardized with individual oysters weighing 1 g DW.

2. Using the advection-diffusion model, how does particle availability down reef vary in response to changed oyster density, water velocity, and oyster size?

Available particles for oysters in the final and bottom grid cell along a reef were compared to the initial particle concentration for oyster densities of 50 oysters m^{-2} and 700 oysters m^{-2} and velocities from Frechette et al. (1989) of 5 cm s^{-1}, 15 cm s^{-1}, and 30 cm s^{-1}. Frechette et al. (1989) parameterized their model with these values for simulating particles above a mussel reef. I ran the simulations for a 100 m long reef with an oyster size of 1 g DW. Environmental variables of salinity and temperature remained optimal, and the initial particle concentration was set at $18*10^{-6}$ mg chlorophyll-a cm^{-3}. The simulations were then run while keeping velocity constant at 15 cm s^{-1} and having oyster reefs with total biomasses of 50 g DW m^{-2} and 700 g DW m^{-2}. In this case, oyster sizes were changed to be 0.5, 1.0, or 1.5 g DW $oyster^{-1}$, with the total number of oysters changing to keep areal biomass constant.

3. How long can a reef be before TSS concentrations are too low for filtration?

I was interested in determining the size of a simulated reef could reach before particles were completely depleted. Because this size is likely a function of particle concentration and velocity, simulations were completed to compute particle uptake

for a wide range of these variables for both 700 oysters m^{-2} and 50 oysters m^{-2} using the advection-diffusion particle model. The velocities were chosen as the normal range of velocities that occur in the mainstream lower Potomac River from the NOAA Chesapeake Bay Interpretive Buoy System (http://buoybay.noaa.gov/). According to the filtration rate equations, oysters prefer TSS values between 4 and 25 mg L^{-1}, and the TSS values are proportional to chlorophyll concentration, *C*. The range of initial particles correlated to TSS values in a range just above and below the optimum range of concentrations for filtration. I programmed the model simulations so that the steady state solutions terminated at the length of the reef when the TSS reached below 4 mg L^{-1}, where oysters would lower their filtration rate. The oyster sizes were kept at 1 g DW, and salinity and temperature were held at optimum levels with only TSS affecting filtration.

4. How long can a reef be to minimize particle gradients to a 10% decrease from initial concentrations?

The same simulations were then run to calculate length and particle uptake with the objective of keeping particle gradients across a reef at a minimum. I adopted the objective of 10% or less difference between initial and final chlorophyll concentrations for an oyster bed after the approach of Bacher et al. (2003), a study which examined effects of particle gradients on scallops. When the percent difference between the initial concentration and the grid concentration hit above 10%, the steady-state solution was suspended at that location. The velocities ranged from 5-200*10^3 cm hr^{-1}, and the initial concentrations corresponded to TSS values of greater than 4 mg L^{-1} and higher, in this case, rather than also incorporating a value

lower than 4 mg L^{-1}. Again, oyster size remained 1 g DW, and salinity and temperature were held at optimal levels.

3. RESULTS

3.1. Model Complexity

Results of the simulations comparing model complexity (Table 3) indicate a clear difference between the two particle models. Overall, the more complex, advection-diffusion model simulated lower particle uptake rates, indicating lower particle availability for oysters. The magnitude of the difference between the simulated results of each model varied with oyster density and current speed. Particle uptake rate at specific reef locations and the total reef uptake are shown in Figures 4 through 7 for the four simulations described in Table 3.

When looking at simulated patterns of uptake with reef distance (Figures 4-7), the advection model results in uptake that decreases in a linear fashion with distance from the particle source, while the advection-diffusion model exhibits steeply decreasing uptake rates at the leading edge of the reef. Recall here that the advection-diffusion model divides the vertical water column into multiple grid cells, with particle removal through oyster filtration only in the bottom cell. In contrast, the advection model assumes filtration of the entire water column.

Output from the first simulation, using the higher oyster density and velocity, are shown in Figure 4. The advection-diffusion model results in a 33% decrease in total particle uptake, computed as the summation of the particle removal along the length of the reef. Using the same oyster density but lower velocity, the second simulation resulted in a steeper decrease of particle uptake rates along the axis of the

reef for the advection-diffusion model (Figure 5). Total computed particle removal for this simulation was 84% lower than that of the advection model. Figure 5 also displays the oscillatory behavior of the model when particle concentrations are close to the values that result in a declined filtration rate to 10% of the maximum filtration rate (Table 1 *f(TSS)).* The TSS limitation factor is formulated to have high (25 mg L^{-1}) and low (4 mg L^{-1}) cutoff concentrations. Empirical studies indicate these filter feeders reduce filtering at low TSS levels due to low particle availability (Cerco and Noel 2005) and at higher TSS levels due to physiological issues (Loosanoff 1962). In Figure 5, the TSS levels are fluctuating around 4 mg L^{-1}, and the oysters exhibit comparable shifts between maximum filtration and reduced filtration.

Resulting particle uptakes calculated from the third run, when the parameterization described a lower oyster density in conjunction with higher velocity, are shown in Figure 6. In this case, the differences between the two models are minor, with a 3% difference in total uptake between the advection and advection-diffusion model. For the final run, parameterized with both low oyster density and velocity, the advection-diffusion model output is, again, lower than that of the simpler advection model. These results are reported in Figure 7, with 26% less total particle uptake for the advection-diffusion model.

These simulations indicate that reefs with low velocities and/or higher oyster densities show a larger difference in model output between the two approaches. In addition to comparing model output for each of the simulations, it is clear from these results that oyster density can have a large impact on the magnitude of particle uptake and removal. The simulations with lower oyster densities resulted in rates that were

over an order of magnitude lower than those predicted by the high density simulations, regardless of current speed conditions or model complexity.

3.3.1. Particle Gradients

The two particle models illustrate two types of particle gradients. The advection model produces a gradual gradient of particles down reef, with concentrations invariant with height. An example of this is shown in Figure 8, using the simulation of higher oyster density and slower velocity conditions produced with the model comparison (Table 3, Run 2). In this figure, the concentration decreases across the reef with distance from the particle source, and the oysters are assumed to have access to the entire water column.

The advection-diffusion simulation produced a finer spatial gradient of particles. With this model, a concentration boundary layer emerges as a result of the advection-diffusion formulation that governs model output. An example of this boundary layer is pictured in Figure 9 using the higher oyster density and slower velocity conditions (Table 3, Run 2), the same conditions used for the results in Figure 8. The particle boundary increases in height with distance from the particle source at the edge of the reef. The particles in the upper water column are essentially unavailable to these oysters. Note here that the scale encompasses lower concentrations when using the advection-diffusion model (Figure 9) in comparison to the simpler advection model (Figure 8). Since a difference was found between the particle models, and because the advection-diffusion model provides more mechanistic detail that has been observed in empirical studies, the remaining simulated results were calculated with the higher complexity model.

3.2. Particle Availability Down-Reef

Figure 10 graphs the initial concentration of particles at the leading edge of a reef, along with the concentration in the final grid cell of a 100 m reef at the substrate (z=1) under varying conditions of velocity and oyster density. An oyster density of 50 oysters m^{-2}, with each oyster weighing 1 g DW, was used in the simulations pictured in Figure 10. For velocities of 5, 15, and 30 cm s^{-1}, particle concentrations at this location declined by 21%, 8%, and 4%, respectively. When oyster densities were increased to 700 oysters m^{-2}, again weighing 1 g DW, model output depicted a more dramatic particle concentration decline of 81%, 58%, and 40%, respectively, also graphed in Figure 10. Similar to the findings reported for the model comparisons, the greater oyster density and lower velocity conditions resulted in the largest particle changes across a reef and lower particle availability to oysters in subsequent grid cells.

In addition to velocity and density, oyster size can also affect particle availability down a reef. Figure 11 shows the effects of oyster size on particle availability over a 100 m reef when velocity is 15 cm s^{-1}. Here, the oyster biomass remained constant, with oyster size and density changing. The larger oysters had slightly more particles available to them after 100 m. As indicated in the filtration rate equation (Equation 1), filtration is scaled with oyster size, and smaller oysters are capable of filtering and removing more particles per their body size, in comparison to larger oysters, creating slight differences in reef particle removal.

3.3. Reef Size to Deplete TSS

As previously mentioned, oysters slow filtration when TSS levels are below 4 mg L^{-1}, indicating a depleted food source. When these particle levels are reached, the model depicts an oscillatory effect that occurs as diffusion replenishes particles to the bottom grid cells and then oysters deplete them again. This pattern was observed when oyster densities were high and velocity low in the model comparison (Figure 5). Simulations here calculated the length and total associated particle uptake at which TSS concentrations first reach less than 4 mg L^{-1}, where this modelled oscillation would begin to occur.

The initial particle concentrations and velocities were varied to identify the predicted lengths where low TSS first occurs as a function of these variables. Salinity and temperature remained optimal, and the population of oysters were assumed to be 1 g DW per individual. Figure 12a graphs the predicted reef length (m) to low TSS for an oyster density of 700 oysters m^{-2}. The total particle removals corresponding to these reef lengths are graphed in Figure 12b, computed as the sum of the particle uptake until the reef reached the low TSS values. Higher velocities and higher initial concentrations resulted in longer reefs and greater particle uptake, which is to be expected from the governing equations.

The same velocities and initial particle concentrations were then run with densities of 50 oysters m^{-2}, and these results are graphed in Figure 13. Comparing the results of the simulations in Figures 12a and 13a, the predicted reef sizes to low TSS levels were greater for the lower oyster density. This is a result of lower filtration occurring in a grid cell leading to less particle removal rates across a reef. In terms of

total uptake for these reefs sizes, the total particle uptake on less dense reefs is comparable to those reefs with higher oyster densities (Figure 12b and Figure 13b). The increased reef length was able to compensate for the lower per unit area filtration associated with the lower density.

3.4. Reef Size to Minimize Particle Gradient

While the previous exercise to determine a predicted reef length at which TSS concentrations decline to levels that essentially shut down filtration is informative, it is unlikely that a population of oysters could withstand such extreme food limitations. Additional analyses of the simulation output focused on determining the length of reef and associated particle uptake when initial input concentrations (C) was reduced by 10%. Again, varying velocities and initial particle concentrations were tested, while oyster size and environmental conditions remained the same as in the previous simulations. These results are plotted in Figure 14 for oyster densities of 700 oysters m^{-2} and Figure 15 for oyster densities of 50 oysters m^{-2}. Due to the lower total filtration in a given grid cell, lower densities of oysters support longer predicted reef lengths. The lower density in this case allowed for greater total particle uptake before a 10% particle decline difference, in comparison to the higher density (Figure 14b vs. Figure 15b).

Examining the differences between the reef sizes and uptakes until low TSS occurs and until a 10 % decrease in particles is observed offers additional insights. I compared the ratio of the two lengths for each different parameterization (a total of 210 simulations). The reef lengths at which the 10% gradient is reached are shorter than the reef lengths to low TSS. For all 210 simulations, I calculated the median of

this difference for the two oyster densities. The reef length where the predicted gradient reaches 10% was 354 times shorter when oyster density is 700 oysters m^{-2} and 22 times shorter when oyster density is 50 oysters m^{-2}, across all values of TSS and velocity tested. The total uptake decreases between the two reef sizes by a median difference of 154 fold for 700 oysters m^{-2} and 11 fold for 50 oysters m^{-2}. It is noteworthy that the difference between the two reef lengths is greater than the difference between the total uptake. This indicates that more uptake occurs at the edge of the reef, and the length and uptake are not linearly correlated, which was also indicated in the model comparison graphs (Figures 4-7) for the advection-diffusion model.

4. DISCUSSION

4.1. Complexity

Increasing the complexity of the particle model to include more mechanistic detail resulted in consistently lower particle uptake rates, with the magnitude of this difference dependent on the parameterization of forced mainstream velocity and oyster density values. The more complex, advection-diffusion model captured the hydrodynamic effects on particle concentration gradients and the emergence of a concentration boundary layer.

Empirical studies have documented this boundary layer above shellfish beds (Butman et al. 1994; Jones et al. 2009; Petersen et al. 2013; Saurel et al. 2013; Wildish and Kristmanson 1984; Frechette et al. 1989). For example, Wildish and Kristmanson et al. (1984) measured ATP and bacterial numbers at two heights above mussels in a flume, finding lower concentrations near the filter feeders. Jones et al.

(2009) found a similar pattern in their field experiment over a mixed species suspension feeding population, including clams, finding decreased chlorophyll-a near the substrate. Considering that these patterns were observed in field and flume conditions, and that the simulations in this study using the advection-diffusion model resulted in substantial differences in predicted uptake rates, I recommend including diffusion in coupled physical-biological models of *C. virginica*.

Model complexity could be further increased. For example, an internal boundary layer, also known as a momentum boundary layer, could be modeled. In this case, the velocity gradient with height would change across the reef as a result of substrate roughness and drag effects caused by the suspension feeders (Frechette et al. 1989). However, adding detail to parameterize at larger spatial scales complicates the use of this type of model, requiring more data, and therefore more effort. A trade-off exists between increasing complexity and meeting the objectives defined for using a model to address a given ecological question. Following the principle of Occam's razor, models should be kept the simplest for what is being described (Myung and Pitt 1997). The necessary complexity depends on the end goals of the user. The model is used for determining the limits of reef size that keep particle gradients low and describing the concentration of particles being removed from the water column, an important implication for improving water quality. Whether a momentum boundary layer is essential to accomplish this more accurately is a question future studies must balance against the added data requirements such a mechanism will require for application of the model.

4.2. Supporting Reef Size as a Function of Environmental Parameters

The morphology of reefs should be supportive of oyster growth to sustain a population over time. However, the optimal location for oyster growth is heterogeneous across the reef. As distance from the edge increased across a bed in a segmented flume, Rheault and Rice (1996) reported reduced oyster growth rate and condition index, where chlorophyll concentration was reduced from 100% to approximately 11% in the final chamber. As indicated by this potential change in oyster health and growth, environmental conditions can give an indication of supported reef size for a given area. A reef length where TSS regularly reaches a minimum value and slows filtration is not sustainable for *C. virginica*.

Comparison of the calculated reef sizes and current oyster reef sizes indicate that length does matter. Reefs are often measured in terms of total area (Kennedy and Sanford 1999; Maryland Department of Natural Resources 1997), lacking specific length and width dimensions. The oyster reefs in the Great Wicomico River, a restoration site in a tributary of the Chesapeake Bay, are as large as $7.16*10^4$ m^2 (Southworth et al. 2010). Though reefs are typically oblong (Kennedy and Sanford 1999), estimating dimensions assuming the reef is square results in lengths on the order of 200-300 m.

Using the results of the advection-diffusion model, it is possible to explore predicted, supportive reef lengths in the context of particle concentrations, oyster densities, and current velocity. This is not a bioenergetics growth model, so the effects of decreased food concentration with reef length are not assessed in terms of oyster growth. Instead, a 10% particle concentration decline, adopted from Bacher et

al. (2003), or less is chosen as a proxy for a thriving reef to avoid the changes to *C. virginica* health condition with decreasing food concentration documented by Rheault and Rice (1996).

According to Figure 14a, the simulated reef length to a 10% decline of particle availability is up to 14 meters when oyster density is 700 oysters m^{-2}. This value is the maximum predicted reef length from this series of simulations, modeled using the highest initial particle concentration and velocities. This length is substantially lower than 200 meters, the approximate length found in the Great Wicomico River. When the oyster density is 50 oysters m^{-2} and there are lower velocities simulated, the length to a 10% decrease in particles is comparable to the 200-300 meters found in the Great Wicomico study (Figure 15a). Figure 15a also shows that larger velocities and initial particle concentrations can lead to even longer reefs before a 10% decline in particles is observed. These velocities may be less common, as they are based on mainstream values. As reefs are typically in shallower areas, they experience slower velocities than the mainstream channel current (Allen 1985) and are thus susceptible to these lower velocities.

In addition to limiting food supply gradients, knowing if oysters are receiving an adequate food supply is important. Tenore and Dunstan (1973) report greatest food assimilation efficiency for oysters at concentrations of 300 μg C L^{-1}, with an increase in pseudofeces production above this level. Using a ratio of 42 C : 1 chlorophyll (Cloern et al. 1995; Brush et al. 2005), this can be converted into chlorophyll units as $7.14*10^{-6}$ mg cm^{-3} to arrive at the approximate concentration oysters for optimal assimilation efficiency. Concentrations below these levels were

reached in a few simulation scenarios as seen in the boundary layer concentrations in Figure 9, and the final concentrations for Figures 10 and 11. These low chlorophyll concentration areas should be avoided as they may not provide sufficient food.

Other processes excluded from this model may help to sustain longer reef lengths than those predicted here. In the advection-diffusion model, the $\frac{dC}{dt}$ term was removed (see Equation 6 vs. Equation 7) because the concentration of phytoplankton was assumed to not change with time, but this is not likely. Nutrient increases have been documented near reefs, likely stimulating *in situ* primary production as a result of increased remineralization facilitated by the oyster reefs themselves. Petersen et al. (2013) documented increasing NH_4 near mussel beds, a result of biodeposition. Another study by Kellogg et al. (2013), calculated the nitrogen fluxes above restored oyster beds and found higher fluxes of NH_4 compared to a control site, as well as increased rates of denitrification. Exploring whether these nitrogen recycling processes balance the loss of nitrogen through denitrification to result in increased primary production would be a worthwhile modeling exercise to explore, especially given the results found here.

4.3. Insights for Restoration and Aquaculture

Both restoration and aquaculture are ongoing efforts in Chesapeake Bay. The main restoration technique is to create or find sites of hard substrate for oyster larvae to settle on, as oysters permanently cement to a surface. Often, spat-on-shell, or juvenile oysters, are also deposited on these sites (http://chesapeakebay.noaa.gov/oysters/technical-aspects-of-oyster-restoration). In aquaculture, oysters can be grown in cages or bags, which protect the oysters from predators, either near an estuary

bottom or supported at the surface with floats (http://chesapeakebay.noaa.gov/fish-facts/oysters).

In order to have a thriving and growing population of oysters, restored oyster reefs and aquaculture should keep gradients of food particles at a minimum across a reef while also maintaining the magnitude of particle concentrations at a level sufficient for growth. The advection-diffusion model developed here can be used to calculate these associated reef lengths and concentrations. If there is a potential restoration site, the velocity could be measured with a laser Doppler velocimeter (LDV) at varying water column heights (e.g. Butman et al. 1994), and upstream chlorophyll could be measured with a sonde. Then, the appropriate reef length, parallel to the dominant direction of flow, can be calculated with the model and implemented at the site in the restoration effort. Since the modeled length is considered to be the length parallel to the unidirectional flow, and the width is simply 1 meter, the output of this model describes a section of the reef. This section of reef (1 m*reef length) could be extended in the direction that is perpendicular to the flow, extending the width of the reef, as long as flow conditions remain constant. I recognize that flow directions can vary, making the solution more complex. If anything, the unidirectional, simpler flow conditions in the model presented here provide a more conservative estimate of particle transport, and as such provide predictions for initial siting and design that will likely fall well within the optimum particle gradients for a given site.

Alternatively, if a restoration or aquaculture effort is constrained by costs to a specific acreage, the hybrid particle transport and filtration rate model can be used to

determine the optimal environmental conditions conducive for oyster filtration rates and particle uptake that support growth. For example, in the case of a project that is budgeted to restore a 50 m long oyster reef, necessary water velocity and TSS concentrations, along with salinity and temperature conditions, could be evaluated in both the model and potential restoration sites to identify an optimal location. If you restore to the 50 oyster m^{-2} restoration goals, according to the results from the parameterization in this study, you would need velocities to be greater than approximately 35,000 cm hr^{-1} (or about 10 cm s^{-1}) to maintain high particle supplies under optimal temperature and salinity conditions.

4.4. Future Directions

Coupled biological-physical models, such as this advection-diffusion model, enhance our predictions of spatial particle concentrations. These spatial considerations of particle concentrations would benefit existing models such as the Cerco and Noel (2005) growth model, Powell et al. (1992) population model, and Fulford et al. (2007) clearance rate model. These models, which could also be improved by incorporating a different filtration rate (further explained in Chapter 1), do not account for changing particle concentrations across a reef.

Food availability models for oysters have been previously developed (e.g. Wilson-Ormond et al. 1997) that account for horizontal advective movement over an oyster bed, but results from simulations here indicate that without including diffusive movement, these simpler formulations likely overestimate food availability and particle uptake over the oyster reef. The Wilson-Ormond et al. (1997) model, describes particle availability in terms of the percentage of particles removed. They

determined that velocities greater than 6 cm s^{-1} provided enough replenishment of food. From my model outputs, a higher velocity would be necessary to keep replenishment sustainable, likely indicating the effects of adding the 2-D spatial gradient of particles. Similarly, efforts to apply clearance rate models to estuarine ecosystems as a means of estimating the impact of oysters on water quality and clarity (Fulford et al. 2007; Newell and Koch 2004) generally do not include hydrodynamic considerations. Clearance rate models have been valuable in extending laboratory studies of filtration to ecosystem-scale processes. However, matching these to reef-scale particle transport and uptake processes is critical to reconsidering the likely role of physical processes in the feedbacks that oyster reefs have on estuarine water quality.

Another model that may benefit from incorporation of the advection-diffusion particle model and filtration model described here is the Farm Aquaculture Resource Management (FARM) model, an online user-friendly tool (www.farmscale.org/; Ferreira et al. 2007). The FARM model is designed to determine productivity of an aquaculture "farm" for a given location and practices. Carrying capacity, cost-benefit concerns, and the potential impact on restoring water quality are all considerations of this modeling platform, combining physical and shellfish growth models. The physical models include advection but do not include vertical diffusion and particle boundary layers, thus it would profit from incorporating the more complex, advection-diffusion model. Additionally, the growth model is parameterized for five aquaculture species, including the Pacific oyster, *Crassostrea gigas* (Ferreira et al. 2007). It could also be expanded to include *C. virginica* and use the filtration rate

equation (Equation 1) within that growth model. A screenshot of this model interface is shown in Figure 16.

In future work, more components can be added to the particle model. In reality, the magnitude of velocity changes with time and direction of flow changes with the tides. Rather than assuming a steady-state solution, dynamic simulations could be run to allow for changing salinity and temperature with time of year.

More hydrodynamic effects could be incorporated into the models, if determined to be necessary. One effect is the changing velocity profiles across a reef, leading to increasing boundary layer thickness. Another effect, ignored in this model, is of the exhalent current on the flow regime and re-entrainment of particles. Monismith et al. (1990) found that bivalves that possess siphons can have localized effects on boundary layer flow with small jet currents created by the siphons. Oysters lack siphons, so flow effects and re-suspension of waste particles likely are not as significant in comparison to a bivalve like the clam.

The simulations were run with same-sized oysters, but multiple size classes in a given area would increase realism. The principle of self-thinning (White et al. 2007), used for plant communities, could be applicable. This principle indicates that as individual size increases, community abundance decreases, which could translate to decreased oyster density and smaller oyster sizes as distance from the source of new organic matter increases. Changing densities and areal biomass in accordance with the ¾ power scaling of the self-thinning rule could be included as a function of distance in future versions of this model.

The spatial context for the model could also be modified for floating aquaculture techniques. Depth would need to be altered, and it is likely that additional hydrodynamic processes describing effects on flow by the cages and turbulent mixing would be important for delivery of particles.

5. CONCLUSION

From the findings in this study, describing particle gradients in a spatially-explicit framework with coupled biological-physical models can greatly affect calculated oyster particle removal rates and remaining particle availability to down-reef oysters. The more complex, advection-diffusion model, creating a concentration boundary layer, indicates the depletion of particles near a reef can only support certain lengths of reefs before food limitation occurs. The length of this reef is dependent on oyster size and density, velocity, and surrounding particle concentrations. Examining the added effects of complexity in this study points out that past benthic clearance rates may need to be revised to account for these new considerations.

LITERATURE CITED

Allen, J.R.L. (1985). Principles of physical sedimentology. George Allen & Unwin, London.

Allen, S., Carpenter, A.C., Luckenbach, M., Paynter, K. Sowers, A., Wesson, J., & Westby, S. (2011). Restoration goals, quantitative metrics and assessment protocols for evaluating success on restored oyster reef sanctuaries. Report of the Oyster Metrics Workgroup Submitted to the Sustainable Fisheries Goal Implementation Team of the Chesapeake Bay Program.

Bacher, C., Grant, J., Hawkins, A.J.S., Fang, J., Zhu, M, & Besnard, M. (2003). Modelling the effect of food depletion on scallop growth in Sungo Bay (China). *Aquatic Living Resources, 16*, 10-24.

Brush, M.J., Brawley, J.W., Nixon, S.W., & Kremer, J.N. (2002). Modeling phytoplankton production: problems with the Eppley curve and an empirical alternative. *Marine Ecology Progress Series, 238*, 31-45.

Butman, C.A., Frechette, M., Geyer, W.R., & Starczak, V.R. (1994). Flume experiments on food supply to the blue mussel Mytilus edulis L. as a function of boundary-layer flow. *Limnology and Oceanography, 39* (7), 1755-1768.

Cerco, C. F. & Noel, M.R. (2005). Evaluating ecosystem effects of oyster restoration in Chesapeake Bay. *A Report to the Maryland Department of Natural Resources*.

Cerco, C.F., & Noel, M.R. (2007). Can oyster restoration reverse cultural eutrophication in Chesapeake Bay? *Estuaries and Coasts*, 30 (2), 331-343.

Clauser, F.H. (1956). The turbulent boundary layer. *Advances in Applied Mechanics, 4*, 1-51.

Cloern, J.E., Grenz, C., & Vidergar-Lucas, L. (1995). An empirical model of phytoplankton chlorophyll:carbon ratio – the conversion factor between productivity and productivity and growth rate. *Limnology and Oceanography, 40*(7), 1313-1321.

Doiron, S. (2008). Reference Manual for Oyster Aquaculturists. *New Brunswick Department of Agriculture, Fisheries and Aquaculture*.

Edelstein-Keshet, L. (2005). Mathematical models in biology. Society for Industrial and Applied Mathematics, Philadelphia, PA.

Ferreira, J.G., Hawkins, A.J.S., & Bricker, S.B. (2007). Management of productivity, environmental effects and profitability of shellfish aquaculture - the Farm Aquaculture Resource Management (FARM) model. *Aquaculture, 264*, 160-174.

Frechette, M., Butman, C.A., & Geyer, R.W. (1989). The importance of boundary-layer flows in supplying phytoplankton to the benthic suspension feeder, *Mytilus edulis* L. *Limnology and Oceanography, 34(*1), 19-36.

Fulford, R.S., Breitburg, D.L., Newell, R.I.E., Kemp, W. M., & Luckenbach, M. (2007). Effects of oyster population restoration strategies on phytoplankton biomass in Chesapeake Bay: A flexible modeling approach. *Marine Ecology Progress Series, 336*, 43-61.

Hornberger, G. & Wiberg, P. (2005) Finite Difference Solutions for Transient Problems. In: Numerical Methods in the Hydrological Sciences. Special Publication Series 57. American Geophysical Union, 1-20.

Jones, N.L., Thompson, J.K., Arrigo, K.R., & Monismith, S.G. (2009). Hydrodynamic control of phytoplankton loss to the benthos in an estuarine environment. *Limnology and Oceanography, 54*(3), 952-969.

Kellogg, L.M., Cornwell, J.C. Owens, M.C., & Paynter, K.T. (2013). Denitrification and nutrient assimilation on a restored oyster reef. *Marine Ecology Progress Series, 480*, 1-17.

Kennedy, V.S & Sanford, L.P. (1999) In: Luckenbach, M.W, Mann, R., & Wesson, J.A. (eds) Oyster reef habitat restoration: A synopsis and synthesis of approaches. Virginia Institute of Marine Science Press, Gloucester Point, VA, 25-46.

Loosanoff, V.L. (1962). Effects of turbidity on some larval and adult bivalves. *Proceedings of the Fourteenth Annual Gulf and Caribbean Fisheries Institute, 14*, 80-94.

Maryland Department of Natural Resources. (1997). Report: Maryland's historic oyster bottom; A geographic representation of the traditional named oyster bars.

Monismith, S.G., Koseff, J.R., Thompson, J.K., O'Riordan, C.A., & Nepf, H.M. (1990). A study of model bivalve siphonal currents. *Limnology and Oceanography, 35(*3), 680-696.

Myung, I.J, & Pitt, M.A. (1997). Applying Occam's razor in modelling cognition: A Bayesian approach. *Psychonomic Bulletin & Review, 4* (1), 79-95.

Newell, R.I.E & Koch, E.W. (2004). Modeling seagrass density and distribution in response to changes in turbidity stemming from bivalve filtration and seagrass sediment stabilization. *Estuaries, 27* (5), 793-806.

North, E.W., Schlag, Z., Hood, R.R., Li, M., Zhong, L., Gross, T., & Kennedy, V.S. (2008) Vertical swimming behavior influences the dispersal of simulated oyster larvae in a coupled-particle tracking and hydrodynamic model of Chesapeake Bay. *Marine Ecology Progress Series, 359,* 99-115.

Petersen, J.K., Marr, M., Ysebaert, T., & Herman, P.M.J. (2013). Near-bed gradients in particles and nutrients above a mussel bed in the Limfjorden: Influence of physical mixing and mussel filtration. *Marine Ecology Progress Series, 490*, 137-146.

Powell, E.N, Hofmann, E.E., Klinck, J.M., & Ray, S.M. (1992). Modeling oyster populations I. A commentary on filtration rate. Is faster always better? *Journal of Shellfish Research, 11*(2), 387-398.

Rheault, R.B. & Rice, M.A. (1996). Food-limited growth and condition index in the eastern oyster, *Crassostrea virginica* (Gmelin 1791), and the bay scallop, *Argopecten irradians irradians* (Lamarck 1819). *Journal of Shellfish Research, 15*(2), 271-283.

Saurel, C., Petersen, J.K., Wiles, P.J., & Kaiser, M.J. (2013). Turbulent mixing limits mussel feeding: Direct estimates of feeding rate and vertical diffusivity. *Marine Ecology Progress Series, 485*, 105-121.

Simpson, J.H., Berx, B., Gascoigne, J., & Saurel, C. (2007). The interaction of tidal advection, diffusion and mussel filtration in a tidal channel. *Journal of Marine Systems, 68*, 556-568.

Southworth, M., Harding, J.M., Wesson, J.A., & Mann, R. (2010). Oyster (Crassostrea virginica, Gemlin 1791) population dynamics on publics reefs in the Great Wicomico River, Virginia, USA. *Journal of Shellfish Research, 29* (2), 271-290.

Tenore, K.R., & Dunstan, W.M. (1973). Comparison of feeding and biodeposition of three bivalves at different food levels. *Marine Biology, 21*, 190-195.

White, E.P., Ernest, S.K.M., Kerkhoff, A.J., & Enquist, B.J. (2007). Relationships between body size and abundance in ecology. *Trends in Ecology and Evolution, 22*(6), 323-329.

Wilberg, M.J, Livings, M.E., Barkman, J.S., Morris, B.T., & Robinson, J.M. (2011). Overfishing, disease, habitat loss, and potential extirpation of oysters in upper Chesapeake Bay. *Marine Ecology Progress Series, 436*. 131-144.

Wildish, D.J. & Kristmanson, D.D. (1984) Importance to mussels of the benthic boundary layer. *Canadian Journal of Fisheries and Aquatic Science, 41*, 1618-1625.

Wilson-Ormond, E.A., Powell, E.N., & Ray, S.M. (1997). Short-term and small-scale variation in food availability to natural oyster population: Food, flow, and flux. *Marine Ecology, 18*(1), 1-34.

TABLES

Parameter	Function
Temperature	$f(T) = e^{(-0.006*(T-27)^2)}$
Salinity	$f(S) = 1$ when S<5, $f(S) = 0.0926 * \mathrm{S} - 0.139$ when 5≤S≤12 $f(S) = 1$ when S>12
TSS	$f(TSS) = 0.1$ when TSS<4 mg L^{-1} $f(TSS) = 1$ when 4≤TSS≤25 mg L^{-1} $f(TSS) = 10.364 * \ln(TSS)^{-2.0477}$ when TSS>25 mg L^{-1}

Table 1. Functions of environmental parameters for calculation of filtration rate. Each function is scaled between 0 and 1 and then multiplied by a size-dependent maximum filtration rate.

Model Variables	Definition
A	Areas of Incoming and Outgoing Flow (cm^2), $A=w*h$
C	Chlorophyll Concentration (mg cm^{-3})
dx	Change in x (cm)
dz	Change in z (cm)
FR	Oyster Filtration Rate (cm^3 hr^{-1} cm^{-2})
h	Water Column Depth (cm)
K_z	Vertical Turbulent Diffusivity (cm^2 hr^{-1})
$\boldsymbol{u}_*$	Shear Velocity (cm hr^{-1})
u_{bar}	Mainstream Velocity (cm hr^{-1})
u_z	Velocity at Height z (cm hr^{-1})
V	Volume of Cell (cm^3), V=w*h*dx or $V=w*dz*dx$
w	Reef Width (cm)
x	Distance Down Reef, Grid Cell Horizontal Location
z	Height, Grid Cell Vertical Location
z_0	Roughness Parameter (cm)

Table 2. Common variables and definitions used in the advection and advection-diffusion model equations.

	Reef Length (m)	Velocity (cm hr^{-1})	Oyster Density (m^{-2})	Individual Oyster g DW	T (°C)	S	Initial Concentration (mg cm^{-3})
Run 1	10	34000	700	1	27	15	$1.8*10^{-5}$
Run 2	10	3400	700	1	27	15	$1.8*10^{-5}$
Run 3	10	34000	50	1	27	15	$1.8*10^{-5}$
Run 4	10	3400	50	1	27	15	$1.8*10^{-5}$

Table 3. Simulations run for comparison of the advection and advection-diffusion models. For each run, the combination of velocity and oyster density was changed.

FIGURES

Advection Model

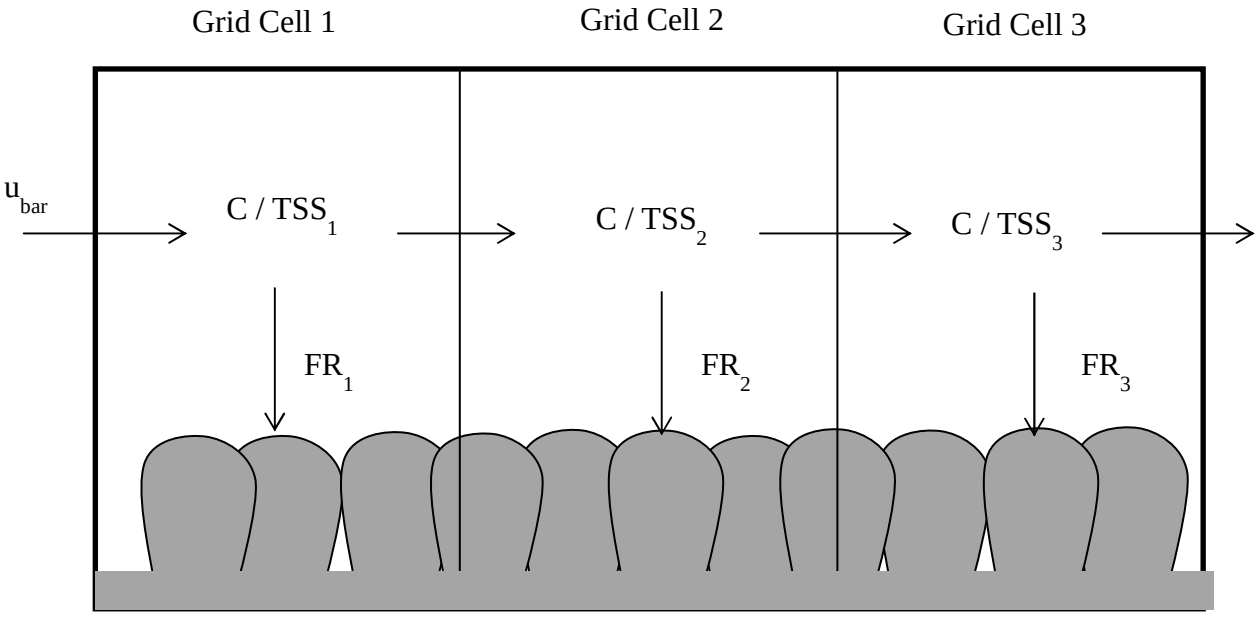

Figure 1. Advection particle model conceptual diagram. Arrows indicate direction of particle loss processes for each grid cell via advection or filtration by oysters.

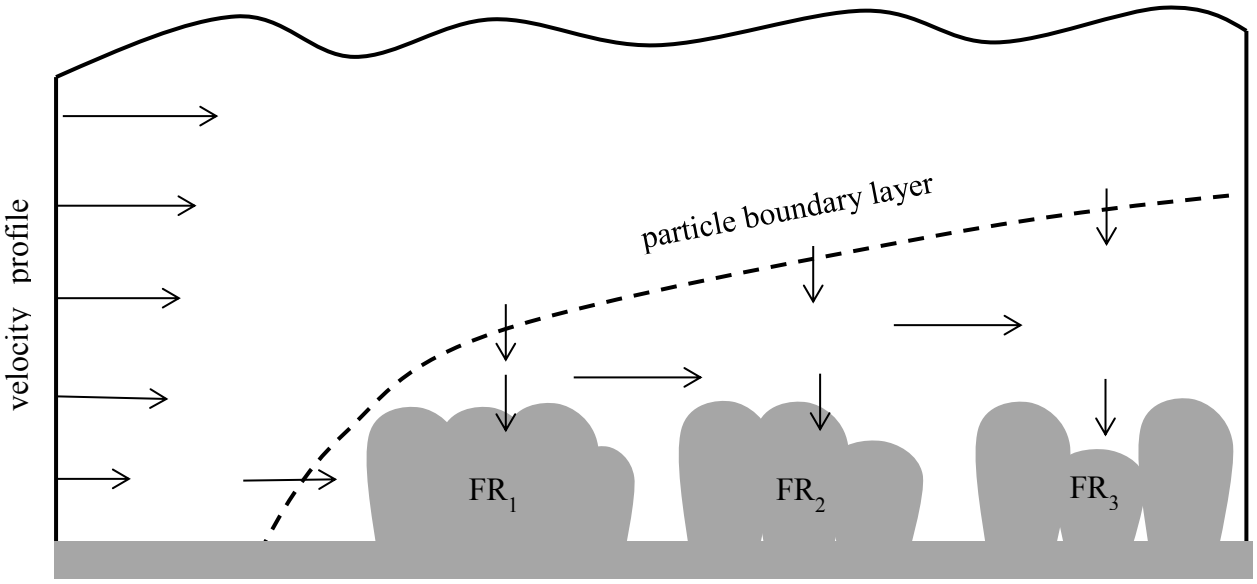

Figure 2. Advection-diffusion model conceptual diagram. Arrows indicate direction of particles and loss processes via advection, diffusion, or filtration. The dotted line represents a particle boundary layer that is formed when variable velocity, diffusion, and a rough substrate combine to affect particle concentrations adjacent to the oyster reef.

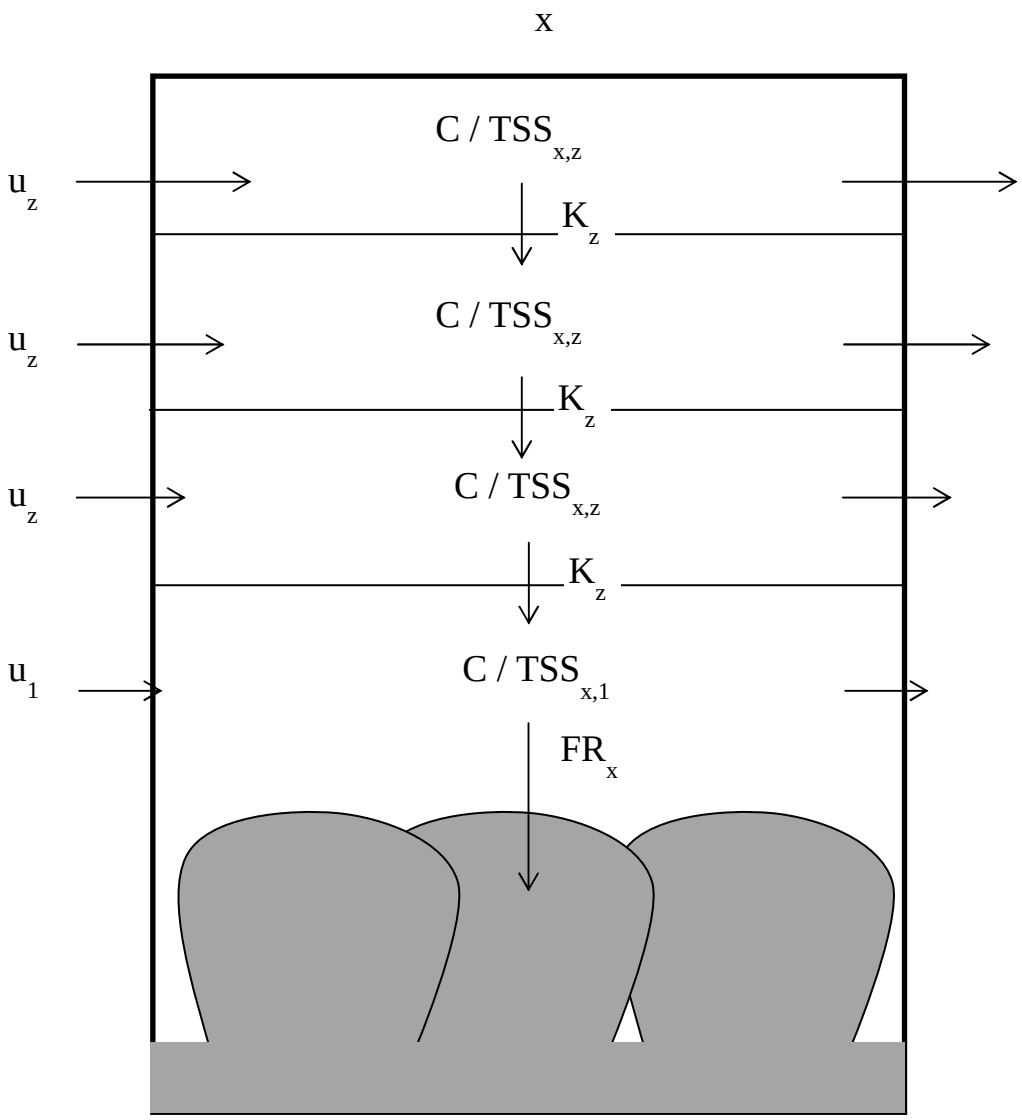

Figure 3. Flows in the advection-diffusion model for the grid cells in the vertical direction at location *x*. Arrows indicate direction of particle movement via advection, diffusion, or filtration by oysters.

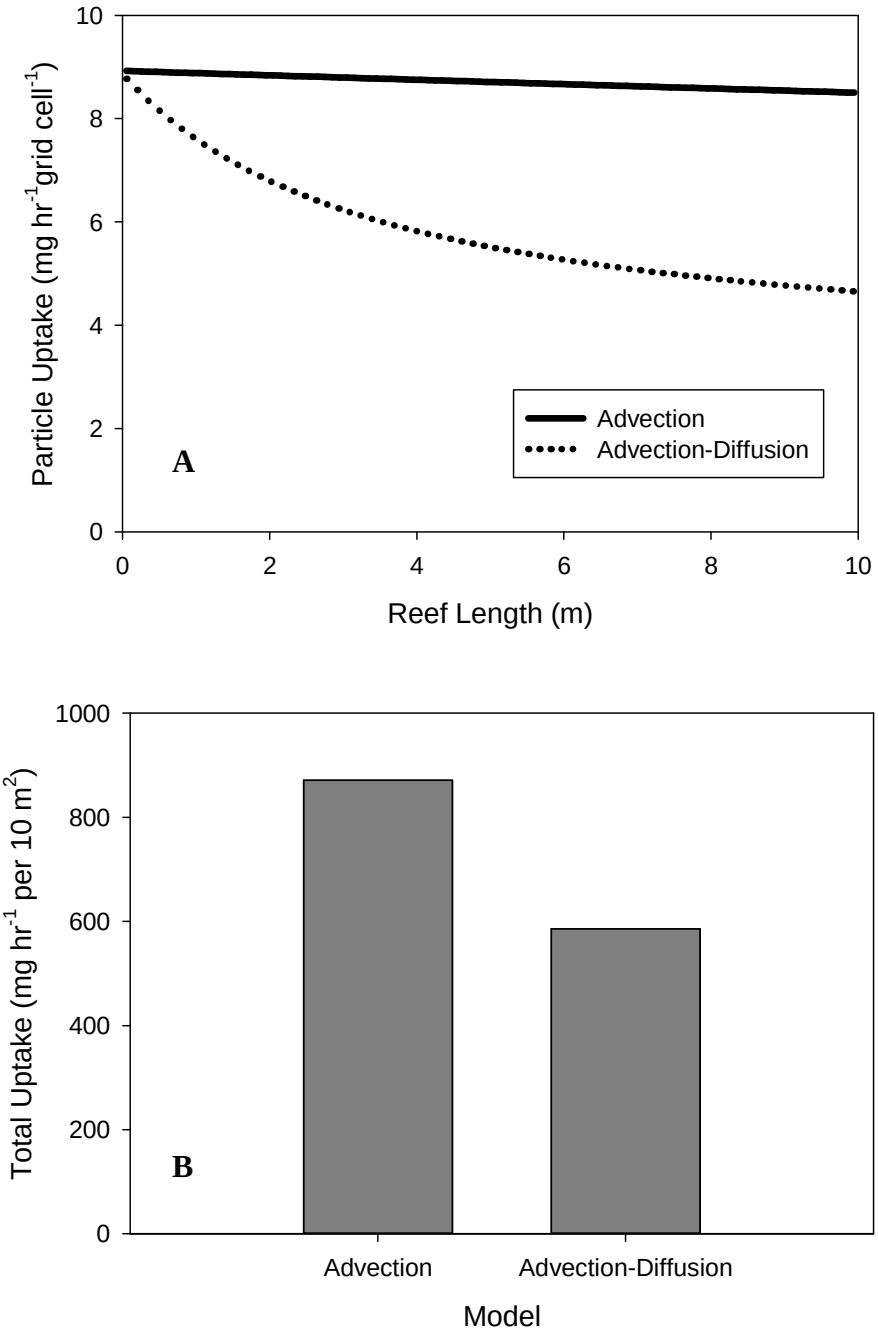

Figure 4. Results of Complexity Comparison Run 1 - Higher Density and Higher Velocity. (a) Reef location and corresponding oyster particle uptake, and (b) the total uptake on a 10 m^2 reef section.

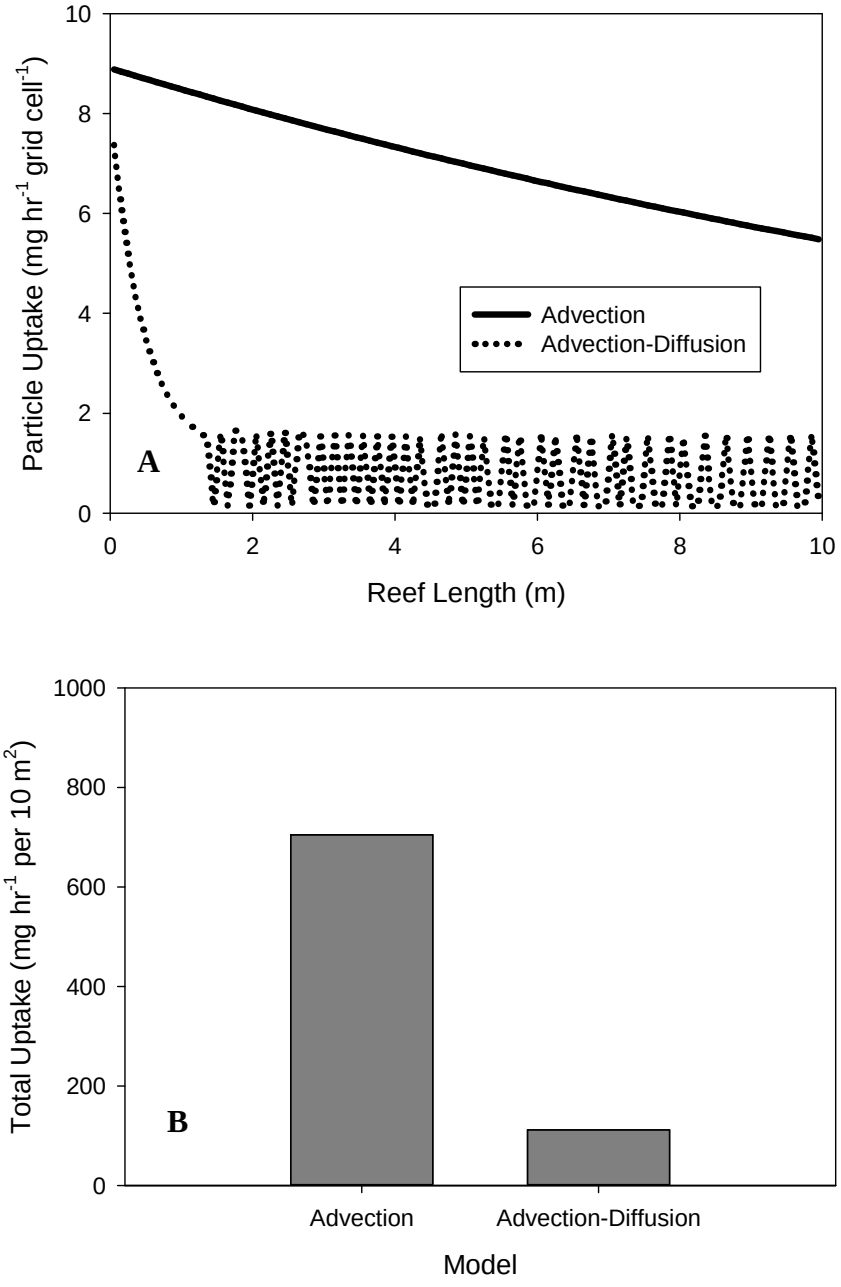

Figure 5. Results of Complexity Comparison Run 2 - Higher Density and Lower Velocity. (a) Reef location and corresponding oyster particle uptake, and (b) the total uptake on a 10 m^2 reef section.

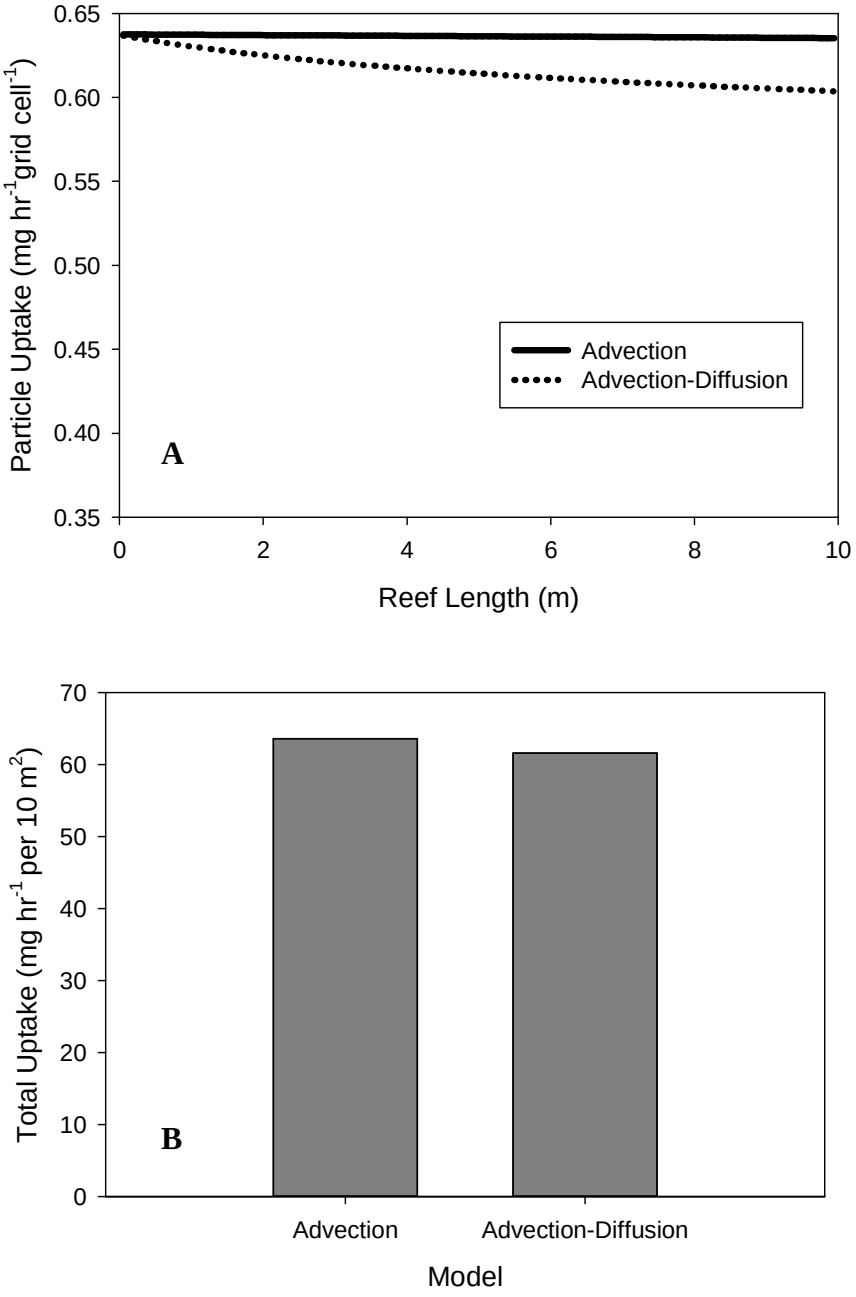

Figure 6. Results of Complexity Comparison Run 3 - Lower Density and Higher Velocity. (a) Reef location and corresponding oyster particle uptake, and (b) the total uptake on a 10 m^2 reef section.

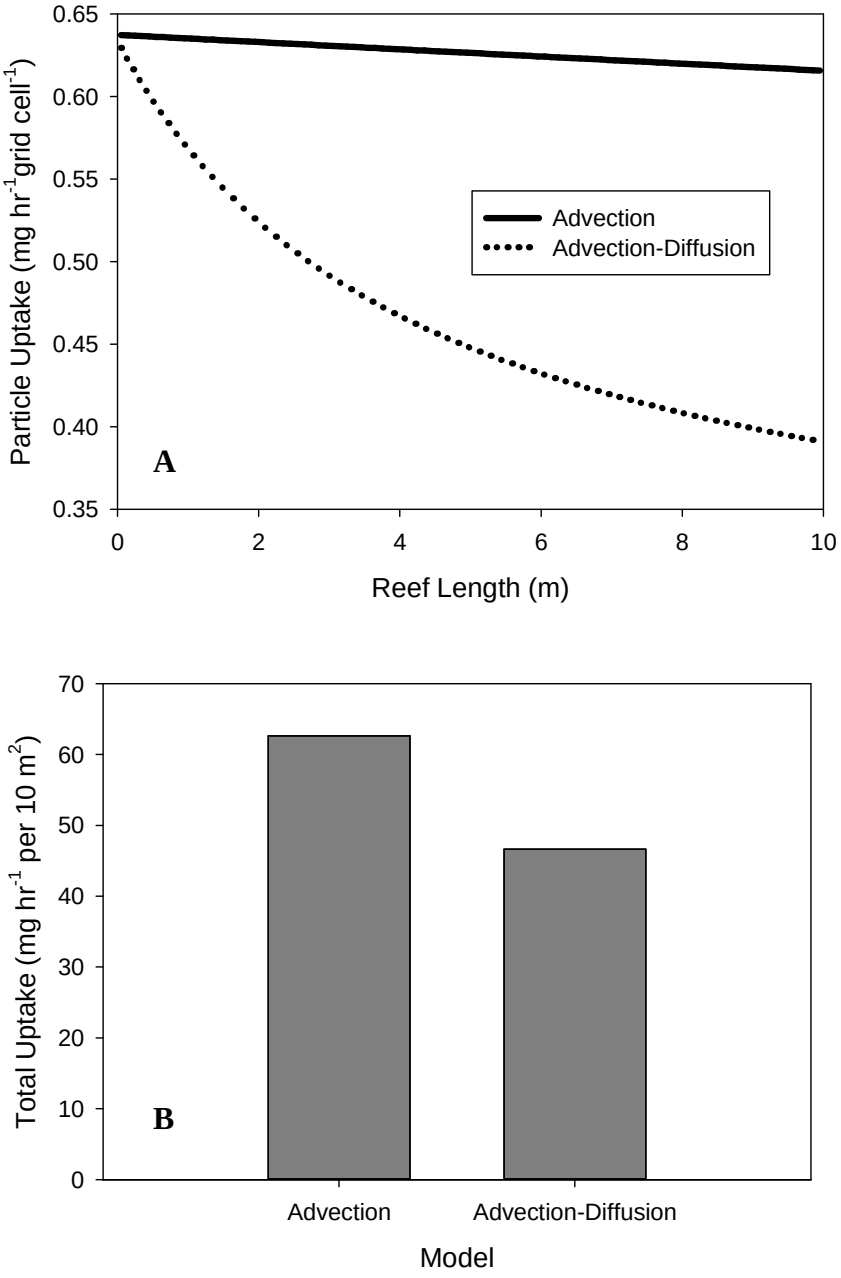

Figure 7. Results of Complexity Comparison Run 4 - Lower Density and Lower Velocity. (a) Reef location and corresponding oyster particle uptake, and (b) the total uptake on a 10 m^2 reef section.

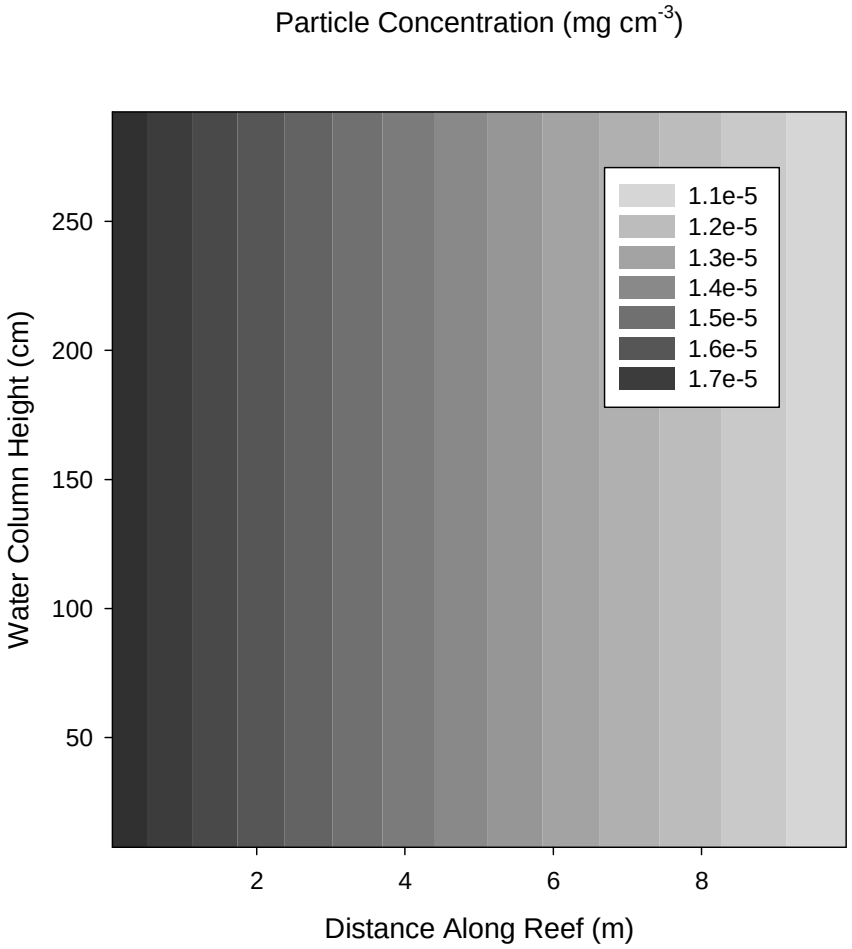

Figure 8. Particle concentration (mg cm^{-3}) contours for the advection model with higher density and lower velocity (Table 3, Run 2). The particles vary across the reef but not with height.

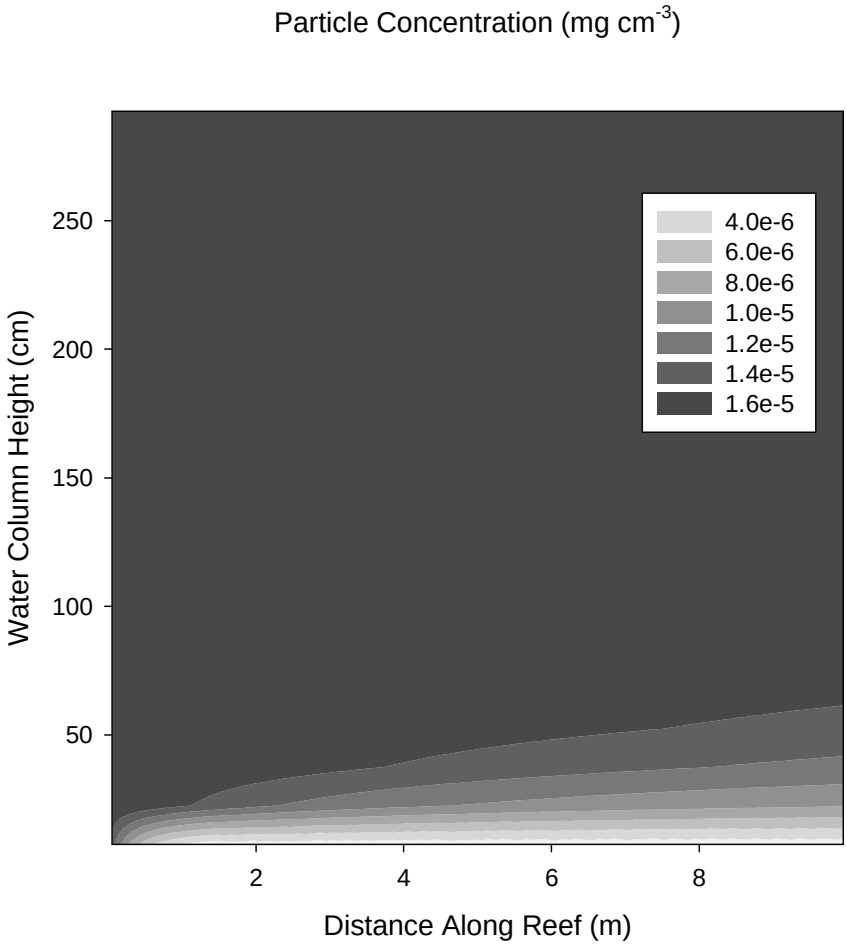

Figure 9. Particle concentration (mg cm^{-3}) contours for the advection-diffusion model with higher density and lower velocity (Table 3, Run 2). A concentration boundary layer occurs near the substrate.

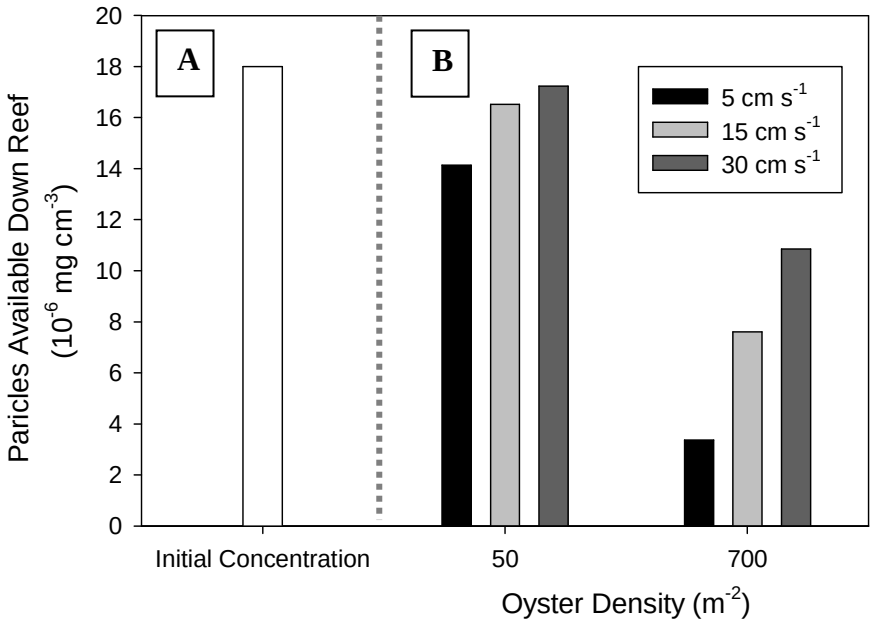

Figure 10. Initial particles (a) and particles available to oysters in the last and bottom (z=1) grid cell (b) when oyster density and velocity are varied for a 100 meter long reef.

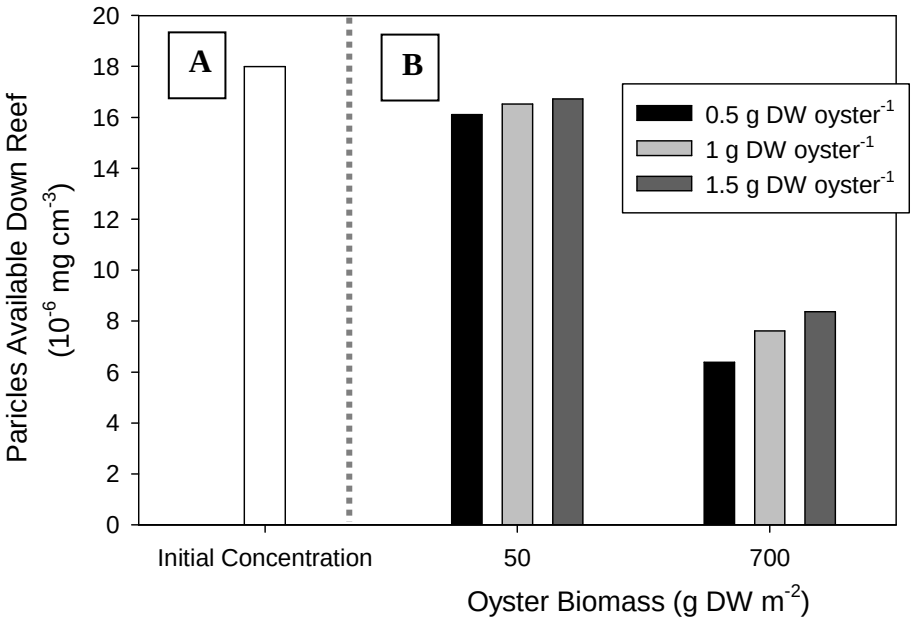

Figure 11. Initial particles (a) and particles available to oysters in the last and bottom (z=1) grid cell (b) when oyster sizes are varied, keeping total areal biomass constant, for a 100 meter long reef when velocity is 15 cm s^{-1}.

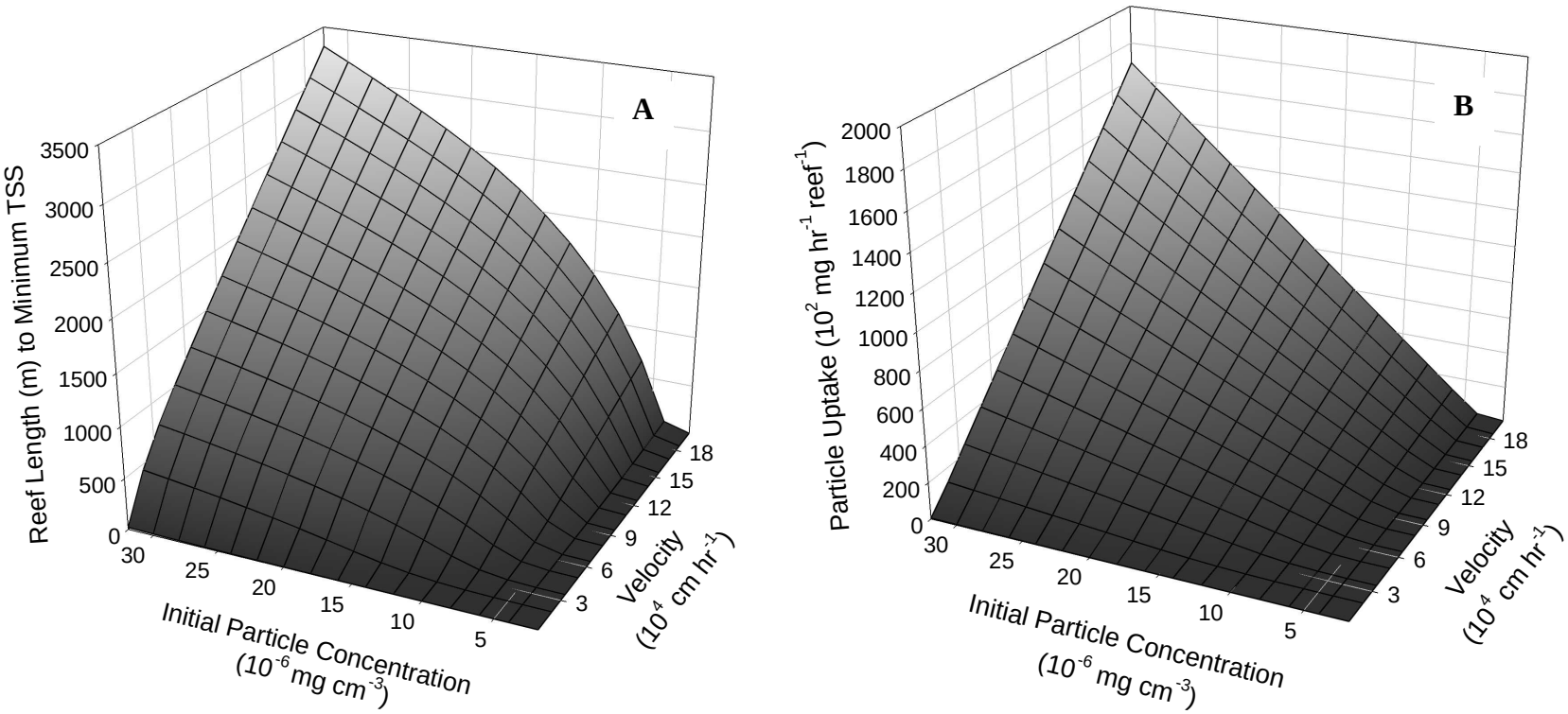

Figure 12. Advection-diffusion model results using 700 oysters m^{-2} over range of velocity and initial particle concentrations for (a) reef length at which particle concentrations drop below 4 mg L^{-1} and (b) the total reef particle removal associated with this reef length.

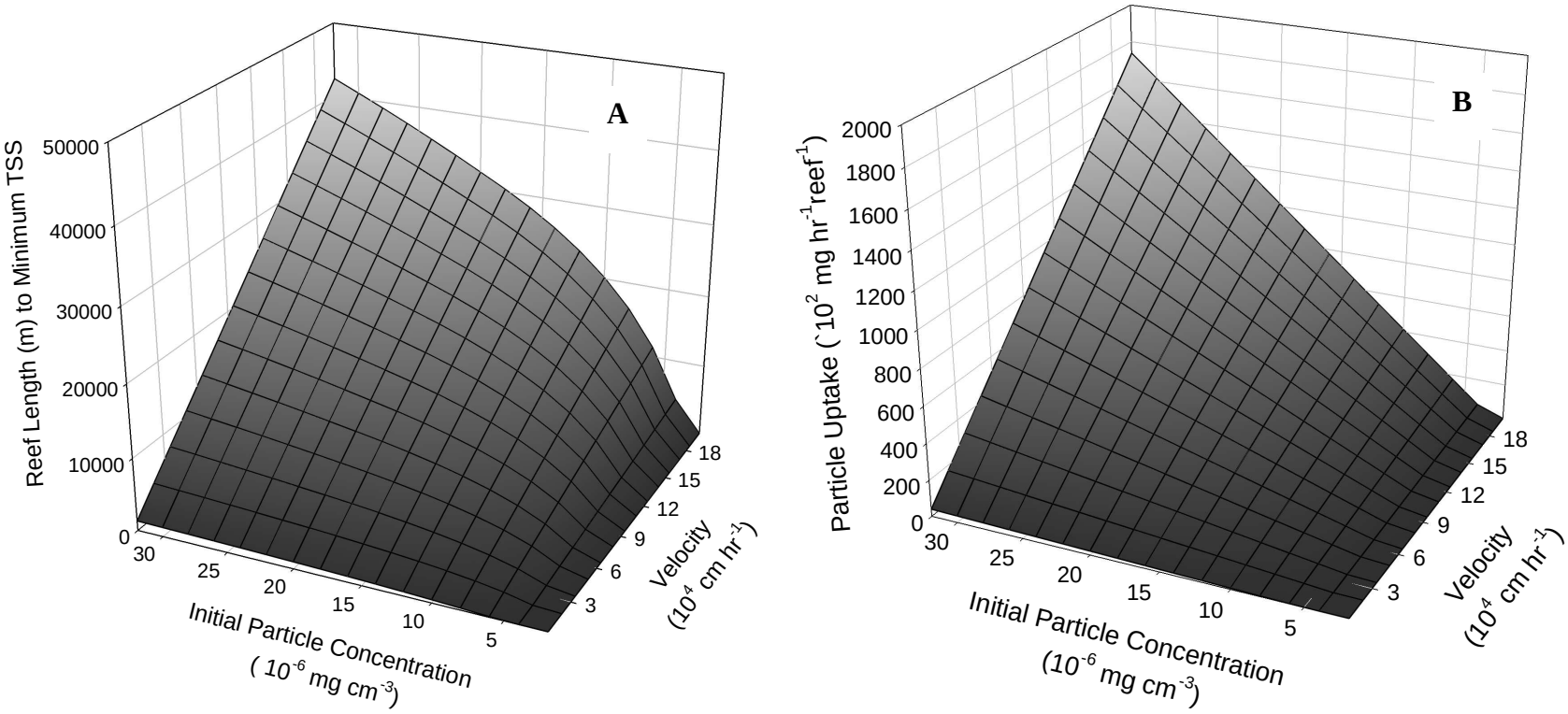

Figure 13. Advection-diffusion model results using 50 oysters m^{-2} over range of velocity and initial particle concentrations for (a) reef length at which particle concentrations drop below 4 mg L^{-1} and (b) the total reef particle removal associated with this reef length.

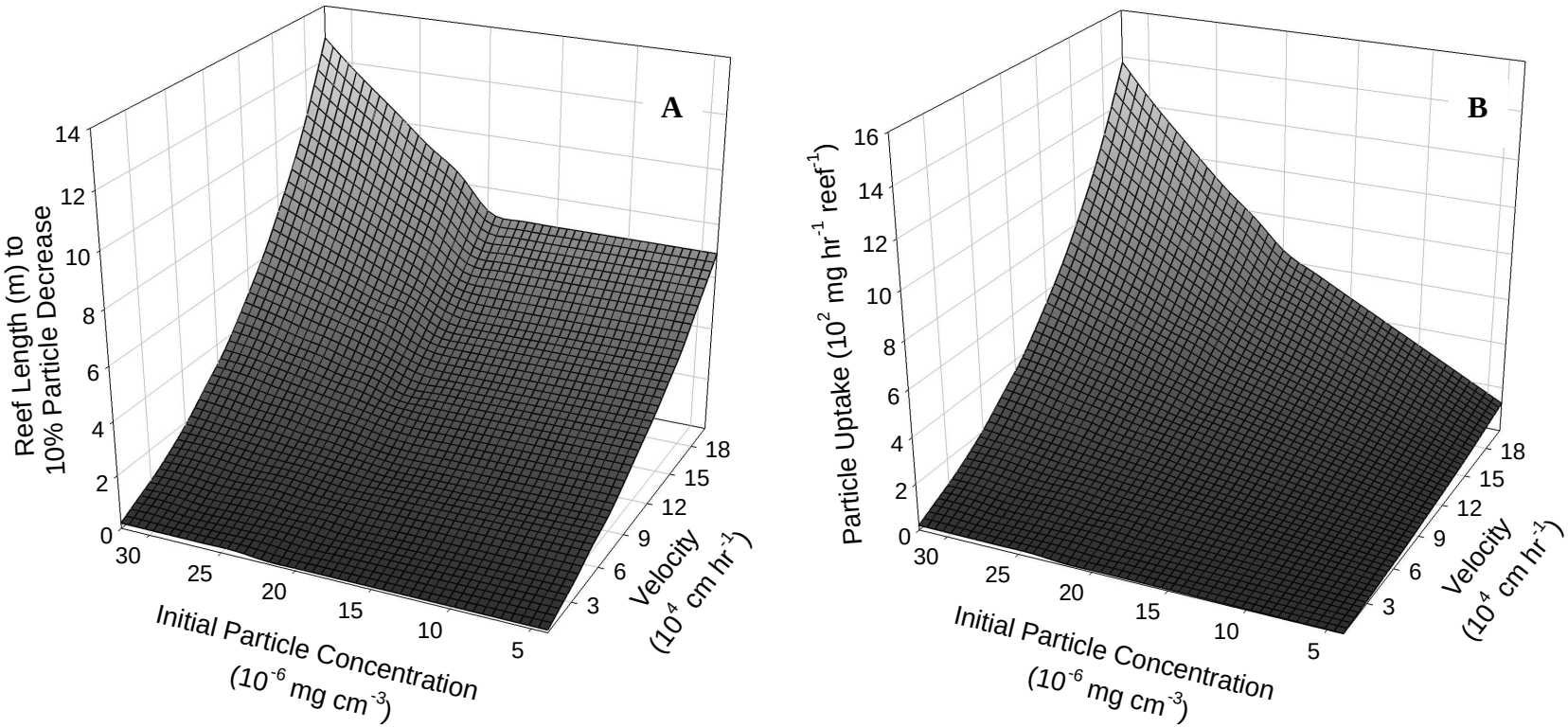

Figure 14. Advection-diffusion model results using 700 oysters m^{-2} over range of velocity and initial particle concentrations for (a) reef length at which the cross length concentration gradient is 10% and (b) the total reef particle removal associated with this reef length.

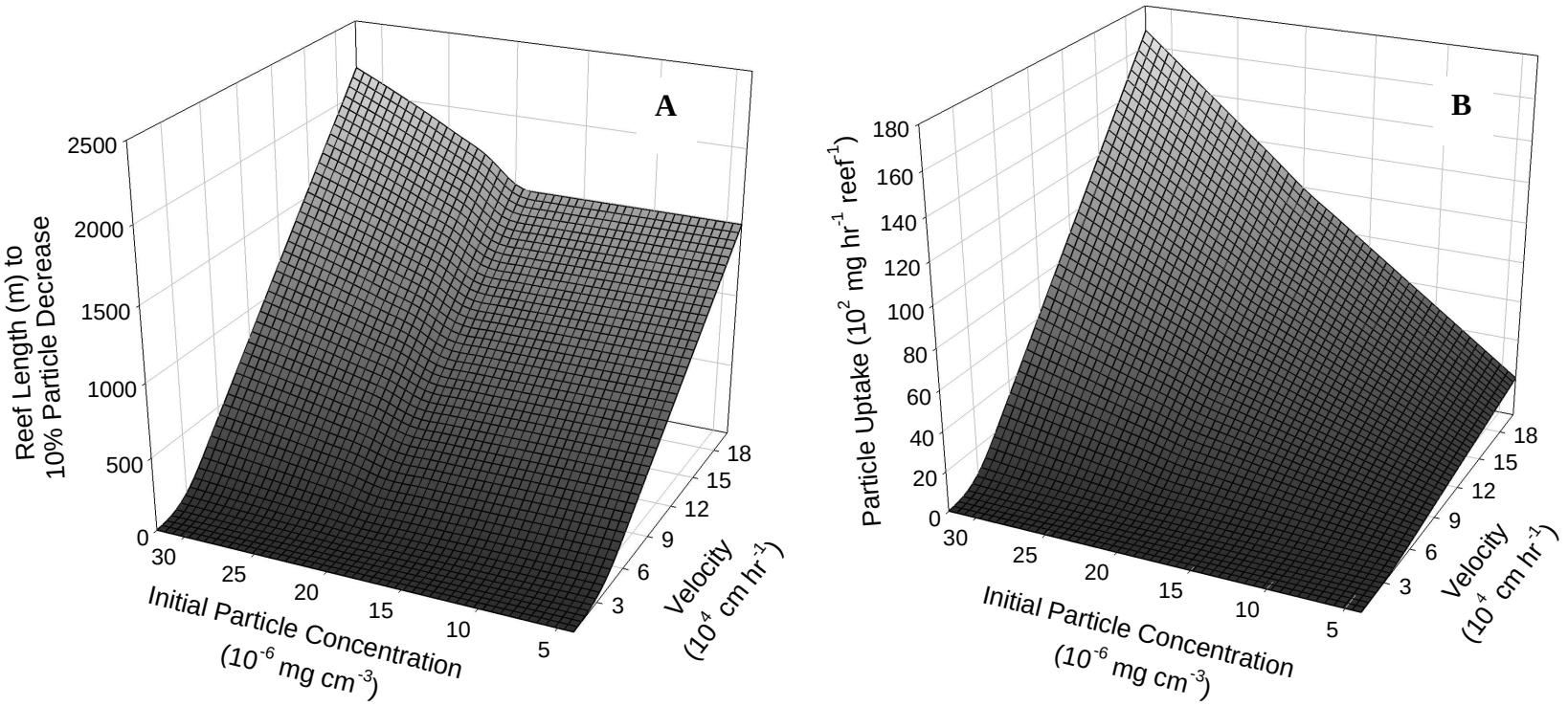

Figure 15. Advection-diffusion model results using 50 oysters m^{-2} over range of velocity and initial particle concentrations for (a) reef length at which the cross length concentration gradient is 10% and (b) the total reef particle removal associated

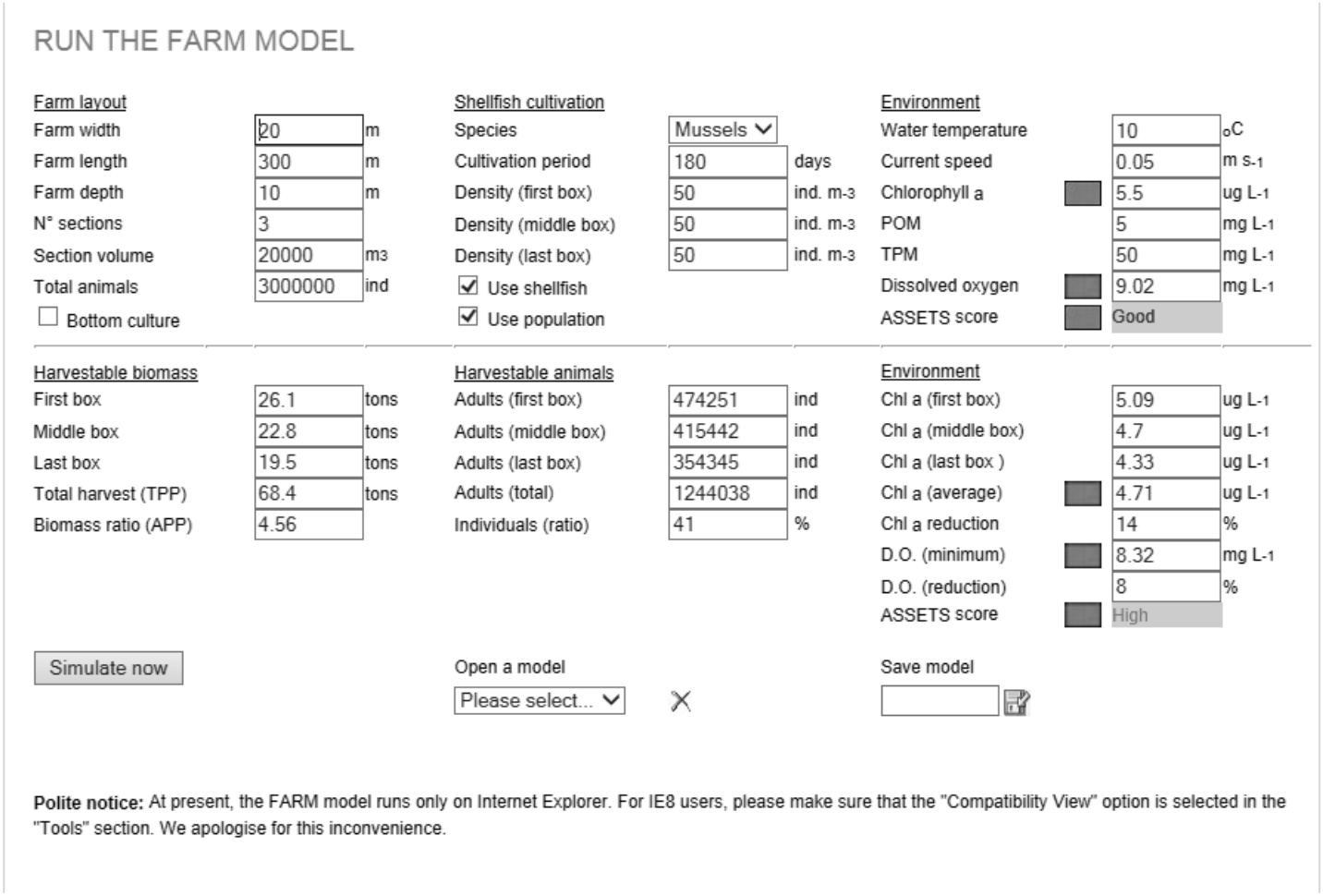

Figure 16. FARM model interface. Inputs include the farm layout, shellfish cultivation, and environmental variables. The outputs include harvestable biomass, harvestable animals, and the environmental variables.

Appendix A

Conversions

To compare filtration rates, conversions are necessary. Simple dimensional analysis convert time and volume units. Other necessary conversion factors are described here.

Oyster Weight

Grams of oyster carbon, *g C,* and grams dry weight, *g DW,* are interchangeable with the fraction: 0.5 *g C*: 1 *g DW* (Cerco and Noel 2005). Allometric relationships between oyster biomass, *DW* (g), and oyster height, *H* (mm), are related as

$$DW = 0.00008 * H^{2.175}$$

For this equation, I measured oyster dry weights and lengths for 1, 2, and 3 year old oysters and for larger oysters with unknown ages. Ross and Luckenbach (2006) also examine the relationship of height and weight and found the relationship to be $DW=0.00003*H^{2.3952}$. The graph on the next page displays the power function fit from my empirical data and the regression equation reported by Ross and Luckenbach (2006), which are comparable, justifying the use of my height and weight relationship.

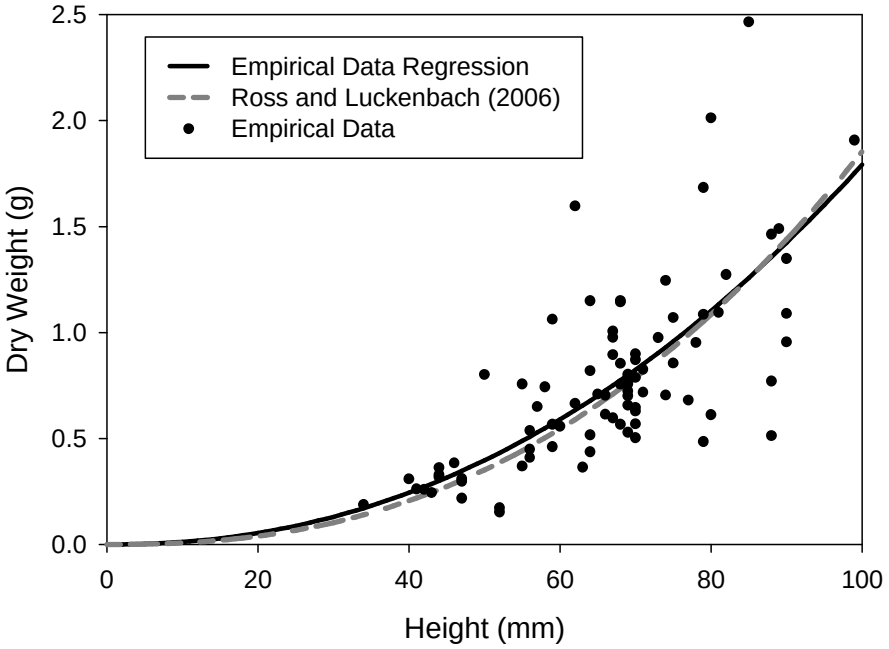

Empirical data and regressions from my empirical data and Ross and Luckenbach (2006) for the height (mm) vs. dry weight (g) relationship.

Standardized Filtration Rates

Filtration rates vary with oyster dry weight, thus to standardize for 1 g DW oysters, the corrected filtration rate for a 1 g DW oyster, *X*, is

$$X = \frac{Y}{DW^{-0.28}}$$

(Fulford et al. 2007; Newell and Koch 2004)

Where *Y* is the given filtration rate. An exponent of -0.28 is used (Fulford et al. 2007) to keep filtration on a per weight basis.

Appendix B

MATLAB Coding

Advection Code

The following codes run the advection model, including the files ParticleCapture1Db.m, Filtration2.m, and SteadyStateb.m.

ParticleCapture1Db.m

```
% Script to run all the codes in order

%THESE PARAMETERS CAN BE CHANGED
clear
%Oyster Parameters
N=700;      %number of oysters per m^2
g=1;     %size in grams of oysters
oysterheight=((g/0.00008)^(1/2.175))/10; %cm  from DW=0.00008*H^2.175 where H
is in mmm

%Box Set Up
L=10*100;         %length of reef(cm)
w= 100;           %width of volume of interest (cm)
depth=3*100;      %depth of water column(cm)


z0=oysterheight/30;  %roughness parameter

%Parameter Set Up (T,S,velocity)
S=15;  %salinity units
T=27;    %degrees C
velocity=34000; %cm/hr

%Outside Chlorophyll Concentration (mg/cm^3) and TSS concentration mg/L
Parout=18*10^-6;
outTSS=Parout*1309916;

%%%%%%%%%%%%%%%%%%%%%%%%%%%%%%%%%%%%%%%%%%%%%%%%%%%%%%%%%%%%%%%%%%%%%%%%%%%%%%%

Filtration2

SteadyStateb

%Particle Uptake (mg/hr)
Uptake=nan(1,Boxnum);

for x=1:Boxnum;
    Uptake(x)=C(x)*alpha(x)*w*dx; %Filtration rate* bottom area * the
particles in bottom box
end
```

Filtration2.m

```
%Filtration Rate for the given box

%Maximum Filtration per m^2
Frmax=([0.17*(g).^0.6486])/24*N;   %(m^3/hr/m^2)

%Environmental Limitations for each day

fT=exp(-0.006*(T-27).^2);  %fT function

if (S<5)
    fS=0
elseif (S>12)
    fS=1
elseif (S>=5) && (S<=12)
fS=(0.0926*S)-0.139;
end

%Filtration Rate for each day

Fr2=Frmax.*fT.*fS;  %Fr of each box
```

SteadyStateb.m

```
%Filtration rate at time t for given boxes without the TSS limitation factor
(cm^3/hr/cm^2)
Filtration=Fr2.*(100); %Including unit conversion

%Conversion
fraction=1309916;   %Muliplied by Chl to give TSS concentration

%Box size
dxs=(0.5*velocity*depth)/Filtration %size needed for stability
dx=10  %cm
if dxs<dx
    dx=dxs
end

Boxnum=ceil(L/dx)
for x=2:Boxnum;  %Length Position
    X(1)=dx*0.5
    X(x)=X(x-1)+dx
end

%Matrix set up of variable components
C=nan(1,Boxnum);  %Par=particles--->in this case chlorophyll
TSS=nan(1,Boxnum);  %TSS levels of the boxes
fTSS=nan(1,Boxnum); %fTSS levels of the boxes
alpha=nan(1,Boxnum); %Filtration rate of the boxes

%Governing Equation:
%Cn+1=Cn*(1-(alpha*dx/velocity*h))

%First Box Concentration
if (outTSS>25) %f(TSS)
            fTSS(1)=10.364*(log(outTSS)).^-2.0477;
     elseif (outTSS<4)
            fTSS(1)=0.1;
         elseif (outTSS>=4) && (outTSS<=25);
            fTSS(1)=1;
     end
            alpha(1)=Filtration*fTSS(1);
C(1)=Parout*(1-((alpha(1)*dx)/(velocity*depth)));
TSS(1)=C(1)*fraction

%Rest of Boxes Concentration
for x=1:Boxnum-1;
   C(x+1)=C(x)*(1-((alpha(x)*dx)/(velocity*depth)));
   TSS(x+1)=C(x+1)*fraction;
   if (TSS(x+1)>25);
                     fTSS(x+1)=10.364*(log(TSS(x+1))).^-2.0477;  %Using if
then statements for TSS
                elseif (TSS(x+1)<4);
                    fTSS(x+1)=0.1;
               elseif (TSS(x+1)>=4)&&(TSS(x+1)<=25);
                   fTSS(x+1)=1;
   end
```

```
                    alpha(x+1)=Filtration*fTSS(x+1);
end
```

Advection-Diffusion Code

The following codes run the advection-diffusion model, including the files ParticleCapture.m, Filtration2.m, and Diffusivity.m.

ParticleCapture.m

```
% Script to run all the codes in order

%THESE PARAMETERS CAN BE CHANGED
clear
%Oyster Parameters
N=700;    %number of oysters per m^2
g=1;     %size in grams of oysters
oysterheight=((g/0.00008)^(1/2.175))/10; %cm  from DW=0.00008*H^2.175 where H
is in mmm

%Box Set Up
L=100*100;         %length of reef(cm)
w= 100;         %width of volume of interest (cm)
depth=3*100;    %depth of water column(cm)

z0=oysterheight/30;  %roughness parameter

%Parameter Set Up (T,TSS,S,velocity)
S=15;  %salinity units
T=27;    %degrees C
velocity=108000; %cm/hr

%Outside Chlorophyll Concentration (mg/cm^3) and TSS concentration mg/L
Parout=18*10^-6;
outTSS=Parout*1309916;

%%%%%%%%%%%%%%%%%%%%%%%%%%%%%%%%%%%%%%%%%%%%%%%%%%%%%%%%%%%%%%%%%%%%%%%%%%%%

Filtration2

Diffusivity

%Particle Uptake (mg/hr)
Uptake=nan(1,Boxnum);

for x=1:Boxnum;
    Uptake(x)=C(x,1)*alpha(x)*w*dx; %Filtration rate * area*the particles in
bottom box
end
```

Filtration2.m

```
%Filtration Rate

%Maximum Filtration in a m^2
Frmax=([0.17*(g).^0.6486])/24*N;   %(m^3/hr/m^2)

%Environmental Limitations for each day

fT=exp(-0.006*(T-27).^2);  %fT function

if (S<5)
    fS=0
elseif (S>12)
    fS=1
elseif (S>=5) && (S<=12)
fS=(0.0926*S)-0.139;
end

%Filtration Rate for each day

Fr2=Frmax.*fT.*fS;  %Fr of each box
```

Diffusivity.m

```
%Filtration rate at time t for given boxes without the TSS limitation factor
(cm^3/hr/cm^2)
Filtration=Fr2.*(100); %Including unit conversion

%Conversion
fraction=1309916;   %Muliplied by Chl to give TSS concentration

%Heights Above Bottom
deltad=depth/20; %Want 20 different heights
z1(1)=0.5*deltad;  %to find the height in the middle of a box
for z=2:1:20
    z1(z)=z1(z-1)+deltad;  %height above bottom
end
%z1 is the actual height above the bottom

%Velocity Calculations
%Ubar and Ustar
ubar=velocity; %vertically averaged velocity or maintream velocity
ustar=ubar*(2*depth-(z0))/(5*(z0+depth*(log(depth/z0)-1)));  %ustar
u=nan(size(z1)); %velocity
for z=1:20;
  u(z)=(ustar/0.4)*log(z1(z)/z0);
end

%Height Dependent Only Parameters (Diffusivity)
K=nan(size(z1));
dkdz=nan(size(z1));
for z=1:20;
    K(z)=0.4*ustar*z1(z)*(1-(z1(z)/depth));
    dkdz(z)=0.4*ustar*(1-2*(z1(z)/depth));
end

%Box Set up
dz=deltad;
us=(ustar/0.4)*log((depth*0.5)/z0);
Ks=0.4*ustar*z1(z)*(1-((depth*0.5)/depth));
dcs=((dz^2)*us)/(5*Ks);  %Stability Criteria
dx=10 %cm  %Box size unless needed to be smaller
if dcs<dx
    dx=dcs
end
Boxnum=ceil(L/dx)
for x=2:Boxnum;  %Length Position
    X(1)=dx*0.5
    X(x)=X(x-1)+dx
end

%Set up Matrices
C=nan(Boxnum,20);
fTSS=nan(1,Boxnum);
alpha=nan(1,Boxnum);
TSS=nan(1,Boxnum);
```

```
%Governing Equation
%C(x+1,z)=C(x,z)+(dx/u(z))*[C(x,z+1)*((dkdz(z)/(2*dz))+(K(z)/(dz^2)))+...
%C(x,z)*(-2*K(z)/(dz^2))+C(x,z-1)*(-dkdz(z)/(2*dz)+K(z)/(dz^2))]

%First Box Concentration
if (outTSS>25) %f(TSS)
   fTSS(1)=10.364*(log(outTSS)).^-2.0477;
elseif (outTSS<4)
   fTSS(1)=0.1;
elseif (outTSS>=4) && (outTSS<=25);
   fTSS(1)=1;
end
alpha(1)=Filtration*fTSS(1);
C(1,1)=Parout+(dx/u(1))*(Parout*((dkdz(1)/(2*dz))+(K(1)/(dz^2)))+...
    Parout*(-2*K(1)/(dz^2))+Parout*(-dkdz(1)/(2*dz)+K(1)/(dz^2))-...
    (alpha(1)*Parout/dz));
TSS(1)=C(1,1)*fraction;
for z=2:20;
C(1,z)=Parout+(dx/u(z))*(Parout*((dkdz(z)/(2*dz))+(K(z)/(dz^2)))+...
    Parout*(-2*K(z)/(dz^2))+Parout*(-dkdz(z)/(2*dz)+K(z)/(dz^2)));
end

%Rest of Boxes Concentration
for x=1:Boxnum-1;
   C(x+1,1)=C(x,1)+(dx/u(1))*(C(x,2)*((dkdz(1)/(2*dz))+(K(1)/(dz^2)))+...
       C(x,1)*(-2*K(1)/(dz^2))+C(x,1)*(-dkdz(1)/(2*dz)+K(1)/(dz^2))-...
       (alpha(x)*C(x,1)/dz));
   TSS(x+1)=C(x+1,1)*fraction;
   if (TSS(x+1)>25);  %Using if then statements for TSS effect
       fTSS(x+1)=10.364*(log(TSS(x+1))).^-2.0477;
   elseif (TSS(x+1)<4);
       fTSS(x+1)=0.1;
   elseif (TSS(x+1)>=4)&&(TSS(x+1)<=25);
       fTSS(x+1)=1;
   end
   alpha(x+1)=Filtration*fTSS(x+1);

C(x+1,20)=C(x,20)+(dx/u(20))*(C(x,20)*((dkdz(20)/(2*dz))+(K(20)/(dz^2)))+...
       C(x,20)*(-2*K(20)/(dz^2))+C(x,19)*(-dkdz(20)/(2*dz)+K(20)/(dz^2)));
   for z=2:19;
   C(x+1,z)=C(x,z)+(dx/u(z))*(C(x,z+1)*((dkdz(z)/(2*dz))+(K(z)/(dz^2)))+...
       C(x,z)*(-2*K(z)/(dz^2))+C(x,z-1)*(-dkdz(z)/(2*dz)+K(z)/(dz^2)));
   end
end
```

Calculating Lengths and Total Uptake

For varying velocity and initial particle concentrations, plotting3d.m was used in conjunction with a function created with ParticleCapture.m. The Diffusivity.m code is altered to suspend calculations at given conditions. Both variations of Diffusivity.m are below.

plotting3d.m

```
velocity1=[5000:15000:200000];  %Velocity
Parout1=[4*10^-6:2*10^-6:32*10^-6]; %Initial Particle Concentrations

[yyyyy,xxxx]=meshgrid(Parout1,velocity1)
Uptake2=nan(size(xxxx));            %Uptake
ReefLength=nan(size(yyyyy));        %Reef Length

for kk=1:length(Parout1);
    for ii = 1:length(velocity1);

[Uptake2(ii,kk),ReefLength(ii,kk)]=ParticleCapture(xxxx(ii,kk),yyyyy(ii,kk));
%Run the Particle Capture.m function
      end
end
```

ParticleCapture.m
Function

```
function [Uptake2, ReefLength]=ParticleCapture(velocity, Parout)

% Script to run all the the codes in order

%THESE PARAMETERS CAN BE CHANGED

%Oyster Parameters
N=50;    %number of oysters per m^2
g=1;     %size in grams of oysters
oysterheight=((g/0.00008)^(1/2.175))/10; %cm  from DW=0.00008*H^2.175 where H
is in mmm

%Box Set Up
w= 100;         %width of volume of interest (cm)
depth=3*100;    %depth of water column(cm)

z0=oysterheight/30;  %roughness parameter

%Parameter Set Up (T,TSS,S,velocity)
S=15;  %salinity units
T=27;    %degrees C


%Outside Chlorophyll Concentration (mg/cm^3) and TSS concentration mg/L

outTSS=Parout*1309916;

%%%%%%%%%%%%%%%%%%%%%%%%%%%%%%%%%%%%%%%%%%%%%%%%%%%%%%%%%%%%%%%%%%%%%%%%%%%%

Filtration2

Diffusivity

%Particle Uptake (mg/hr)

Uptake2=sum(Uptake);
ReefLength=(length(TSS)*dx)/100 %meters long

end
```

Diffusivity.m

```
%Filtration rate at time t for given boxes without the TSS limitation factor
(cm^3/hr/cm^2)
Filtration=Fr2.*(100); %Including unit conversion

%Conversion
fraction=1309916;   %Muliplied by Chl to give TSS concentration

%Heights Above Bottom
deltad=depth/20; %Want 20 different heights
z1(1)=0.5*deltad;  %to find the height in the middle of a box
for z=2:1:20
    z1(z)=z1(z-1)+deltad;  %height above bottom
end
%z1 is the actual height above the bottom

%Velocity Calculations
%Ubar and Ustar
ubar=velocity; %vertically averaged velocity or maintream velocity
ustar=ubar.*(2*depth-(z0))/(5*(z0+depth*(log(depth/z0)-1)));  %ustar
u=nan(size(z1))'; %velocity
for z=1:20;
  u(z)=(ustar/0.4).*log(z1(z)/z0);
end

%Height Dependent Only Parameters (Diffusivity)
K=nan(size(z1));
dkdz=nan(size(z1));
for z=1:20;
    K(z)=0.4*ustar*z1(z)*(1-(z1(z)/depth));
    dkdz(z)=0.4*ustar*(1-2*(z1(z)/depth));
end

%Box Set up
dz=deltad;
us=(ustar/0.4)*log((depth*0.5)/z0);
Ks=0.4*ustar*z1(z)*(1-((depth*0.5)/depth));
dcs=((dz^2)*us)/(5*Ks);  %Stability Criteria
dx=10; %cm  %Box size unless needed to be smaller
if dcs<dx
    dx=dcs;
end



%Governing Equation
%C(x+1,z)=C(x,z)+(dx/u(z))*[C(x,z+1)*((dkdz(z)/(2*dz))+(K(z)/(dz^2)))+...
%C(x,z)*(-2*K(z)/(dz^2))+C(x,z-1)*(-dkdz(z)/(2*dz)+K(z)/(dz^2))]

%First Box Concentration
if (outTSS>25) %f(TSS)
   fTSS(1)=10.364*(log(outTSS)).^-2.0477;
elseif (outTSS<4)
   fTSS(1)=0.1;
elseif (outTSS>=4) && (outTSS<=25);
```

```
   fTSS(1)=1;
end
alpha(1)=Filtration*fTSS(1);
C(1,1)=Parout+(dx/u(1))*(Parout*((dkdz(1)/(2*dz))+(K(1)/(dz^2)))+...
    Parout*(-2*K(1)/(dz^2))+Parout*(-dkdz(1)/(2*dz)+K(1)/(dz^2))-...
    (alpha(1)*Parout/dz));
TSS(1)=C(1,1)*fraction;
for z=2:20;
C(1,z)=Parout+(dx/u(z))*(Parout*((dkdz(z)/(2*dz))+(K(z)/(dz^2)))+...
    Parout*(-2*K(z)/(dz^2))+Parout*(-dkdz(z)/(2*dz)+K(z)/(dz^2)));
end

%Rest of Boxes Concentration

 for x=1:100000000
   if (Parout-C(x,1))/Parout>0.1
     break
   end
   C(x+1,1)=C(x,1)+(dx/u(1))*(C(x,2)*((dkdz(1)/(2*dz))+(K(1)/(dz^2)))+...
       C(x,1)*(-2*K(1)/(dz^2))+C(x,1)*(-dkdz(1)/(2*dz)+K(1)/(dz^2))-...
       (alpha(x)*C(x,1)/dz));
   TSS(x+1)=C(x+1,1)*fraction;

   if (TSS(x+1)>25);  %Using if then statements for TSS effect
       fTSS(x+1)=10.364*(log(TSS(x+1))).^-2.0477;
   elseif (TSS(x+1)<4);
       fTSS(x+1)=0.1;
   elseif (TSS(x+1)>=4)&&(TSS(x+1)<=25);
       fTSS(x+1)=1;
   end
   alpha(x+1)=Filtration*fTSS(x+1);

C(x+1,20)=C(x,20)+(dx/u(20))*(C(x,20)*((dkdz(20)/(2*dz))+(K(20)/(dz^2)))+...
       C(x,20)*(-2*K(20)/(dz^2))+C(x,19)*(-dkdz(20)/(2*dz)+K(20)/(dz^2)));
   for z=2:19;
   C(x+1,z)=C(x,z)+(dx/u(z))*(C(x,z+1)*((dkdz(z)/(2*dz))+(K(z)/(dz^2)))+...
       C(x,z)*(-2*K(z)/(dz^2))+C(x,z-1)*(-dkdz(z)/(2*dz)+K(z)/(dz^2)));
   end
 end

for x=1:length(TSS);
   Uptake(x)=C(x,1)*alpha(x)*w*dx; %Filtration rate * area*the particles in
bottom box
end
```

Diffusivity.m

```
%Filtration rate at time t for given boxes without the TSS limitation factor
(cm^3/hr/cm^2)
Filtration=Fr2.*(100); %Including unit conversion

%Conversion
fraction=1309916;   %Muliplied by Chl to give TSS concentration

%Heights Above Bottom
deltad=depth/20; %Want 20 different heights
z1(1)=0.5*deltad;  %to find the height in the middle of a box
for z=2:1:20
    z1(z)=z1(z-1)+deltad;  %height above bottom
end
%z1 is the actual height above the bottom

%Velocity Calculations
%Ubar and Ustar
ubar=velocity; %vertically averaged velocity or maintream velocity
ustar=ubar.*(2*depth-(z0))/(5*(z0+depth*(log(depth/z0)-1)));  %ustar
u=nan(size(z1))'; %velocity
for z=1:20;
  u(z)=(ustar/0.4).*log(z1(z)/z0);
end

%Height Dependent Only Parameters (Diffusivity)
K=nan(size(z1));
dkdz=nan(size(z1));
for z=1:20;
    K(z)=0.4*ustar*z1(z)*(1-(z1(z)/depth));
    dkdz(z)=0.4*ustar*(1-2*(z1(z)/depth));
end

%Box Set up
dz=deltad;
us=(ustar/0.4)*log((depth*0.5)/z0);
Ks=0.4*ustar*z1(z)*(1-((depth*0.5)/depth));
dcs=((dz^2)*us)/(5*Ks);  %Stability Criteria
dx=10; %cm  %Box size unless needed to be smaller
if dcs<dx
    dx=dcs;
end



%Governing Equation
%C(x+1,z)=C(x,z)+(dx/u(z))*[C(x,z+1)*((dkdz(z)/(2*dz))+(K(z)/(dz^2)))+...
%C(x,z)*(-2*K(z)/(dz^2))+C(x,z-1)*(-dkdz(z)/(2*dz)+K(z)/(dz^2))]

%First Box Concentration
if (outTSS>25) %f(TSS)
   fTSS(1)=10.364*(log(outTSS)).^-2.0477;
elseif (outTSS<4)
   fTSS(1)=0.1;
elseif (outTSS>=4) && (outTSS<=25);
```

```
   fTSS(1)=1;
end
alpha(1)=Filtration*fTSS(1);
C(1,1)=Parout+(dx/u(1))*(Parout*((dkdz(1)/(2*dz))+(K(1)/(dz^2)))+...
    Parout*(-2*K(1)/(dz^2))+Parout*(-dkdz(1)/(2*dz)+K(1)/(dz^2))-...
    (alpha(1)*Parout/dz));
TSS(1)=C(1,1)*fraction;
for z=2:20;
C(1,z)=Parout+(dx/u(z))*(Parout*((dkdz(z)/(2*dz))+(K(z)/(dz^2)))+...
    Parout*(-2*K(z)/(dz^2))+Parout*(-dkdz(z)/(2*dz)+K(z)/(dz^2)));
end

%Rest of Boxes Concentration


 for x=1:100000000
   if TSS(x)<4
     break
   end
   C(x+1,1)=C(x,1)+(dx/u(1))*(C(x,2)*((dkdz(1)/(2*dz))+(K(1)/(dz^2)))+...
       C(x,1)*(-2*K(1)/(dz^2))+C(x,1)*(-dkdz(1)/(2*dz)+K(1)/(dz^2))-...
       (alpha(x)*C(x,1)/dz));
   TSS(x+1)=C(x+1,1)*fraction;

   if (TSS(x+1)>25);  %Using if then statements for TSS effect
       fTSS(x+1)=10.364*(log(TSS(x+1))).^-2.0477;
   elseif (TSS(x+1)<4);
       fTSS(x+1)=0.1;
   elseif (TSS(x+1)>=4)&&(TSS(x+1)<=25);
       fTSS(x+1)=1;
   end
   alpha(x+1)=Filtration*fTSS(x+1);

C(x+1,20)=C(x,20)+(dx/u(20))*(C(x,20)*((dkdz(20)/(2*dz))+(K(20)/(dz^2)))+...
       C(x,20)*(-2*K(20)/(dz^2))+C(x,19)*(-dkdz(20)/(2*dz)+K(20)/(dz^2)));
   for z=2:19;
   C(x+1,z)=C(x,z)+(dx/u(z))*(C(x,z+1)*((dkdz(z)/(2*dz))+(K(z)/(dz^2)))+...
       C(x,z)*(-2*K(z)/(dz^2))+C(x,z-1)*(-dkdz(z)/(2*dz)+K(z)/(dz^2)));
   end
 end

for x=1:length(TSS);
   Uptake(x)=C(x,1)*alpha(x)*w*dx; %Filtration rate * area*the particles in
bottom box
end
```

Literature Cited

Allen, J.R.L. (1985). Principles of physical sedimentology. George Allen & Unwin, London.

Allen, S., Carpenter, A.C., Luckenbach, M., Paynter, K. Sowers, A., Wesson, J., & Westby, S. (2011). Restoration goals, quantitative metrics and assessment protocols for evaluating success on restored oyster reef sanctuaries. Report of the Oyster Metrics Workgroup Submitted to the Sustainable Fisheries Goal Implementation Team of the Chesapeake Bay Program.

Bacher, C., Grant, J., Hawkins, A.J.S., Fang, J., Zhu, M, & Besnard, M. (2003). Modelling the effect of food depletion on scallop growth in Sungo Bay (China). *Aquatic Living Resources, 16,* 10-24.

Barrera-Escorcia, G., Vanegas-Perez, C., & Wong-Chang, I. (2012). Filtration rate, assimilation and assimilation efficiency in *Crassostrea virginica* (Gmelin) fed with *Tetraselmis suecica* under cadmium exposure. *Journal of Environmental Science and Health Part A, 45,* 14-22.

Bayne, B.L. (1971a) Oxygen consumption by three species of lamellibranch mollusk in declining ambient oxygen tension. *Comparative Biochemistry and Physiology A, 40*, 955-970.

Bayne, B.L. (1971b). Ventilation, the heart heat and oxygen uptake by *Mytilus edulis* in declining oxygen tension. *Comparative Biochemistry and Physiology A, 40,* 1065-1085.

Brown, J.H., Gillooly, J.F., Allen, A.P., Savage, V.M., & West, G.B. (2004). Toward a metabolic theory of ecology. *Ecology, 85* (7), 1771-1789.

Brush, M.J., Brawley, J.W., Nixon, S.W., & Kremer, J.N. (2002). Modeling phytoplankton production: problems with the Eppley curve and an empirical alternative. *Marine Ecology Progress Series, 238,* 31-45.

Butman, C.A., Frechette, M., Geyer, W.R., & Starczak, V.R. (1994). Flume experiments on food supply to the blue mussel Mytilus edulis L. as a function of boundary-layer flow. *Limnology and Oceanography, 39* (7), 1755-1768.

Cerco, C. F. & Noel, M.R. (2005). Evaluating ecosystem effects of oyster restoration in Chesapeake Bay. *A Report to the Maryland Department of Natural Resources*.

Cerco, C.F., & Noel, M.R. (2007). Can oyster restoration reverse cultural eutrophication in Chesapeake Bay? *Estuaries and Coasts,* 30 (2), 331-343.

Chesapeake Bay Program (2009, Nov. 2). *Eastern Oyster*. Retrieved November 11, 2010, from Bay Field Guide: http://www.chesapeakebay.net/american_oyster.htm

Clauser, F.H. (1956). The turbulent boundary layer. *Advances in Applied Mechanics, 4*, 1-51.

Cloern, J.E., Grenz, C., & Vidergar-Lucas, L. (1995). An empirical model of phytoplankton chlorophyll:carbon ratio – the conversion factor between productivity and productivity and growth rate. *Limnology and Oceanography, 40*(7), 1313-1321.

Collier, A., Ray, S.M., Magnitzky, A.W., & Bell, J.O. (1953). Effect of dissolved organic substances on oysters. *Fishery Bulletin 84*, 54.

Comeau, L.A., Fabrice, P., Tremblay, R, Bates, S.S., & LeBlanc A. (2008). Comparison of eastern oyster (*Crassostrea virginica*) and blue mussel (*Mytilus edulis*) filtration rates at low temperature. *Canadian Technical Report of Fisheries and Aquatic Sciences 2810.*

Dame, R.F. (1972). The ecological energies of growth, respiration and assimilation in the intertidal American Oyster *Crassostrea virginica. Marine Biology, 17*, 243-250.

Doering, P.H. & Oviatt, C.A. (1986). Application of filtration rate models to field populations of bivalves: an assessment using experimental mesocosms. *Marine Ecology Progress Series, 31*, 265-275.

Doiron, S. (2008). Reference Manual for Oyster Aquaculturists. *New Brunswick Department of Agriculture, Fisheries and Aquaculture*.

Edelstein-Keshet, L. (2005). Mathematical models in biology. Society for Industrial and Applied Mathematics, Philadelphia, PA.

Ferreira, J.G., Hawkins, A.J.S., & Bricker, S.B. (2007). Management of productivity, environmental effects and profitability of shellfish aquaculture - the Farm Aquaculture Resource Management (FARM) model. *Aquaculture, 264*, 160-174.

Frechette, M., Butman, C.A., & Geyer, R.W. (1989). The importance of boundary-layer flows in supplying phytoplankton to the benthic suspension feeder, *Mytilus edulis* L. *Limnology and Oceanography, 34(*1), 19-36.

Fulford, R.S., Breitburg, D.L., Newell, R.I.E., Kemp, W. M., & Luckenbach, M. (2007). Effects of oyster population restoration strategies on phytoplankton biomass in Chesapeake Bay: A flexible modeling approach. *Marine Ecology Progress Series, 336,* 43-61.

Fulton, E.A., Smith, A.D.M., & Johnson, C.R. (2003). Effect of complexity on marine ecosystem models. *Marine Ecology Progress Series, 253,* 1-16.

Gerritsen, J., Holland, A.F., & Irvine, D.E. (1994). Suspension-feeding bivalves and the fate of primary production: An estuarine model applied to the Chesapeake Bay. *Estuaries, 17* (2), 403-416.

Grizzle, R.E., Greene, J.K., & Coen, L.D. (2008). Seston removal by natural and constructed intertidal eastern oyster (*Crassostrea virginica*) reefs: A comparison with previous laboratory studies, and the value of in situ methods. *Estuaries and Coasts, 31,* 1208-1220.

Gutierrez, J.L., Jones, C.G., Strayer, D.L, & Iribarne, O.O. (2003). Mollusks as ecosystem engineers: the role of shell production in aquatic habitats. *Oikos 101*, 79-90.

Hornberger, G. & Wiberg, P. (2005) Finite Difference Solutions for Transient Problems. In: Numerical Methods in the Hydrological Sciences. Special Publication Series 57. American Geophysical Union, 1-20.

Jones, N.L., Thompson, J.K., Arrigo, K.R., & Monismith, S.G. (2009). Hydrodynamic control of phytoplankton loss to the benthos in an estuarine environment. *Limnology and Oceanography, 54*(3), 952-969.

Jordan, S. (1987). Sedimentation and remineralization associated with biodeposition by the American oyster *Crassostrea virginica* (Gmelin). (Doctoral Dissertation). University of Maryland, College Park, Maryland.

Kellogg, L.M., Cornwell, J.C. Owens, M.C., & Paynter, K.T. (2013). Denitrification and nutrient assimilation on a restored oyster reef. *Marine Ecology Progress Series, 480,* 1-17.

Kemp, W. M., Boynton, W. R., Adolf, J. E., Boesch, D. F., Boicourt, W. C., Brush, G., et al. (2005). Eutrophication of Chesapeake Bay: Historical trends and ecological interactions. *Marine Ecology Progress Series, 303,* 1-29.

Kennedy, V.S & Sanford, L.P. (1999) In: Luckenbach, M.W, Mann, R., & Wesson, J.A. (eds) Oyster reef habitat restoration: A synopsis and synthesis of approaches. Virginia Institute of Marine Science Press, Gloucester Point, VA, 25-46.

Langefoss, C. M. & Maurer D. (1975). Energy portioning in the American oyster, *Crassostrea virginica* (Gmelin). *Proceedings of the National Shellfisheries Association, 65*, 20-25.

Loosanoff, V.L. & Engle, J.B. (1947). Effect of different concentrations of micro-organisms on the feeding of oysters (*O. virginica*). *Fishery Bulletin 42, 51*, 31-57.

Loosanoff, V.L. & Nomejko C.A. (1946). Feeding of oysters in relation to tidal stages and to periods of light and darkness. *Biological Bulletin, 90*(3), 244-264.

Loosanoff, V.L. & Tommers, F.D. (1948). Effect of suspended silt and other substances on rate of feeding of oysters. *Science, 107*(2768), 69-70.

Loosanoff, V.L. (1953). Behavior of oysters in water of low salinities. *Proceedings of the National Shellfisheries Association, 43*, 135-151.

Loosanoff, V.L. (1958). Some aspects of behavior of oysters at different temperatures. *Biological Bulletin, 114*(1), 57-70.

Loosanoff, V.L. (1962). Effects of turbidity on some larval and adult bivalves. *Proceedings of the Fourteenth Annual Gulf and Caribbean Fisheries Institute, 14*, 80-94.

Maryland Department of Natural Resources. (1997). Report: Maryland's historic oyster bottom; A geographic representation of the traditional named oyster bars.

Monismith, S.G., Koseff, J.R., Thompson, J.K., O'Riordan, C.A., & Nepf, H.M. (1990). A study of model bivalve siphonal currents. *Limnology and Oceanography, 35(*3), 680-696.

Myung, I.J, & Pitt, M.A. (1997). Applying Occam's razor in modelling cognition: A Bayesian approach. *Psychonomic Bulletin & Review*, *4* (1), 79-95.

Newell R.I.E. & Langdon C.J. (1996) Mechanisms and physiology of larval and adult feeding. In: Kennedy V.S., Newell R.I.E, & Eble A. (eds) The eastern oyster *Crassostrea virginica*. Maryland Sea Grant College, College Park, MD, 185-230.

Newell, R.I.E & Koch, E.W. (2004). Modeling seagrass density and distribution in response to changes in turbidity stemming from bivalve filtration and seagrass sediment stabilization. *Estuaries, 27* (5), 793-806.

Newell, R.I.E. (1988). Ecological changes in Chesapeake Bay: Are they the result of overharvesting the American Oyster, *Crassostrea virginica*? *Understanding the Estuary: Advances in Chesapeake Bay Research. Chesapeake Research Consortium Publication 129,* 536-546.

Newell, R.I.E., Fisher, T.R., Holyoke, R.R., & Cornwell, J.C. (2005). Influence of eastern oysters on nitrogen and phosphorus regeneration in Chesapeake Bay, USA. In: Dame, R. & Olenin, S. (eds) The comparative roles of suspension feeders in ecosystems. NATO Science Series: IV-Earth and Environmental Sciences. Springer, Netherlands, 47, 93-120.

NOAA Fisheries Eastern Oyster Biological Review Team. (2007). Status review of the Eastern Oyster (Crassostrea virginica): Report to the National Marine Fisheries Service, Northeast Regional Office. *NOAA.*

North, E.W., Schlag, Z., Hood, R.R., Li, M., Zhong, L., Gross, T., & Kennedy, V.S. (2008) Vertical swimming behavior influences the dispersal of simulated oyster larvae in a coupled-particle tracking and hydrodynamic model of Chesapeake Bay. *Marine Ecology Progress Series, 359,* 99-115.

Palmer, R.E. (1980). Behavioral and rhythmic aspects of filtration in the bay scallop, *Argopecten irradians concentricus* (Say), and the oyster, *Crassostrea virginica* (Gmelin). *Journal of Experimental Marine Biology and Ecology,* 45, 273-295.

Peters, R.H (1983). The ecological implications of body size. Cambridge University Press, New York, 1-23.

Petersen, J.K., Marr, M., Ysebaert, T., & Herman, P.M.J. (2013). Near-bed gradients in particles and nutrients above a mussel bed in the Limfjorden: Influence of physical mixing and mussel filtration. *Marine Ecology Progress Series, 490*, 137-146.

Powell, E.N, Hofmann, E.E., Klinck, J.M., & Ray, S.M. (1992). Modeling oyster populations I. A commentary on filtration rate. Is faster always better? *Journal of Shellfish Research, 11*(2), 387-398.

Powell, E.N, Hofmann, E.E., Klinck, J.M., & Ray, S.M. (1994). Modeling oyster populations IV: Rates of mortality, population crashes, and management. *Fishery Bulletin, 92,* 347-373.

Rheault, R.B. & Rice, M.A. (1996). Food-limited growth and condition index in the eastern oyster, *Crassostrea virginica* (Gmelin 1791), and the bay scallop, *Argopecten irradians irradians* (Lamarck 1819). *Journal of Shellfish Research, 15*(2), 271-283.

Riisgard, H.U. (1988). Efficiency of particle retention and filtration rate in 6 species of Northeast American bivalves. *Marine Ecology Progress Series, 45* (3), 217-223.

Riisgard, H.U. (2001). On measurement of filtration rates in bivalves-the stony road to reliable data: review and interpretation. *Marine Ecology Progress Series, 211*, 275-291.

Ross, P.G., & Luckenbach, M.W. (2006). Relationships between shell height and dry tissue biomass for the eastern oyster (*Crassostrea virginica)*. 9th International Conference on Shellfish Restoration, Charleston, S.C. November 2006.

Saurel, C., Petersen, J.K., Wiles, P.J., & Kaiser, M.J. (2013). Turbulent mixing limits mussel feeding: Direct estimates of feeding rate and vertical diffusivity. *Marine Ecology Progress Series, 485*, 105-121.

Savage, V.M., Gillooly, J.F., Brown, J.H., West, G.B., & Charnov, E.L. (2004). Effects of body size and temperature on population growth. *The American Naturalist, 163*(3), 429-441.

Sibly, R.M., Grimm, V., Martin, B.T., Johnston, A.S.A, Kulakowska, K, Topping, C.J., et al. (2013). Representing the acquisition and use of energy by inidviduals in agent-based models of animal populations. *Methods in Ecology and Evolution, 4*, 151-161.

Simpson, J.H., Berx, B., Gascoigne, J., & Saurel, C. (2007). The interaction of tidal advection, diffusion and mussel filtration in a tidal channel. *Journal of Marine Systems, 68*, 556-568.

Southworth, M., Harding, J.M., Wesson, J.A., & Mann, R. (2010). Oyster (Crassostrea virginica, Gemlin 1791) population dynamics on publics reefs in the Great Wicomico River, Virginia, USA. *Journal of Shellfish Research, 29* (2), 271-290.

Tamburri, M.N. & Zimmer-Faust, R.K. (1996). Suspension feeding: Basic mechanisms controlling recognition and ingestion of larvae. *Limnology and Oceanography, 41*(6), 1188-1197.

Tenore, K.R., & Dunstan, W.M. (1973). Comparison of feeding and biodeposition of three bivalves at different food levels. *Marine Biology, 21*, 190-195.

Ward, J.E., Newell, R.I.E., Thompson, R.J., & MacDonald, B.A. (1994). In vivo studies of suspension-feeding processes in the eastern oyster, *Crassostrea virginica* (Gmelin). *Biological Bulletin, 186*, 221-240.

White, E.P., Ernest, S.K.M., Kerkhoff, A.J., & Enquist, B.J. (2007). Relationships between body size and abundance in ecology. *Trends in Ecology and Evolution, 22*(6), 323-329.

Wilberg, M.J, Livings, M.E., Barkman, J.S., Morris, B.T., & Robinson, J.M. (2011). Overfishing, disease, habitat loss, and potential extirpation of oysters in upper Chesapeake Bay. *Marine Ecology Progress Series, 436*, 131-144.

Wilberg, M.J., Wiedenmann, J.R., & Robinson, J.M. (2013). Sustainable exploitation and management of autogenic ecosystem engineers: application to oysters in Chesapeake Bay. *Ecological Applications, 23*(4), 766-776.

Wildish, D.J. & Kristmanson, D.D. (1984) Importance to mussels of the benthic boundary layer. *Canadian Journal of Fisheries and Aquatic Science, 41,* 1618-1625.

Wilson-Ormond, E.A., Powell, E.N., & Ray, S.M. (1997). Short-term and small-scale variation in food availability to natural oyster population: Food, flow, and flux. *Marine Ecology, 18*(1), 1-34.